

Effects of A β Oligomers and State-Dependent Channel Blockers on High Voltage-Activated Calcium Channels

David Hermann

2013

Dissertation

submitted to the

Combined Faculties for the Natural Sciences and for Mathematics

of the Ruperto-Carola University of Heidelberg, Germany

for the degree of

Doctor of Natural Science

presented by

David Hermann, MSc in Neurosciences

born in Erlangen

Declarations according to § 8 (3) b) and c) of the doctoral degree regulations: a) I hereby declare that I have written the submitted dissertation myself and in this process have used no other sources or materials than those expressly indicated, b) I hereby declare that I have not applied to be examined at any other institution, nor have I used the dissertation in this or any other form at any other institution as an examination paper, nor submitted it to any other faculty as a dissertation.

Darmstadt, _____

Effects of A β Oligomers and State-Dependent Channel Blockers on High Voltage-Activated Calcium Channels

Referees:

Prof. Dr. Andreas Draguhn

Prof. Dr. Stephan Frings

Referees Prof. Dr. Andreas Draguhn
Department of Neuro- and Sensory Physiology
Institute for Physiology and Pathophysiology
University of Heidelberg
Im Neuenheimer Feld 326, 69120 Heidelberg, Germany

Prof. Dr. Stephan Frings
Department of Molecular Physiology
Centre for Organismal Studies
University of Heidelberg
Im Neuenheimer Feld 504, 69120 Heidelberg, Germany

Oral Examiners Dr. Johann Bollmann
Department of Biomedical Optics
Max Planck Institute for Medical Research
Jahnstrasse 29, 69120 Heidelberg, Germany

Dr. Wolfgang Kelsch
Department of Psychiatry and Psychotherapy
Central Institute of Mental Health
University Heidelberg
J5, 68159 Mannheim, Germany

Local Supervisor Dr. Volker Nimmrich
Department of Pharmacology
AbbVie GmbH & Co. KG
Knollstraße 50, 67061 Ludwigshafen/Rhein, Germany

Date of Oral Examination

Acknowledgements

This work was carried out at and supported by the AbbVie (former: Abbott) GmbH & Co. KG in Ludwigshafen and the Ruperto-Carola University of Heidelberg.

First and foremost, I owe many thanks to my supervisor in Ludwigshafen, Dr. Volker Nimmrich who has given me excellent scientific and professional guidance and supported me throughout all the 4 years at AbbVie and beyond. I feel very privileged to have worked together with Michael Bahr, Tanja Georgi and Siena Kiess, who I admire not only for their expert technical knowledge and methodological skills. I would further like to express my gratitude to Dr. Karsten Wicke, who has been overly supportive and provided valuable senior scientific advice. This also holds true for Prof. Dr. Gerhard Gross whose efforts made funding of this project at AbbVie possible in the first place. Special thanks go to Dr. Mario Mezler, who had a major impact on this thesis by, among other things, providing the transfected cell lines and sharing his profound knowledge on assay development together with Dr. Andrew Swensen, located at Abbott Park in Illinois, U.S.A. I am also very thankful for constant high quality supply of A β globulomer provided by Andreas Striebinger from the lab of Dr. Stefan Barghorn and the remarkable technical support received from the whole Nanion Technologies GmbH team, especially Dr. Ali Obergrußberger.

Success of this PhD project was only achievable because of the full, continuous and outstanding scientific, technical, and practical support by Prof. Dr. med. Andreas Draguhn and his department at the University of Heidelberg – from the very beginning to the very end. I am especially thankful for all expert remarks I received from Dr. Claus Bruehl regarding electrophysiological procedures and experimental design throughout the whole project. Furthermore, it needs to be emphasized that wrapping up this thesis was only possible because of the reliable cell culture maintenance by Nadine Zuber and the extraordinary efforts by Fabian Roth, giving me practical experimental training after closing time and on weekends. In addition, I would also like to thank Prof. Dr. Stefan Frings for investing his valuable time as my second referee.

My family, especially Valeska, has always been a wonderful source of encouragement providing me with the determination and strength to overcome any obstacle, I love you.

Contents

List of Abbreviations	xi
Abstract	xiii
Zusammenfassung	xv
1 Introduction	1
1.1 Alzheimer's Disease (AD)	1
1.1.1 Clinical and Socioeconomic Facts	1
1.1.2 Histopathology of AD and Function of the Hippocampal Formation	3
1.1.3 Molecular Mechanisms	6
1.1.3.1 The Cholenergetic and Glutamate Hypotheses: Rationale for Current Drug Treatment	6
1.1.3.2 The Amyloid Hypothesis	9
1.1.3.3 Ion Channel-Related Synaptic Pathophysiology	13
1.2 High Voltage-Activated Calcium Channels	18
1.2.1 Structure and Pharmacological Characterization	19
1.2.2 Terminology of Channel States and Transitions	23
1.2.3 Function and Mechanisms of Inactivation	24
1.3 Drug Discovery Targeting Ion Channels	28
1.3.1 Ion Channels as Drug Targets	28
1.3.2 High Throughput Methods	30
1.3.3 State-Dependent Channel Modulation	32
1.3.4 P/Q-type Calcium Channels as Potential Drug Target	35
Aims of the Study	37
2 Materials and Methods	39
2.1 Chemicals and Biologics	39
2.2 Generation of Cell Lines and High Throughput Screening	40
2.3 Patch Clamp Recordings	42
2.3.1 Manual Patch Clamp	43
2.3.1.1 Voltage-clamp	43
2.3.1.2 Current-clamp	45
2.3.2 Automated Patch Clamp	46
2.4 Hippocampal Slice Culture Preparation	48
2.5 Field Potential Recordings	50

2.6	Data Analysis	51
2.7	Statistics.....	53
3	Results	55
3.1	Effects of Oligomeric A β on Synaptic Transmission are Calcium Channel-Dependent.....	56
3.2	Oligomeric A β Modulates Recombinant Calcium Channels	59
3.2.1	Biophysical and Pharmacological Validation of Functional Channel Expression.....	59
3.2.2	A β Oligomers Facilitate Channel Activation at Intermediate Depolarized Potentials.....	66
3.2.3	Effects of A β Oligomers Appear to be Independent of Channel State..	71
3.3	Identification of Novel State-Dependent P/Q-type Calcium Channel Blockers..	72
3.3.1	Inactivation of Recombinant Channels Accumulates over Time.....	73
3.3.2	Channel Activation, but not Inactivation is Similar between Manual and Automated Patch Clamp.....	77
3.3.3	Compound Screening Reveals Novel Channel Blockers.....	81
3.3.4	Characterization of State-Dependency of Selected Compounds.....	86
3.4	State-Dependent Block of Calcium Channels Prevents Oligomeric A β -induced Synaptic Deficits	88
4	Discussion	91
4.1	Overactivation of Presynaptic Calcium Channels as a Potential Molecular Mechanism in AD	92
4.1.1	Presynaptic Calcium Channel Block Reverses Oligomeric A β -induced Deficits in Synaptic Transmission.....	93
4.1.2	Oligomeric A β Augments Presynaptic Calcium Channel Currents	95
4.2	Development of State-Dependent P/Q-type Calcium Channel Blockers	100
4.2.1	Appropriate Screening Protocol Selection Depends on Disease- and Channel-Specific Properties	102
4.2.2	Compound Screening Reveals Novel Channel Blockers.....	105
4.2.3	State-Dependent Calcium Channel Block Ameliorates Oligomeric A β -induced Deficits in Synaptic Transmission.....	109
4.3	Conclusion and Outlook	110
	Publications	111
	Bibliography	113
	List of Tables and Figures	141

List of Abbreviations

A β	Amyloid- β
AD	Alzheimer's Disease
APP	Amyloid Precursor Protein
CA1/3	Cornu Ammonis 1/3
CNS	Central Nervous System
fEPSP	Field Excitatory Postsynaptic Potential
FLIPR	Fluorometric Imaging Plate Reader
GHK	Goldman-Hodgkin-Katz
HVA	High Voltage-Activated
LMW	Low Molecular Weight
LTP	Long Term Potentiation
NMDA	N-methyl-D-aspartate

Abstract

Alzheimer's disease (AD) is accompanied by increased brain levels of soluble amyloid- β (A β) oligomers (McLean et al., 1999). It has been suggested that A β oligomers directly impair synaptic function (Haass and Selkoe, 2007) and modulate high voltage-activated calcium channels (Sberna et al., 1997; Bobich et al., 2004; Nimmrich et al., 2008a). State-dependent drugs are hypothesized to target pathologically overactivated channels without altering physiological activity, which may reduce adverse side effects (Winqvist et al., 2005). Here, the effect of A β globulomer, a synthetic, stable, and pathologically relevant oligomeric A β preparation (Barghorn et al., 2005; Gellermann et al., 2008), on high voltage-activated calcium channels was further elucidated. Furthermore, it was tested whether novel state-dependent calcium channel blockers can ameliorate oligomeric A β -induced deficits in synaptic transmission.

First, the effect of oligomeric A β on excitatory synaptic transmission was investigated in rat organotypic hippocampal slice cultures. Specific block of P/Q-type and N-type calcium channels by ω -agatoxin IVA and ω -conotoxin MVIIA, respectively, completely reversed A β oligomer-induced deficits. By contrast, (additional) L-type calcium channel block by nimodipine (Diochot et al., 1995; Furakawa et al., 1999), a potential antidementia medicine (Birks and López-Arrieta, 2002), was ineffective. As assessed by whole cell patch clamp analysis, oligomeric A β shifted the activation of P/Q-type and N-type calcium channels, recombinantly expressed in HEK293 cells, to more hyperpolarized values. Application of non-aggregated A β peptide had no effect. These findings suggest that overactivation of presynaptic calcium channels by oligomeric A β may lead to functional synaptic deficits, which can be prevented with presynaptic calcium channel blockers.

In a second part of this work, novel state-dependent calcium channel blockers were identified (published in Mezler et al., 2012a) and their potential to protect from A β -induced functional deficits investigated. Compounds were initially detected by a fluorescence imaging plate reader-based primary high throughput screen (previously performed at Abbott) using HEK293 cells recombinantly expressing P/Q-type calcium channels. For subsequent compound validation using a more direct measure of channel function, an automated patch clamp secondary screening assay was

established and incorporated into the hit-to-lead cycle of a drug discovery process. Representative compounds out of this screen were characterized for state-dependent P/Q-type calcium channel block by manual patch clamp recordings. Finally, these blockers were able to protect from A β -induced functional decline in synaptic transmission similarly as the state-independent peptide toxins.

Findings from this work hint towards the therapeutic potential of state-dependent presynaptic calcium channel block, which needs to be further elucidated in an *in vivo* model of AD. As P/Q-type calcium channel gain-of-function is also associated with migraine and epilepsy, novel specific channel blockers may also alleviate symptoms of other neurological diseases, beyond AD.

Zusammenfassung

Die Alzheimer-Krankheit geht im Gehirn mit einem erhöhten Spiegel von löslichen Amyloid- β (A β) Oligomeren einher (McLean et al., 1999). Es wird vermutet, dass A β Oligomere unmittelbar synaptische Funktion schädigen (Haass and Selkoe, 2007) und spannungsaktivierte Kalziumkanäle beeinflussen (Sberna et al., 1997; Bobich et al., 2004; Nimmrich et al., 2008a). Für zustandsabhängige Wirkstoffe wird angenommen, dass diese auf pathologisch überaktivierte Kanäle wirken ohne deren physiologische Aktivität zu beeinflussen, was unerwünschte Nebenwirkungen reduzieren würde (Winqvist et al., 2005). In der vorliegenden Arbeit wird der Effekt von A β Globulomer, einer synthetischen, stabilen und pathologisch relevanten oligomeren A β Präparation (Barghorn et al., 2005; Gellermann et al., 2008), auf spannungsaktivierte Kalziumkanäle weiter aufgeklärt. Darüber hinaus wurde getestet, ob neuartige zustandsabhängige Kalziumkanalblocker A β Oligomer-induzierte Defizite der synaptischen Übertragung lindern können.

Zuerst wurde der Effekt von oligomerem A β auf exzitatorisch synaptische Übertragung organotypischer hippocampaler Schnittkulturen der Ratte untersucht. Spezifischer P/Q-Typ und N-Typ Kalziumkanalblock, jeweils durch ω -agatoxin IVA beziehungsweise ω -conotoxin MVIIA, kehrte die A β Oligomer-induzierten Defizite vollständig um. Im Gegensatz dazu war (zusätzlicher) L-Typ Kalziumkanalblock durch nimodipine (Diochot et al., 1995; Furakawa et al., 1999), ein potenzielles Antidementivum (Birks and López-Arrieta, 2002), unwirksam. Durch Whole Cell Patch Clamp Untersuchungen wurde ermittelt, dass oligomeres A β die Aktivierung von – in HEK293 Zellen rekombinant exprimierten – P/Q-Typ und N-Typ Kalziumkanälen zu hyperpolarisierenden Spannungswerten verschoben wurde. Applikation von nicht aggregiertem A β Peptid hatte keinen Effekt. Diese Befunde lassen vermuten, dass Überaktivierung präsynaptischer Kalziumkanäle durch oligomeres A β zu funktionellen synaptischen Defiziten führen kann, die durch präsynaptische Kalziumkanalblocker verhindert werden können.

Im zweiten Teil dieser Arbeit wurden neuartige zustandsabhängige Kalziumkanalblocker identifiziert (publiziert in Mezler et al., 2012a) und deren Potenzial untersucht A β -induzierte funktionelle Defizite zu verhindern. Substanzen wurden zunächst durch ein Fluorescence Imaging Plate Reader-basiertes primäres

Hochdurchsatz-Screening (im Vorfeld bei AbbVie durchgeführt) mittels HEK293 Zellen identifiziert, die rekombinant P/Q-Typ Kalziumkanäle exprimieren. Für anschließende Substanzvalidierung wurde eine direktere Messung der Kanalfunktion etabliert, ein automatischer Patch Clamp Sekundärscreen, der in den Hit-To-Lead Zyklus eines Wirkstoffentwicklungsprogramms eingebettet wurde. Die Zustandsabhängigkeit des P/Q-Typ Kalziumkanalblocks repräsentativer Substanzen dieses Screenings wurde durch manuelle Patch Clamp Messungen charakterisiert. Letztlich waren diese Blocker in der Lage vor den A β -induzierten Defiziten in synaptischer Übertragung, ebenso wie die zustandsunabhängigen Peptidtoxine, zu schützen.

Die Ergebnisse dieser Arbeit deuten auf das therapeutische Potential eines zustandsabhängigen präsynaptischen Kalziumkanalblocks hin, was durch ein *in vivo* Model der Alzheimer-Krankheit weiterer Aufklärung benötigt. Da erhöhte P/Q-Typ Kalziumkanalfunktion auch mit Migräne und Epilepsie in Verbindung gebracht wird, könnten neuartige spezifische Kalziumkanalblocker auch die Symptome anderer neurologischer Erkrankungen, neben der Alzheimer-Krankheit, lindern.

1 Introduction

1.1 Alzheimer's Disease (AD)

The most common form of dementia, AD, which ultimately ends fatally, was initially described by Alois Alzheimer more than a century ago. Due to the worldwide increasing life expectancy, AD has been increasingly receiving attention by the scientific community and the public since the 1960s. The following chapter will provide an insight into the current and predicted number of demented patients, the detrimental effects of private caregiving to family members and the economical burden dementia imposes on governments around the world. Moreover, a brief overview is given about the clinical manifestations and disease progression of AD as well as the currently available pharmacological treatment options. The subsequent section will review the histopathological hallmarks of AD. As the hippocampal region is one of the primarily affected regions and is also utilized in experimental studies within this PhD work, a short introduction of its anatomical structure and function is included. In the last sections, the rationales and proposed mechanisms of action of the currently marketed drugs is elaborated in more detail. Finally, several currently proposed molecular mechanisms are reviewed focusing on ion channel-related synaptic pathophysiology of AD.

1.1.1 Clinical and Socioeconomic Facts

For 2010, worldwide 35.6 million people were estimated to be suffering from dementia, a serious loss of cognitive ability (Ferri et al., 2009). Usually this decline in brain function manifests progressively and affects memory, learning, orientation, language, comprehension, judgment and personality. Wimo and Prince (2010) predict the number of demented people to rise to 65.7 and 115.5 million in the years 2030 and 2050, respectively. This report also estimated the current worldwide socioeconomic costs caused by dementia at 604 billion US dollars, with 70% of costs occurring in Western Europe and North America. Dementia has a tremendous impact on the ability to live independently and cognitive impairment was identified as one of the main predictors for institutionalization in the USA (Gaugler et al., 2007).

Moreover, the burden and emotional stress of private care, which is usually carried out by family members or friends of the demented patient, causes very high levels of psychological morbidity among the caregivers, increasing their rate of major depression by 2.8 to 38.7 times (Cuijpers, 2005). This report also emphasizes that by far the strongest factor correlated with dementia is age. The overall prevalence at age 60 and over was estimated at 5-7% in most regions of the world, and starting from age 65 the likelihood of developing dementia roughly doubles every 5 years. Based on a study about early onset dementia within the United Kingdom, Harvey et al. (2003) estimated that this doubling every 5 years already starts at age 35.

Dementia can be caused by a single disease or a mixture of several underlying diseases including AD, vascular dementia, dementia with Lewy-Bodies, and others. AD is the leading cause for dementia, as it has been illustrated by post-mortem analysis of demented people, which identified AD-related pathology in 86% and pure (exclusive) AD pathology in 43% of the cohort (Jellinger, 2006). This is in line with a previous review by Nussbaum and Ellis (2003) stating that about two thirds of all dementias are caused by AD.

Upon diagnosis of AD before age 90, Dodge et al. (2003) found that the remaining life years individuals from an American cohort decreased by about one third to one half. They also report that diagnosed AD patients are burdened with a significantly higher level of disability for the rest of their shortened life. Early phases of AD are marked by a subtle impairment of learning and memory including forgetfulness, whereas at the same time older episodic, semantic and implicit memory remains mostly intact. As cognitive impairments increase, everyday life activities become more and more challenging and the patient requires assistance by another person. As motor impairments manifest and cognitive impairments continue to worsen (e.g., not being able to recognize family members anymore), caregiving becomes increasingly demanding until the patient has to be institutionalized. Late stage AD is accompanied by loss of speech and the inability of patients to feed themselves. The ultimate cause of death often occurs by respiratory system diseases like an acquired inflammation of the lung (Förstl and Kurz, 1999; Brunnstrom and Englund, 2009). When comparing death rates in the USA from the year 2008 with 2000, deaths caused by AD increased by 66% whereas the number of other common causes of

death decreased including stroke, human immunodeficiency virus, prostate cancer, breast cancer, and heart disease (Thies and Bleiter, 2012).

Unfortunately, as of today there is no causative treatment available for AD. First and second line medical treatment is obtained by acetylcholinesterase inhibitors (donepezil, rivastigmine, galantamine and tacrine) and the N-methyl-D-aspartate (NMDA) receptor antagonist memantine, respectively. As these drugs are only effective in about half of the patients slowing down cognitive decline by a mere 6-12 months, they are only considered as symptomatic treatment which does not stop or even reverse the progression of the disease. Despite major investments into basic research and drug development have led to numerous clinical trials (Mangialasche et al., 2010), no new medication for AD has gained approval from regulatory authorities of the United States since 2003.

Considering all of these factors, it is evident that AD is a detrimental disease for both the patient and their relatives. Due to the complete lack of effective therapeutic intervention, those affected have to inevitably face a terminal disease, which gradually diminishes cognitive functions and impacts the personality of the diseased, as well as intensive long-term caretaking, which is physically and emotionally extraordinarily demanding. Moreover, the associated high socioeconomic costs are increasingly becoming an issue for governments and institutions around the world.

1.1.2 Histopathology of AD and Function of the Hippocampal Formation

The diagnosis of AD today is defined by two histopathological hallmarks, which were already described by Alois Alzheimer (1907), after whom this disease was named. These hallmarks are senile plaques, mostly composed out of amyloid (A β) peptide, and neurofibrillary tangles, comprising hyperphosphorylated forms of the microtubule associated protein tau found especially in the cortex and hippocampus (Bouras et al., 1994). In addition, neuronal cell death has been reported (Neary et al., 1986). However, a decrease in the number of neurons has also been observed for normal aging and AD may rather facilitate cell shrinkage within the hippocampus (Simic et al., 1997; Gosche et al., 2002). Even today AD can only be unambiguously confirmed post-mortem based on the demonstration of these A β plaques and neurofibrillary tangles along with amyloid deposits in the cerebral blood-vessels, reactive gliosis,

and neuronal atrophy. Prior to death medical history, mental tests, and exclusion of other diseases allow clinical diagnosis of AD (McKhann et al., 1984; McKhann et al., 2011) with an averaged sensitivity of 81% and specificity of 70% (Knopman et al., 2001). Current clinical diagnosis can, however, only be obtained if the disease has already progressed to a state where cognitive deficits have already manifested. In the future, earlier diagnosis of AD may be feasible with surrogate markers including immunoassays detecting A β and tau phosphorylated at specific epitopes in cerebrospinal fluid. These biomarkers may also serve as diagnostic markers for AD trials (reviewed by Hampel et al., 2010).

The entorhinal cortex, appears be the first structure with histopathological changes in AD (Hyman et al., 1984; Braak et al., 1993; Gómez-Isla et al., 1996). This structure constitutes the main input to the hippocampal formation, which comprises the hallmarks of AD and is also already affected during early stages of the disease (Blennow et al., 1996). The role of the hippocampal region in AD was further supported by animal models of AD (reviewed by Fitzjohn et al., 2008).

The function of the hippocampus in learning and memory was unambiguously demonstrated by Scoville and Milner (1957). After bilateral removal of the hippocampus for treatment of epilepsy, the patient H.M. suffered from permanent anterograde memory impairment hindering encoding of any new long-term memories. Interestingly, although H.M. could not encode new memories, he was still able to recall some retrograde memories especially ones from long ago. It has subsequently been observed in many patients that bilateral hippocampal damage induces severe loss of (at least) anterograde episodic memory (reviewed by Spiers et al., 2001). On a molecular level, learning and memory is associated with synaptic plasticity (Hebb, 1949). Within the hippocampus several forms of plasticity can be observed including long-term potentiation (LTP; Bliss and Lomo, 1973). Initial support for the theory of LTP as neurophysiological correlate of learning and memory has been collected by Morris et al. (1986), providing experimental evidence that hippocampal LTP measured *in vitro* is required for formation of memories *in vivo*. As a consequence, disturbances in LTP may contribute to the clinical symptoms in AD (Rowan et al., 2003). In addition to its function in memory, is noteworthy that the hippocampus is also involved in other tasks like spatial navigation, as initially described by O'Keefe and Dostrovsky (1971).

Another, more technical, reason why this region has been intensively studied is because of its relatively simple, three-layered anatomical structure and well-defined cytoarchitecture. Hippocampal circuitry is organized in a highly ordered manner with lamina-specific connections of afferent fibers. This also holds true for isolated hippocampal slice cultures, where termination of hippocampal afferents does not lead to significant translaminal sprouting of the remaining intrinsic fibers (Frotscher et al., 1995; Frotscher et al., 1997). Furthermore, synaptic field potentials have symmetry along the septotemporal axis. Thus, slices taken from different transversal parts of the hippocampus show similar electrophysiological patterns increasing the reproducibility of the respective electrophysiological field recordings.

In the following, the anatomy of the hippocampus is briefly reviewed (Amaral and Witter, 1989), focusing on its trisynaptic pathway. Anatomically, the hippocampus is located within the medial temporal lobe, is part of the limbic system and consists of the entorhinal cortex, dentate gyrus, cornu ammonis (CA1-3) fields, and subiculum. The major input afferent to the hippocampal formation arises from the perforant path fibers originating from the adjacent entorhinal cortex. They synapse in the outer molecular layer of the granule cells in the dentate gyrus and in the stratum lacunosum-moleculare at distal apical dendrites. Signals from the granule cells are conveyed via their axonal projections called mossy fibers to the pyramidal cell layer of the CA3 region. The signal is then further transduced via the Schaffer collateral, which innervate proximal apical dendrites in the stratum radiatum of pyramidal CA1 cells by releasing the excitatory neurotransmitter glutamate. The stratum pyramidale comprises the cell bodies of the pyramidal neurons and synapses from a variety of interneurons. Recurrent connections of pyramidal cells within the CA1 region mainly synapse on the basal dendrites in the stratum oriens. In contrast, dendrites from different types of interneurons receive input from both stratum radiatum and stratum oriens (Buhl et al., 1996; Halasy et al., 1996). The CA1 region projects to the adjacent subiculum and the entorhinal cortex, thereby closing the loop between the entorhinal cortex and hippocampus. Most sensory input to the hippocampus is received through the entorhinal cortex, which after the loop in the hippocampus conveys the signal back to the same cortical area that it originally received the input from. Furthermore, a smaller fraction of subcortical afferents terminate diffusely on different kinds of target cells (Wyss et al., 1979). As a consequence, isolated studies

of transverse hippocampal sections still inherit a large portion of the hippocampal circuitry.

Stimulation of the Schaffer collateral results in a negative shift in the extracellular field potential measured in the stratum radium (reflecting the current sink of the postsynapse) and a positive potential measured in the pyramidal layer (representing the corresponding current source close to the soma). The initial change in potential is solely due to excitatory transmission, since the Schaffer collateral fibers release the neurotransmitter glutamate. After a few milliseconds the excitatory potential is superimposed by feed forward and feed backward inhibitory currents of bistratified cells, innervating stratum radiatum, or basket cells which synapse perisomatically at the pyramidal cell layer (Buzsáki, 1984; Buhl et al., 1996; Halasy et al., 1996).

1.1.3 Molecular Mechanisms

Despite extensive studies especially within the last three decades, the precise molecular causes leading to AD have not been understood. Several competing mechanisms of actions have been proposed and (partially) evaluated in the clinic. This chapter will first review the scientific rationale which led to the drugs currently in clinical use for treatment of AD. Then, the amyloid hypothesis of AD will be introduced and discussed, also referring to findings from related clinical trials. Finally, based on this hypothesis, findings regarding ion channel-dependent synaptic pathophysiology will be reviewed.

1.1.3.1 The Cholinergic and Glutamate Hypotheses: Rationale for Current Drug Treatment

As of today, several competing hypotheses for mechanisms of action exist for AD; the first one was termed the cholinergic hypothesis and introduced by Bartus et al. (1982), who based this theory mainly on two sets of findings. On the one hand, the neurotransmitter acetylcholine plays an important role in learning and memory (Drachman and Leavitt, 1974). On the other hand, AD studies exhibited central nervous system (CNS) deficits in synthesis and release of acetylcholine, choline

uptake, and loss of cholinergic neurons from the nucleus basalis pointing towards a substantial cholinergic deficit in AD (Bowen et al., 1976; Davies and Maloney, 1976; Perry et al., 1977; Whitehouse et al., 1982). These changes were observed by post-mortem biopsy, correlated with the cognitive impairment of AD patients (Perry et al., 1978), and were found within a year of the onset of symptoms of dementia (Bowen et al., 1982), suggesting that the deficit might be causative for AD.

The therapeutic strategy of increasing acetylcholine levels in patients, through inhibition of acetylcholinesterase, has resulted in four of currently five approved drugs for the treatment of AD. However, cholinergic treatment is only considered to be symptomatic. In addition, the therapeutic benefit is limited as progression of AD is only postponed in a fraction of patients by several months after treatment of donepezil (Steele and Glazier, 1999). Although, there have been reports that positive long-term effects compared to placebo control are not detectable (Courtney et al., 2004; Petersen et al., 2005), meta-analyses by Lanctot et al. (2003) and Birks (2006) concluded that increasing cholinergic levels through acetylcholinesterase inhibitors lead to a significant therapeutic effect. Recently, EVP-6124 (EnVivo Pharmaceuticals), a novel $\alpha 7$ nicotinic acetylcholine receptor partial agonist (Prickaerts et al., 2012), has recently shown efficacy in a phase 2b trial for symptomatic treatment of AD (Hilt et al., 2012). It remains to be seen in a larger cohort, if this positive modulation of acetylcholine-mediated transmission may be superior compared to acetylcholinesterase inhibitors for the treatment of AD or whether cholinergic-dependent treatment can be additive.

Also, glutamatergic neurotransmission in the neocortex and hippocampus was found to be disrupted in AD patients (Maragos et al., 1987; Palmer and Gershon, 1990; Myhrer, 1998). In the hippocampus, glutamate levels as well as NMDA binding are decreased especially for pyramidal CA1 neurons (Greenamyre et al., 1987; Ulas et al., 1992). As glutamate is crucial for learning and memory (Bliss and Collingridge, 1993; Riedel et al., 2003), alterations in the glutamatergic system has also been implicated as a contributor to the clinical symptoms of AD. Glutamate may be a secondary cause of neuronal damage in AD via excitotoxicity, which appears to be primarily NMDA receptor-mediated (reviewed by Greenamyre and Young, 1989; Harkany et al., 2000). NMDA receptor activation was also found to stimulate A β

production, which in turn affects synaptic transmission (reviewed by Butterfield and Pocernich, 2003).

Several NMDA antagonists have failed in the clinic as neuroprotective agents for the treatment of AD due to side effects, including hallucinations, agitation, or anesthesia (Olney et al., 1991; Krystal et al., 1994). This was partly associated with high NMDA binding affinity also altering physiological channel function (Kornhuber and Weller, 1997). Memantine, an uncompetitive low to moderate affinity NMDA blocker, showed neuroprotective potential in preclinical AD models *in vivo* (Barnes et al., 1996; Danysz and Parsons, 2003) and *in vitro* (Nimmrich et al., 2010). In the clinic, memantine has shown modest effects in moderate-to-severe AD (Reisberg et al., 2003) and has exhibited no severe psychotomimetic adverse effects (Orgogozo et al., 1991; Winblad and Poritis, 1999). It was approved by regulatory authorities in Europe and the U.S. for the treatment of moderate to severe AD, respectively, and also exhibits beneficial effects in patients receiving donepezil (Tariot et al., 2004). Based on a recent meta-analysis by Schneider et al. (2011) there is no evidence that memantine is beneficial during earlier stages of AD and cognitive benefits during moderate AD are smaller than for acetylcholinesterase inhibitors.

Moreover, other therapeutic approaches are being pursued for AD. For example, block of the serotonin 5-HT₆ receptor enhances (e.g., cholinergic) neurotransmission (Upton et al., 2008; Rossé and Schaffhauser, 2010) and led to successful clinical phase 2 trials. For SB-742457 (GlaxoSmithKline) efficacy and tolerability was shown in mild-to-moderate AD patients (Maher-Edwards et al., 2010). Upon additive treatment with donepezil, this compound (Maher-Edwards et al., 2011) and the 5HT-6 antagonist Lu-AE58054 (Press release, Lundbeck, 2012) also slowed cognitive decline of moderate AD patients. Other approaches include antioxidants like vitamin E (Petersen et al., 2005; Galasko et al., 2012), anti-inflammatory drugs like ibuprofen (Tabet and Feldmand, 2003), and acetylsalicylic acid (Jaturapatporn et al., 2012), which however have not resulted into new drug approvals. For example, dimebon, an antihistamine drug used in Russia with several additional mechanisms of action including neuroprotective effects on mitochondria and block of multiple ion channels (Bachurin et al., 2001; Bachurin et al., 2003), revealed very promising potential in a phase 2 study (Doody et al., 2008). Unfortunately, dimebon failed to show efficacy in the subsequent phase 3 trial (Jones, 2010).

1.1.3.2 The Amyloid Hypothesis

Identification of the amino acid sequence of the main constituent of amyloid plaques by Glenner and Wong (1984) and Masters et al. (1985) set the stage for the amyloid hypothesis. It proposes that accumulation of A β constitutes the primary cause for AD pathology and suggests that tau pathology is a downstream event induced by an imbalance of A β production and clearance (Hardy and Allsop, 1991). In the following, the genetic evidence and results from animal models supporting this hypothesis are described. Subsequently, some clinical trials will briefly be summarized, which aimed at reducing A β plaque levels but have not so far resulted in any drug approval. Finally, converging evidence is presented, which suggests that AD pathology is only mediated by certain forms and epitopes of A β and not, as originally believed, by insoluble A β plaques - one hallmark of AD.

Table 1.1 Genetic factors predisposing to AD (adapted from Selkoe, 1996)

Gene defect	Age of AD onset	A β phenotype
APP	Early	↑ production of total A β or A β_{1-42} peptides
Apolipoprotein E4 polymorphism	Late	↑ density of A β plaques and vascular deposits
Presenilin-1	Early	↑ production of A β_{1-42} peptides
Presenilin-2	Early	↑ production of A β_{1-42} peptides

The A β hypothesis is strongly supported by genetic evidence (Table 1.1). As stated previously, AD is a predominately disease of the elderly, but there is also early-onset AD (before age 60 or 65), which makes up about 1-5% of all cases. Although only about 13% of these can be attributed to familiar forms in a dominant autosomal manner (Campion et al., 1999), these cases have been crucial in depicting pathogenic pathways of AD. Associated with early-onset are mutations in the genes encoding the amyloid precursor protein (APP), presenilin-1, and presenilin-2. A β generation occurs via cleavage of APP, an integral membrane protein involved in synaptogenesis (Wang et al., 2009), by the enzyme β -secretase and the protease complex γ -secretase. Mutations of the APP gene cause early onset AD (Chartier-Harlin et al., 1991; Goate et al., 1991; Murrell et al., 1991) and lead to overexpression of total A β levels (Citron et al., 1992) or an increase in the

A β_{42} -to-A β_{40} ratio (Suzuki et al., 1994). Mutations of the presenilin-1 and presenilin-2 genes increase the production of A β_{42} by altering APP metabolism via interaction with γ -secretase and their mutations (Scheuner et al., 1996; Citron et al., 1997; De Strooper et al., 1998; Wolfe et al., 1999). Furthermore, the E4 allele of apolipoprotein, a cholesterol transport protein capable of binding to A β (Strittmatter et al., 1993), confers a higher likelihood especially for late-onset (after 60 or 65 of age) of AD (Corder et al., 1993). Creation of several transgenic mice models, which in part resemble AD-like pathology, has further supported the significance of these genetic alterations (reviewed by McGowan et al., 2006).

It should be noted, however, that alterations of tau protein and A β levels in human cerebrospinal fluid (CSF) are not exclusively linked to AD, but also to other forms of dementia (Spillantini et al., 1998; Gloeckner et al., 2008). Moreover, it has not been unambiguously proven that A β induces tau pathology. For example, one conflicting finding is that tau pathology seems to correlate more closely with neuronal loss than A β plaques (Schmitz et al., 2004). However, experimental data from transgenic mice models of AD showed that clearance of A β also decreases levels of neurofibrillary tangles (Oddo et al., 2004), but not vice versa. In addition, application of A β in turn induced neurofibrillary tangles and thereby neuronal loss (Lewis et al., 2001). So it has been postulated that the pathological assembly of A β induces tau-related pathology and may lead to the development of AD (Oddo et al., 2006). Moreover, APP is located on chromosome 21 and patients with Down syndrome (trisomy 21) develop amyloid deposits and early onset AD until age 40 (Olson and Shaw, 1969; Glenner and Wong, 1984; Wisniewski et al., 1985; Teller et al., 1996; Lott and Head, 2005). This is supportive of the hypothesis by Hardy and Allsop (1991) that A β deposition may be major events and precede tau pathology in AD.

A β aggregation into insoluble plaques has long been associated with neurotoxicity (Lashuel et al., 2002). In turn, one therapeutic approach has been to lower the plaque load, which was supported by studies in APP-overexpressing transgenic mice (Schenk et al., 1999). However, this approach has not (yet) led to a successful drug approval. In 2002, active immunization with AN-1792 (Elan Pharmaceuticals) against A β in a phase 2b study successfully lowered A β plaque load. Unfortunately, the treated individuals still developed dementia as found in a follow-up study (Gilman et al., 2005; Holmes et al., 2008). Furthermore, this study had to be aborted due to the

severe side effect of meningitis in 6% of patients. Therefore, antibodies for passive immunization have been developed, which are less likely to induce an inflammatory response (McLaurin et al., 2002; Dodel et al., 2010). The follow-on project of AN-1792 is Bapineuzumab (also termed AAB-001 or ELN115727: Pfizer, Johnson & Johnson, and Elan) a monoclonal antibody, which was also designed to bind to and clear A β plaques in patients with mild to moderate AD. After promising results obtained in a 6 month long phase 2b study (ClinicalTrials.gov identifier NCT00663026, no significant effects were observed in the following 1.5 year long phase 3 studies on a total of 2,452 patients (NCT00574132, NCT00575055), leading to recent discontinuation of bapineuzumab (Press release Johnson&Johnson, 2012). Another monoclonal antibody directed against plaques, called Solanezumab (LY2062430, Lilly), has also failed its primary endpoints in a recent 1.5 year long phase 3 study on 2,050 patients with mild to moderate AD (Press release Lilly, 2012). However, significant effects of slowed cognitive decline were reported in a secondary subgroup analysis comprising only patients with mild AD. As a consequence, this implies that plaque load reduction may be efficacious only for mild AD. This in line with a hypothesis from Golde et al. (2011) trying to explain the observed failures in clinical development of candidate drugs for AD. This may be caused by the fact that candidates are optimized on preclinical models which represent prestages or milder forms of AD-like pathology compared to the enrolled patients with more advanced disease progression. Another promising drug candidate currently tested in multiple phase 3 studies is Gammagard (an immunoglobulin for intravenous administration, Baxter), containing antibodies extracted from human plasma which may lower A β plaque burden. A three year follow-up study on a previous, small scale phase 2 study revealed that AD patients, who have previously received the highest dose of gammagard, did not exhibit any progression of cognitive decline (Relkin et al., 2012).

In parallel to efforts to facilitate A β clearance, other drug candidates aimed at decreasing A β production. For example, semagacestat (LY450139, Eli Lilly), a γ -secretase and β -secretase inhibitor, proceeded into two clinical phase 3 studies. However, studies had to be aborted as this candidate actually worsened disease progression (press release Eli Lilly, 2010). Unfortunately, these negative results concerning facilitated cognitive decline were again observed in a phase 2 study with avagcestat (BMS-708136, Bristol-Myers Squibb), a γ -secretase inhibitor which is effective in lowering A β concentrations (Coric et al., 2012). Other trials have also

failed to show efficacy (Green et al., 2009). These results question the therapeutic benefit of γ - and β -secretase inhibitors for AD and suggest that lowering overall levels of A β might even be malignant. This would imply that, under certain circumstances, A β may actually support neuronal function. In fact, a dual mechanism of action of A β as neurotrophic and neurotoxic agent has been described (Yankner et al., 1990; Zou et al., 2002; Atwood et al., 2003).

Within the amyloid hypothesis, it has not been unambiguously elucidated which form, epitope, or accumulation of A β may lead to the cognitive decline. A β monomers assemble to form several soluble oligomeric, then fibrillar forms which gradually form insoluble plaques (Selkoe, 2002). At first functional deficits were primarily attributed to the insoluble A β plaques. However, there is now converging evidence that other forms or epitopes of soluble A β may to some extent or even predominantly affect neuronal function. This shift in paradigm was initially supported by findings which have shown that the severity of cognitive decline is only poorly correlated with plaque load, and some patients, who have many plaque deposits, show only mild cognitive impairment (Blennow et al., 1996). This was also observed in mouse models of AD. In the absence of A β plaques functional synaptic deficits (Hermann et al., 2009) and impairment of learning and memory were observed (Westerman et al., 2002) suggesting that soluble A β forms rather than plaques might be responsible for dementia (Hardy and Selkoe, 2002; Mattson, 2004; Haass and Selkoe, 2007; McDonald et al., 2010). This was supported by numerous studies showing that LTP is decreased and long-term depression facilitated by synthetic A β (Cullen et al., 1997; Barghorn et al., 2005) as well as A β derived from natural sources (Walsh et al., 2002; Klyubin et al., 2008; Shankar et al., 2008a) *in vitro* and *in vivo*. Both physiological parameters correlate with morphological alternations in spine density (Engert and Bonhoeffer, 1999; Matsuzaki et al., 2004; Zhou et al., 2004) and with deficits in learning and memory (Morris et al., 1986). In line with this, it was found that soluble A β was localized near synapses (Kokubo et al., 2005a; Noguchi et al., 2009) and may bind to neurons (Lacor et al., 2007). These findings studies suggest that alterations in synaptic transmission via soluble A β occur early in the disease progress causing synaptic decline, which finally leads to memory dysfunction. This refined amyloid hypothesis is supported by the fact that soluble A β and synapse loss is more strongly correlated with severity of dementia in AD compared to plaque load, neurofibrillary tangles, and cholinergic disturbances as reported by numerous studies

(DeKosky and Scheff, 1990; Masliah et al., 1990; Terry et al., 1991; DeKosky et al., 1996; Lue et al., 1999; McLean et al., 1999; Wang et al., 1999).

Of soluble A β forms, monomers do neither affect synaptic function *in vitro* (Nimmrich et al., 2008a) nor cognitive function *in vivo* (Cleary et al., 2005). Moreover, they are rather regarded as neurotrophic instead of neurotoxic (Zou et al., 2002; Atwood et al., 2003; Giuffrida et al., 2009). This may in part explain, why efforts aiming at lowering overall A β levels, e.g., through modulation of the γ -secretase complex, have so far failed to show efficacy in a phase 3 study (see p.11). Consequently, overall reduction of the A β level might not be therapeutically beneficial. As mentioned above, it is an ongoing matter of debate what the toxic species A β is. On the one hand, the size of aggregated A β oligomers may constitute its function, as toxic effects have been attributed e.g., to A β dimers (Walsh et al., 2002; Klyubin et al., 2008), trimers (Townsend et al., 2006), dodecamers (Lesne et al., 2006), and higher molecular weight aggregates (Noguchi et al., 2009). However, A β may also undergo conformational changes (Ono et al., 2009). Such changes can result into different aggregation pathways, one of them resulting in a stable A β ₁₋₄₂ globulomer epitope formed by a loop of the A β amino acids 20-31 (Yu et al., 2009b) which distinguishes this epitope from other A β monomers, oligomers, and fibrils (Gellermann et al., 2008) and induces synaptic deficits (Barghorn et al., 2005; Nimmrich et al., 2008a; Nimmrich et al., 2010). Therefore, current (preclinical) therapeutic approaches also include exclusive clearance of toxic A β epitopes via conformation-specific antibodies (Hillen et al., 2010).

1.1.3.3 Ion Channel-Related Synaptic Pathophysiology

Besides lowering A β levels, an alternative approach for future AD therapeutics based on the amyloid hypothesis would be to antagonize the effects of oligomeric A β on its (synaptic) targets. Numerous targets for A β have been proposed causing synaptic alterations. Here, findings about the interaction of different forms of A β with ion channels, located in the plasma membrane are being described. Finally, a stable oligomeric A β preparation is introduced, which appears to be pathogenically relevant and well suited for studying the effects of oligomeric A β on ion channels and functional synaptic decline.

In recent years it has become apparent that oligomeric forms of A β rather than monomeric or fibrillar forms are causal to synaptic failure (Walsh and Selkoe, 2007). For example, synaptic spine densities decrease after prolonged exposure to toxic A β (Lacor et al., 2007). Moreover, oligomeric A β inhibits hippocampal LTP *in vitro* (Lambert et al., 1998; Barghorn et al., 2005; Townsend et al., 2006) and *in vivo* (Walsh et al., 2002). Recently, it has been shown that A β dimers, obtained from cerebrospinal fluid samples of AD patients, inhibit LTP, enhance long-term depression, and reduce dendritic spine density in the hippocampus of normal rodents (Klyubin et al., 2008; Shankar et al., 2008b). In addition, A β correlates with impairment of learning and memory in APP rodent models (Ashe, 2001; Cleary et al., 2005). Yet, the precise mechanism of action is still being discussed.

Among others, some ion channels are currently being proposed as synaptic targets. APP overexpression in slice cultures, which will also result in elevated A β levels, exerts both presynaptic and postsynaptic effects. Impaired vesicle recycling and silencing of amino-3-hydroxy-5-methyl-4-isoxazol-propionacid (AMPA) currents were found in cultured hippocampal neurons by Ting et al. (2007). Snyder et al. (2005) have found an A β -induced depression of NMDA currents in cortical neurons, which was attributed to facilitated endocytosis of the receptor *in vitro*. A β -induced deficits in LTP *in vivo* were also described as being NMDA-dependent (Kim et al., 2001).

A number of recent studies report disturbances of the presynaptic neurotransmitter release machinery by oligomeric A β . This is supported by the finding that APP is transported to presynaptic terminals, in the hippocampus of transgenic mice, where it is subsequently cleaved to A β (Lazarov et al., 2002). Furthermore, oligomeric A β co-localizes to axon terminals in AD patients (Kokubo et al., 2005b; Ishibashi et al., 2006; Noguchi et al., 2009). Kelly et al. (2005) reported that A β oligomers decrease dynamin 1 levels, which play a crucial part in endocytosis of synaptic vesicles, possibly caused by cleavage of the protein by calpain. This may lead to a depletion of the readily releasable vesicle pool, which is mediated by a downregulation of the dynamin 1 gene or (presynaptic) NMDA-receptors (Kelly and Ferreira, 2007; Shankar et al., 2007; Abramov et al., 2009), possibly leading to the fatal consequences in AD.

Furthermore, disturbed neuronal intracellular (free) calcium levels were observed in models of aging and AD (Disterhoft et al., 1994). A β was found to alter calcium homeostasis *in vitro* (Mattson et al., 1992) and changes in calcium-dependent

enzymes were reported in AD patients (Green et al., 2007). Intracellular calcium overload may be caused by several mechanisms (Yu et al., 2009a), one of them being interaction of soluble A β with presynaptic voltage-gated calcium channels (reviewed by Nimrich and Ebert, 2009; Demuro et al., 2010). As introduced later, these channels play a crucial role in intracellular calcium influx, vesicle release, and presynaptic plasticity (reviewed by Catterall and Few, 2008).

Modification of all types of high voltage-activated (HVA) calcium channels by A β has been described in several studies, also producing conflicting results. Some studies investigated chronic effects of A β in rat cortical neurons. MacManus et al. (2000) and Ramsden et al. (2002) described an increase in HVA calcium channel currents by full length A β_{1-40} which was most likely mediated via N-type and P/Q-type calcium channels. By contrast, Ueda et al. (1997) chronically applied truncated A β_{25-35} and found decreased cell viability which could be attenuated by nimodipine, an unselective L-type calcium channel blocker, but not by specific N-type or P/Q-type calcium channel blockers. Moreover, after chronic exposure to A β_{25-35} they also found an increase in calcium currents which was also insensitive to specific N-type or P/Q-type calcium channel blockers, but could be attenuated by nimodipine. This finding was recently confirmed by Kim and Rhim (2011) who also recorded a current increase from recombinant L-type calcium channels in HEK293 cells after acute treatment with A β_{25-35} . The conflicting results that A β affects different channels may be caused by the use of different preparations. Rovira et al. (2002) found that both A β_{25-35} and A β_{1-40} increased calcium currents in acute hippocampal slices, however the former preparation via L-type whereas the latter via non-L-type calcium channels. Which A β form is most relevant for the pathophysiology of AD has not been elucidated. The relevance of truncated A β_{25-35} for the pathogenesis of AD has been suggested by the fact that this form has been found *in vivo* (Kaneko et al., 2001) and exerts multiple toxic effects *in vitro* as reviewed by Millucci et al. (2010). Whereas full length A β_{1-40} and A β_{1-42} is most abundantly found in AD patients and the alteration of the A β_{1-42} -to-A β_{1-40} ratio is associated with early onset AD (Suzuki et al., 1994; Duff et al., 1996; Scheuner et al., 1996), which strongly suggests the involvement of full length A β in the pathophysiology of AD.

Because A β spontaneously forms aggregates, it needs to be emphasized that the studies cited above used poorly defined A β species for studying functional effects.

The well known rapid aging of A β preparations can influence their biological function: fresh and aged (aggregated) A β_{1-40} can exert opposite effects by increasing (N-type and P/Q-type) and decreasing (only N-type) calcium channel currents, respectively (Ramsden et al., 2002). Similarly, the effects of A β_{1-42} can vary depending on the aggregation and oligomerization status (Innocent et al., 2010). A β species in more sophisticated preparations of A β_{1-42} , like amyloid-derived diffusible ligands, are also poorly defined (Lambert et al., 1998; Hepler et al., 2006). Despite this shortcoming, such preparations have proved useful in identification of the pathological nature of oligomeric A β (Lacor et al., 2007). As of today, many different oligomeric forms of A β have been discovered. A comprehensive overview from Benilova et al. (2012) illustrates that numerous oligomers were found in AD patients, extracted from natural sources and synthetically prepared. To further add to this complexity, polymerization of A β is complex and may occur via metastable intermediates (Lee et al., 2011). Therefore, many oligomeric A β forms are metastable in aqueous solution (Figure 1.1) and may exert different biological effects.

For the purpose of studying the characteristics of pathological A β oligomers in a controlled and reproducible manner, stable and well-defined oligomer preparations were created including A β globulomer, which is formed from synthetic A β_{1-42} (Barghorn et al., 2005). This study showed that A β globulomer predominantly consists of 12-mer A β_{1-42} oligomers. Stability of this preparation was attributed to a conformational switch leading to an A β peptide epitope with a distinct aggregation pathway, independent of the pathway forming fibrils (Gellermann et al., 2008; see upper left corner of Figure 1.1). The fact that A β globulomer inhibits LTP in acute hippocampal slices and that A β globulomer epitopes are found in AD patients as well as in APP overexpressing mouse models, support the pathological relevance of this preparation for AD (Barghorn et al., 2005). It has to be noted that several A β forms have been detected *ex vivo* (Shankar et al., 2008a; Noguchi et al., 2009) and it appears likely that there are several pathologically relevant oligomeric A β species which induce different toxic effects as suggested by findings on different synthetic preparations (reviewed by Benilova et al., 2012). Furthermore, the neurotoxic properties of A β might depend on the mixtures with other A β species (Kuperstein et al., 2010). Keeping these considerations/limitations in mind, we focused on investigating the effects of A β globulomer in order to further elucidate molecular mechanisms of a stable, oligomeric, and non-fibrillar A β preparation.

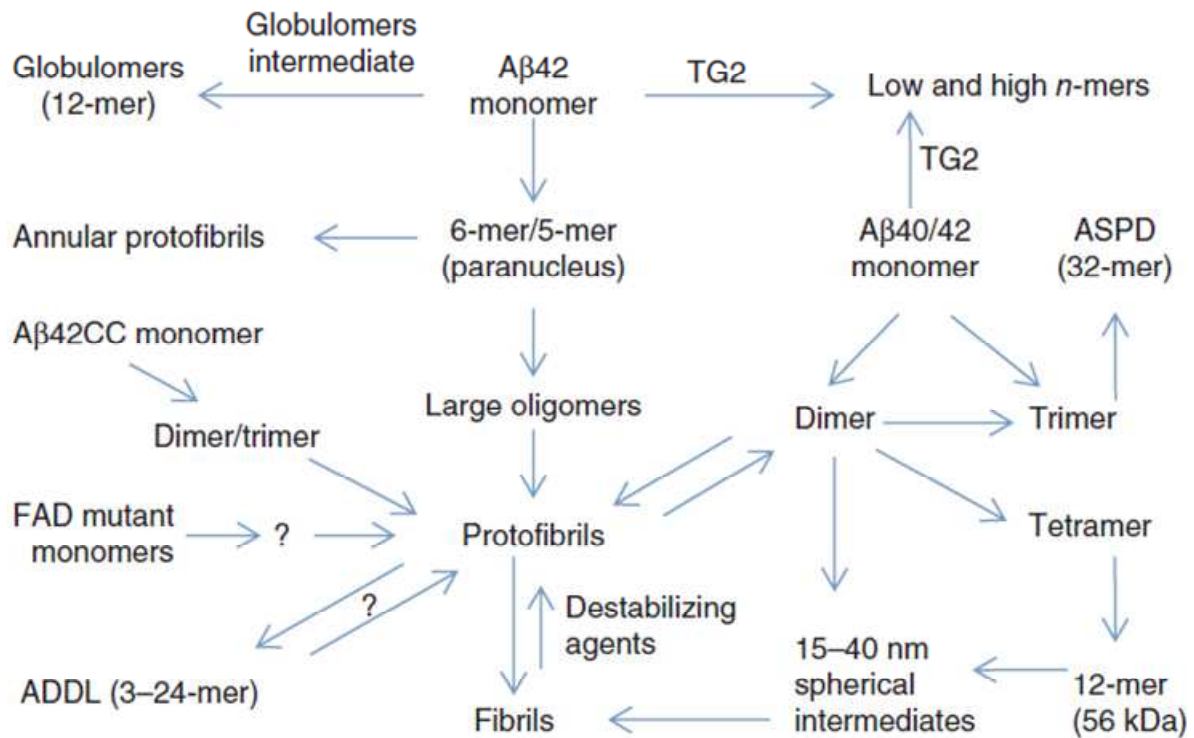


Figure 1.1 Scheme of different natural and synthetic A β assemblies (from Benilova et al., 2012). A β monomers, oligomers, and fibrils exist in a complex equilibrium, sensitive to numerous external factors. Coexistence of several oligomeric populations that do or do not propagate into fibrils is possible. Despite the differences in structure, stability, and concentration, all oligomers may contribute to A β toxicity. ADDL: A β -derived diffusible ligands; ASPD: amylospheroids; TG2: Transglutaminase 2.

A β globulomer was described to affect the frequency of postsynaptic currents in primary hippocampal cell cultures pointing towards a presynaptic target (Nimmrich et al., 2008a). This probably led to a decrease in presynaptic vesicle release, which was found to be caused by a decrease in P/Q-type calcium channel currents *in vitro*. These effects could be reversed by R-roscovitine, a P/Q-type calcium current modulator. In a direct approach of recombinantly expressed P/Q-type calcium currents in *Xenopus* oocytes Mezler et al. (2012a) showed that the α_{1A} subunit of the channel was specifically modulated by A β globulomer leading to an increased calcium influx. It was speculated that this increase might cause excitotoxic synaptic degeneration. The reason for the bidirectional modulation of P/Q-type calcium channels by A β globulomer has not been resolved but might be caused by several factors (and will also be addressed in the discussion). For example, Koch et al. (2004) showed that a peptidic potassium channel blocker can enhance or reduce the potassium current depending on the channel state. Concentration and

state-dependent bidirectional effects have also been observed for R-roscovitine (Buraei and Elmslie, 2008). EVP-6124, a $\alpha 7$ nicotinic acetylcholine modulator and, as described previously, a clinical candidate for the treatment of AD showed concentration-dependent bidirectional effects probably due to a partial agonistic mechanism (Prickaerts et al., 2012). Moreover, the L-type calcium channel agonist Bay K 8644 can also inhibit cardiac calcium channels, which depends on the surrounding voltage (Kass, 1987; Schreibmayer et al., 1992). This indicates that subtle differences in the interaction of a compound with a channel can lead to different functional effects. Therefore, differences between expression systems might explain the bidirectional results from the A β globulomer studies. In fact, A β oligomers have been described to increase and decrease the frequency of postsynaptic currents (Shankar et al., 2007; Abramov et al., 2009), which may be a downstream effect of P/Q-type calcium channel modulation. Furthermore, A β can both increase and decrease LTP (Puzzo et al., 2008).

To conclude, the mechanism of action of oligomeric A β has not yet been completely elucidated partially because many studies used poorly defined preparations (see above). So in this PhD work we tested the effect of a stable A β oligomer preparation on presynaptic calcium channels. In addition to recent findings obtained in *Xenopus* oocytes (Mezler et al., 2012a) and rat primary hippocampal cell cultures (Nimmrich et al., 2008a), we here study the effect of oligomeric A β on recombinant P/Q-type and N-type calcium channels in a human cell line. Moreover, possible state-dependent effects of A β oligomers are being investigated. On a systemic level, we also assessed whether block of P/Q-type, N-type, or L-type calcium channels bears therapeutic potential by preventing functional deficits in an *in vitro* model of A β oligomer-induced synaptic degeneration described in Nimmrich et al. (2010).

1.2 High Voltage-Activated Calcium Channels

This chapter covers theoretical considerations, which might support successful drug development of compounds influencing high voltage-gated calcium channels. First, a brief introduction into the basic properties of the voltage-gated calcium channel family including channel structure, physiological function, and pharmacological properties is provided. Second, the terminology of ion channel states and transitions is listed.

Third, a comprehensive overview is given regarding the mechanisms and kinetics of inactivation in HVA calcium channels. Last, the principle of state-dependence is introduced, as a drug property which probably increases its tolerability in humans, referencing to experimental findings, properties of clinically used substances, and current drug development efforts.

1.2.1 Structure and Pharmacological Characterization

In this subchapter voltage-gated calcium channel structure, ion selectivity, subtype classification and nomenclature, pharmacology, localization, and function is introduced according to Catterall et al. (2005) and (in part) illustrated in Figure 1.2 (p.21).

As determined by studies using channel mutations, ion selectivity in calcium channels is obtained through a selectivity filter of a cluster of four glutamate residues (Yang et al., 1993), which are thought to project into the pore to sort calcium from other ions. The relative permeability sequence has experimentally been determined as calcium > barium > lithium > sodium > potassium > caesium (Hess et al., 1986). As calcium is favored over sodium by a factor of 1000, the calcium current is hardly affected by the extracellular sodium concentration (Polo-Parada and Korn, 1997). In many electrophysiological settings calcium is replaced by barium as a charge carrier, which diminishes (secondary) calcium-dependent effects and therefore unmasks voltage-dependent effects.

Electrophysiological recordings identified voltage-activated calcium currents with distinct characteristics. Depending on the voltage necessary for channel opening, major categorization was carried out into low-voltage and HVA channels. The former comprises T-type calcium currents (also denoted as the $Ca_v3.x$ family), which mediate cardiac pacemaker activity (Satoh, 2003) and thalamic oscillations (Perez-Reyes, 2003) and may be important drug targets for epilepsy and neuropathic pain (Nelson et al., 2006). However, these channels have received little attention as a potential treatment strategy for AD. In part, this is due to the fact that interaction of A β or tau with these channels has not been reported. In addition, *in vitro* data suggests that long-term neuroprotection is rather mediated via HVA (L-type) than T-type calcium channels (Wildburger et al., 2009). HVA channels activate at strongly

depolarized membrane potentials and are multi-subunit complexes. The channels have been further subdivided depending on pore forming subunit, channel kinetics, pharmacology, and cellular distribution (Tsien et al., 1991) yielding L-type, N-type, P/Q-type and R-type calcium channels.

Unlike all other calcium channels, L-type calcium channels (also denoted as the $Ca_v1.x$ family) are modulated by the agonist (-)-Bay K 8644. In addition, they are sensitive to dihydropyridines (e.g., nimodipine), phenylalkamines (verapamil), and benzothiazapines (diltiazem). However, these blockers can also act on other HVA calcium channels (Diochot et al., 1995; Ishibashi et al., 1995; Hockerman et al., 2000). L-type calcium channels are expressed in all excitable and many types of non-excitable cells and are predominately located on cell bodies and proximal dendrites in neuronal cells (Hell et al., 1993). Channels were also found to interact with intracellular calcium stores (Dolmetsch et al., 2001; Thibault et al., 2007) and may regulate gene expression (Murphy et al., 1991). Upon prolonged membrane depolarization, channel inactivation is mostly calcium (Imredy, 1994) and to a lesser extent voltage-dependent (Tsien et al., 1991).

By contrast, most N-type calcium channels ($Ca_v2.2$) display significant voltage-dependent inactivation (Nowycky et al., 1985). They are less sensitive to dihydropyridines, but are inhibited by the peptidic blockers ω -conotoxin extracted from predatory marine snails (Olivera et al., 1987). These channels seem to be exclusively expressed in neuronal tissue (Plummer et al., 1989), cluster at synaptic areas (Jones et al., 1989), are involved in neurotransmitter release (Dutar et al., 1989), and are physically associated with proteins of the release machinery (Leveque et al., 1994; Sheng et al., 1994). However, especially for many synapses in the CNS, neurotransmitter release is not primarily controlled by this channel type (Luebke et al., 1993; Potier et al., 1993).

Neurotransmitter release is also mediated via P/Q-type calcium channels ($Ca_v2.1$), especially in the CNS (Mori et al., 1991; Luebke et al., 1993; Stea et al., 1994). These channels are less sensitive to dihydropyridines and some ω -conotoxins, but are specifically blocked by the funnel web spider toxin ω -agatoxin IVA and ω -agatoxin TK, also termed ω -agatoxin IVB (Adams et al., 1993; Teramoto et al., 1993; Olivera et al., 1994). Initially, P-type and Q-type currents were distinguished due to their different pharmacological affinity to ω -agatoxin-IVA and

electrophysiological properties. However, differences are most likely caused by different splice variants of the pore forming subunit and different complements of auxiliary subunits (Bourinet et al., 1999; Soong et al., 2002).

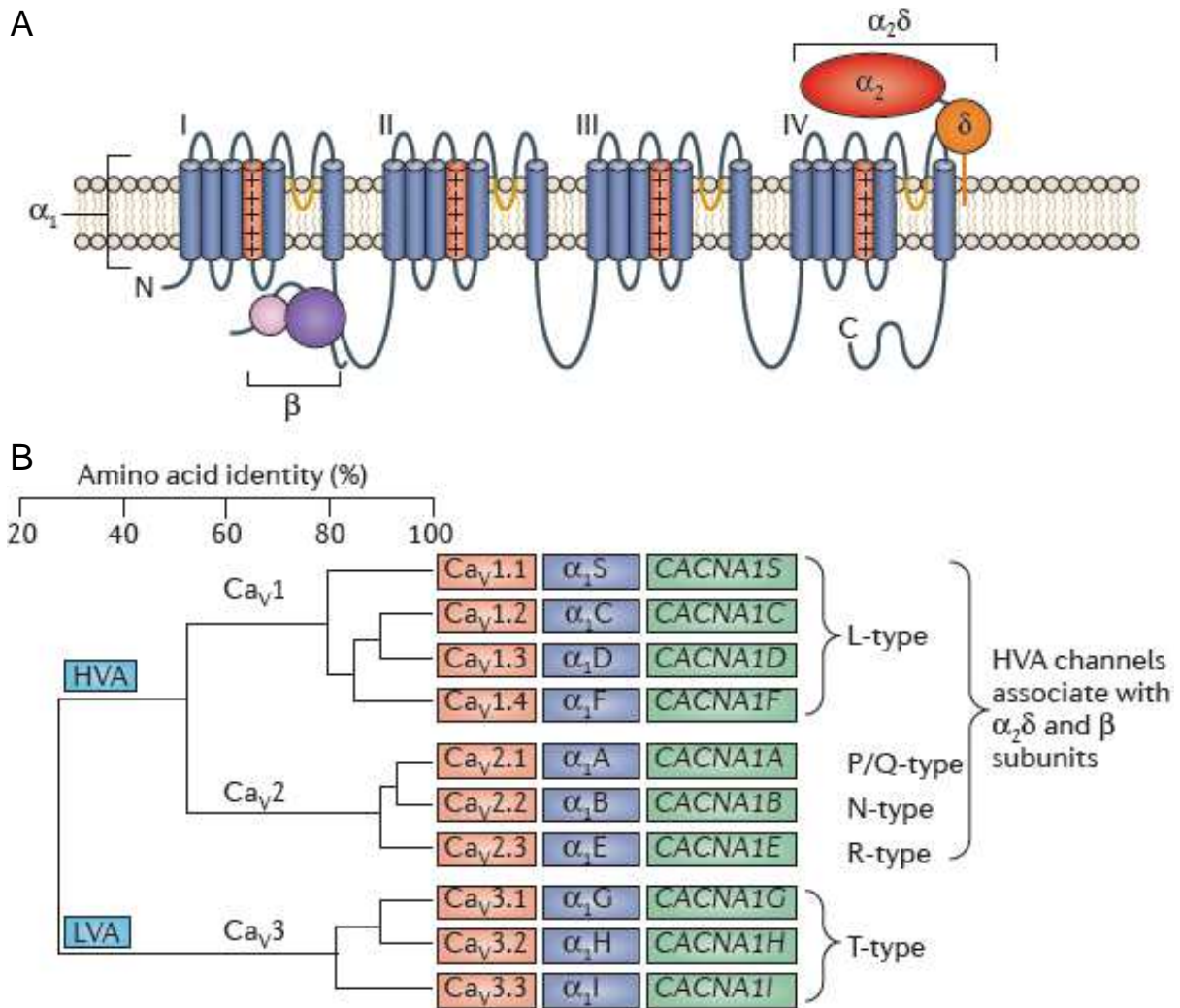


Figure 1.2 Voltage-gated calcium channels (from Dolphin, 2012). (A) Voltage-gated calcium channel α₁ subunits have 24 transmembrane α-helices, organized into four homologous repeats (I–IV). The fourth transmembrane segment S4 of each repeat (red) has approximately five positively charged amino acids and, together with S1, S2, and S3, comprises the voltage-sensing domain of the channel. Yellow segments represent the pore loops. β subunits consist of an Src homology (SH3) domain (pink circle) and a guanylate kinase domain (purple circle), which binds to the intracellular linker between domains I and II of the α₁ subunit. The α₂δ subunit consists of α₂ (red) disulphide-bonded to the δ subunit (orange). The site(s) of interaction between the α₁ subunit and the α₂δ subunit is poorly understood. (B) Dendrogram based on an alignment of the membrane-spanning regions and pore loops of the α₁ subunits. Ca_v1 and Ca_v2 comprise the HVA and Ca_v3 the low-voltage-activated (LVA) channels. Original names (blue), Ca_v nomenclature (red) and gene names (green) of the α₁ subunits are given.

Even after application of dihydropyridines, ω -conotoxins, and ω -agatoxins a small residual HVA R-type calcium current ($\text{Ca}_v2.3$) remains (Zhang et al., 1993). Of the all HVA calcium currents the R-type has been least studied. Results from transgenic mice suggest that rather a family of channels than a single channel mediates this current (Wilson et al., 2000). Dietrich et al. (2003) reported that R-type calcium currents contribute to LTP induction in hippocampal mossy fibers but not to basal transmission or short-term plasticity, which suggests that these channels are remotely localized from the release machinery.

HVA calcium channels are associated with the auxiliary β , $\alpha_2\delta$ (see Figure 1.2, p.21), and in some cases the γ subunit which modulate channel function. The β subunit (reviewed by Buraei and Yang, 2010) enhances expression of the HVA pore forming α_1 subunits by promoting channel insertion into the membrane. The β subunit lacks transmembrane segments and binds to the intracellular I-II loop of the α_1 protein. Four different β subunits have been described, which are encoded by distinct genes. Due to alternative splicing in total 15 different β subunit forms have been described; the β_{1b} subunit was studied in this PhD thesis. β subunits also shift voltage-dependence of activation and inactivation as well as channel kinetics (reviewed by Buraei and Yang, 2010). For example, the rate of voltage-dependent inactivation is increased for β_1 and β_3 , whereas it is often decreased for the β_2 subunit.

Moreover, there are four different $\alpha_2\delta$ extracellularly located subunits, named $\alpha_2\delta_1$ (which was studied in this PhD work), $\alpha_2\delta_2$, $\alpha_2\delta_3$, and $\alpha_2\delta_4$. (reviewed by Dolphin, 2012). They consist out of two disulfide-linked proteins and might be anchored to the membrane by a glycosylphosphatidylinositol anchor (Davies et al., 2010). Recent studies by (Kadurin et al., 2012), however, suggest that this anchor is not indispensable for the function of $\alpha_2\delta$. The main role of this subunit is to increase calcium currents by promoting trafficking of α_1 to the plasma membrane and increasing its turnover time but can also modulate channel function depending on the type of the co-expressed α_1 subunit. Moreover, $\alpha_2\delta$ subunits modulate presynaptic function by increasing the density of synaptic voltage-gated calcium channels and the neurotransmitter release probability (Hoppa et al., 2012). In line with this, the drugs gabapentin and pregabalin, used as antiepileptic agents, are supposed to interact with $\alpha_2\delta$ thereby reducing vesicle release and neuronal excitability (Fink et al., 2002; Taylor et al., 2007; Bauer et al., 2009).

In addition, eight different γ subunit genes have been identified. They often induce a slight hyperpolarizing and depolarizing effect of the voltage-dependence of inactivation and activation, respectively, thereby reducing calcium currents to some extent (Buraei and Yang, 2010). However, unlike the other subunits, the γ subunit is not co-expressed in all calcium channel complexes (especially in the CNS), predominantly associated with L-type calcium channels (Yang et al., 2011), and involved in other functions like regulation of trafficking, localization, and biophysical properties of other ionotropic glutamate receptors (reviewed by Milstein and Nicoll, 2008).

1.2.2 Terminology of Channel States and Transitions

Characterization of e.g., inactivation kinetics is one prerequisite for the development of state-dependent HVA calcium channel blockers. Here, the nomenclature used to characterize transitions of channel states, like inactivation induced by conformational switches (Stotz et al., 2000; Bezanilla, 2002), is being briefly introduced.

Ion channels can exist in an open (conducting) state or in non-conducting closed or inactivated states. The difference between the non-conducting closed and inactivated states is that for the latter the channel is unresponsive to an activating stimulus, comparable to the reduced response of a desensitized receptor. The transition from closed to open is denoted as activation, open to closed is called deactivation, open or closed to inactivated is called open and closed-state inactivation, respectively, and inactivated to open or closed is called recovery from inactivation (Figure 1.3).

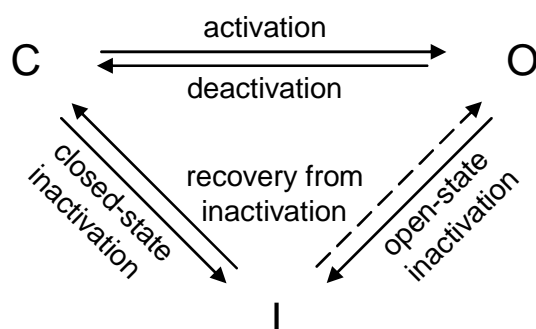


Figure 1.3 Nomenclature of channel state transitions. HVA calcium channels can be present in the non-conducting closed (C) and inactivated (I) states or in the conducting open (O) state. Kinetics of each state transition depend on the surrounding membrane potential. For P/Q-type and N-type calcium channels recovery from inactivation occurs more rapidly to closed (solid lines) than to open (dotted lines) states.

Ion channels can exist in an open (conducting) state or in non-conducting closed or inactivated states. The difference between the non-conducting closed and inactivated states is that for the latter the channel is unresponsive to an activating stimulus, comparable to the reduced response of a desensitized receptor. The transition from closed to open is denoted as activation, open to closed is called deactivation, open or closed to inactivated is called open and closed-state inactivation, respectively, and inactivated to open or closed is called recovery from inactivation (Figure 1.3).

For a subgroup of calcium channels, denoted as voltage-dependent, the probability of being in a certain state depends on the voltage across the cell membrane. At the neuronal resting potential, the HVA calcium channels are mostly present in a closed state. The likelihood for activation increases upon membrane depolarization like action potential arrival. At the same time the probability of channel inactivation increases, which either causes an active decrease in ion conductivity (by open-state inactivation) or a decreased availability for subsequent channel opening (by closed-state inactivation; Patil et al., 1998). For prolonged membrane depolarizations only residual P/Q-type and N-type calcium channel currents, if at all, can be detected (Hans et al., 1999). This implies that under depolarized conditions recovery from inactivation is much slower than inactivation. Thus, for P/Q-type and N-type calcium channels recovery from inactivated states predominantly occurs to closed states during hyperpolarized potentials.

1.2.3 Function and Mechanisms of Inactivation

An effective state-dependent screening protocol should induce stable inactivation. Moreover, as certain pathologies may induce inactivation in different ways as mentioned in the discussion, it might be beneficial for screening protocols to (some extent) mimic the disease-like state of interest. To achieve this, thorough understanding of physiological HVA calcium channel inactivation is a prerequisite. Thus, a comprehensive overview is provided regarding the function, mechanisms, and kinetics of inactivation in HVA calcium channels.

As calcium channel activation occurs at a significantly faster rate than inactivation, membrane depolarization induces channel opening, thereby increasing intracellular calcium concentration. Calcium acts, for example, as a cytoplasmic messenger

activating signaling pathways leading to gene transcription (Dolmetsch et al., 2001) or by triggering neurotransmitter release (Wheeler et al., 1994; Sutton et al., 1999). At the same time calcium channel inactivation prevents prolonged and excessive rise in intracellular calcium concentrations, which may otherwise lead to detrimental cytotoxic effects like apoptosis (Choi, 1988; Orrenius et al., 1989; Cerella et al., 2010). As a functional example, inactivation may contribute to the short-term depression of neurosecretion (Branchaw et al., 1997; Forsythe et al., 1998). Some naturally occurring mutations of the P/Q-type calcium channel were found in humans that modulate its inactivation properties, potentially contributing to respective clinical symptoms such as migraine and ataxia (Matsuyama et al., 1999; Kraus et al., 2000; Wappl et al., 2002). Inappropriate calcium channel inactivation may thus lead to CNS malfunction.

Channel inactivation can be both calcium and voltage-dependent. Calcium dependent modulation is most strongly observed for L-type calcium channels (Peterson et al., 1999; Zuhlke et al., 1999), but is also present for presynaptic P/Q-type calcium channels (Lee et al., 1999). It is induced by a local rise in intracellular calcium concentration and is mediated by the calcium-sensing protein calmodulin which binds directly to multiple sequences of the α_1 calcium channel subunit. This may induce conformational changes of the channel, which modify the probability of the channel to be in a conducting or non-conducting state. Calcium dependent inactivation and facilitation occurs within several milliseconds, and is thereby able to contribute to synaptic short-term plasticity (Forsythe et al., 1998). For presynaptic P/Q-type calcium channels, calcium-dependent modulation is absent if barium replaces calcium as a charge carrier or after intracellular application of BAPTA, a fast calcium chelator (Borst and Sakmann, 1998; Cuttle et al., 1998). This type of inactivation is also less pronounced with coexpression of the β_{1b} subunit, used in this PhD study, than for other β subunits (Lee et al., 2000). Due to its mechanism of action, calcium-dependent inactivation mostly induces open-state rather than closed-state inactivation, which can take place without previous calcium influx.

By contrast, voltage-dependent inactivation can also occur during depolarizations which are sub-threshold to channel opening (Patil et al., 1998). The onset of this type of inactivation can happen at a fast rate (in the range of ms to few s) and at a slow

rate (several s to min). Similar to the ball and chain model applicable to sodium and potassium channels (Armstrong and Bezanilla, 1973; Hoshi et al., 1990), fast voltage-dependent inactivation of calcium channels is induced by an intracellular residue plunging the pore of the channel, which was denoted as a hinged lid mechanism (Figure 1.4; Stotz et al., 2000).

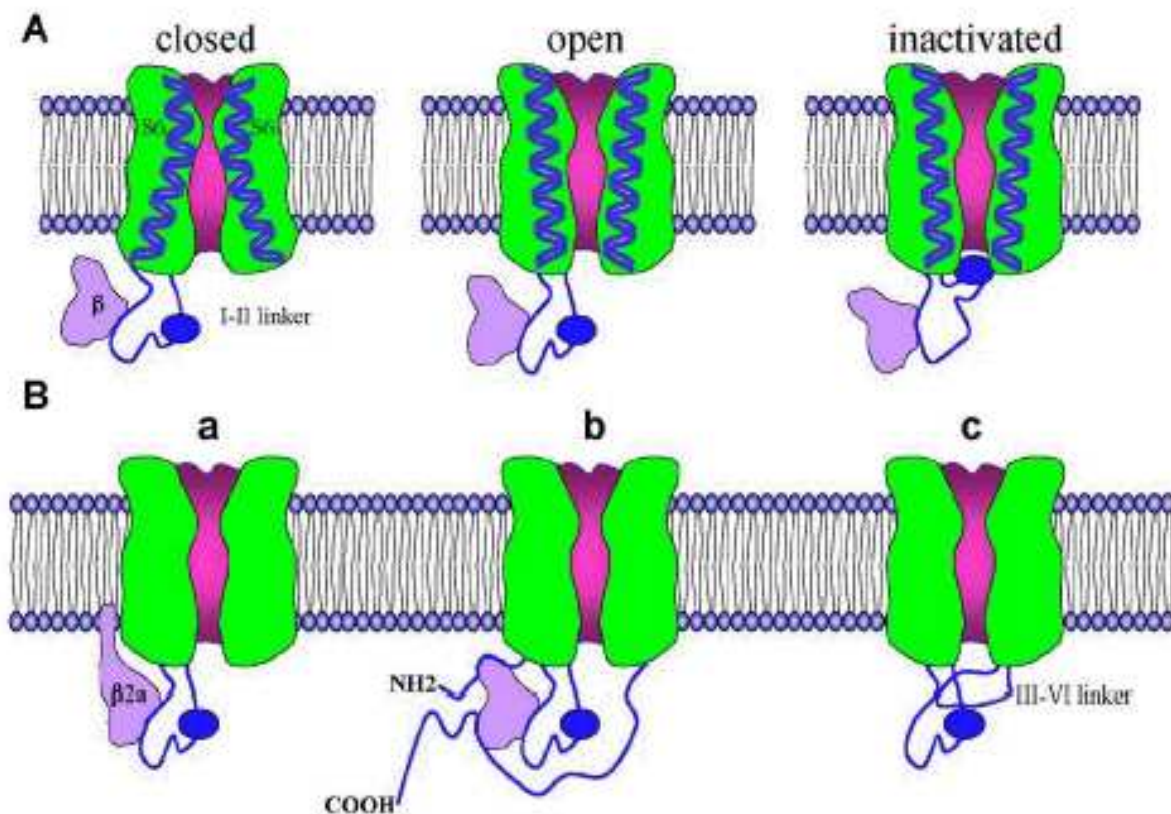


Figure 1.4 Hinged-lid model of fast voltage-dependent inactivation of HVA calcium channels (from Zamponi, 2005). (A) Possible model for calcium channel inactivation, which involves occlusion of the channel pore from the intracellular side by parts of the domain I-II linker of the α subunit. (B) Inhibition of inactivation was found to be mediated by: (a) the β_{2a} subunit; (b) interaction of β subunits with the N-terminus and/or C-terminus indirectly affecting the I-II linker function; (c) In the absence of β subunits, interactions between the I-II and II-IV linker.

Unlike for sodium and potassium channels, the mechanism of fast inactivation for calcium channels is hypothesized to underlie the intracellular domain I-II linker interacting with the S6 transmembrane regions (Stotz and Zamponi, 2001) thereby blocking ion permeability. This interaction can be modulated by other α_1 cytoplasmic loops. For example, intramolecular interaction of the domain III-IV linker with the domain I-II linker was found to slow down inactivation (Geib et al., 2002). In addition,

fast inactivation is also strongly modulated by the auxiliary subunits, especially the β subunit (Varadi et al., 1991). For example, the β_{1b} subunit, which was investigated in this PhD work, tends to increase the rate of inactivation (Isom et al., 1994; Qin et al., 1998). Mechanistically, β subunits may interact with the N-terminus or C-terminus of the α_1 subunit, which in turn may influence the inactivation inducing domain I-II linker (Soldatov, 1998; Stephens et al., 2000; Sandoz et al., 2001). The $\alpha_2\delta$ subunits may also regulate inactivation (Klugbauer et al., 1999; Davies et al., 2007). When coexpressed with the β_{1b} subunit, as in this PhD study, $\alpha_2\delta_1$ was found to significantly facilitate inactivation N-type calcium channel currents in *Xenopus Oocytes* (Canti et al., 2000).

In contrast to fast voltage-dependent inactivation, slow inactivation has been described and understood in much less detail. A couple of studies have described the slow inactivation kinetics in detail. Mostly the inactivation of channels containing the β_2 subunit is dominated by slow kinetics, but also channels with other β isoforms undergo slow inactivation. For example, in a study in *Xenopus oocytes* by Sokolov et al. (2000), on-rates of slow inactivation were calculated to be about a minute, but also depended on the auxiliary β subunit. By contrast, recovery from slow inactivation seemed to be independent of the length of the conditioning prepulse and the β subunit. However, the rate of recovery is slowed for more depolarized membrane holding potentials and inactivation was fully reversible at a holding potential of -80 mV or below, but not at -60 mV. Due to further point mutation studies, this report also suggested that slow inactivation can occur from both open and fast inactivated states (the relation to closed-state inactivation was not elucidated). A complete mechanism of action for slow inactivation has not yet been proposed, but might be similar to the ones of fast inactivation, since also for the slow inactivation point mutations within the cytoplasmic end of the S6 transmembrane regions can selectively abolish slow inactivation of L-type calcium channels (Shi and Soldatov, 2002). Moreover, this study found that inhibition of one type of inactivation facilitates the other type, so fast and slow inactivation might actually be linked.

Functionally, slow inactivation may have implications for synaptic short-term plasticity. For example, after strong physiological channel activation (after trains of action potentials) or pathological membrane depolarization including hypoxic or

ischemic events (Kristian and Siesjö, 1998), more channels are driven into this type of slowly recovering inactivation thereby preventing calcium overload.

The membrane potential in neurons is most of the time too low for opening of HVA calcium channels. Hence, especially for these channels closed-state inactivation that regulates the availability of channels upon action potential arrival might be an important mechanism modulating synaptic transmission. In addition, since voltage-dependent channel inactivation, unlike calcium-dependent inactivation, can induce both open- as well as closed-state inactivation, it is currently perceived as the more relevant type of inactivation within drug development targeting calcium channels in the CNS (Winqvist et al., 2005).

1.3 Drug Discovery Targeting Ion Channels

In the following, the general potential as well as possible pitfalls of ion channels as potential drug targets are being briefly described. Subsequently, current technical advances in patch clamp technology are presented which may overcome a key technical bottleneck in rational drug discovery associated with the limited throughput of manual electrophysiology. Thereafter, the potential of state-dependent target modulation to induce functional selectivity (Urban et al., 2007; Kaczorowski et al., 2008) and to increase the tolerability of future drugs is discussed and exemplified by current N-type calcium channel drug development efforts. In the last subsection, the involvement of P/Q-type calcium channels in other diseases beyond their role for AD (see section 1.1.3.3 p. 13ff), is shortly reviewed along with unselective P/Q-type modulators, which are already in clinical use. Finally, an outlook is given how (more) selective and state-dependent P/Q-type calcium channel modulators might be identified.

1.3.1 Ion Channels as Drug Targets

Only about 22% of proteins in the human genome are located on the cell surface, but they make up 60% of the current drug targets (Overington et al., 2006). Many ion channels are located in the plasma membrane and are typically complex, multimeric, transmembrane proteins that consist of separate pore-forming and accessory

subunits (Ashcroft, 2006). They allow passive ion passage along the electrochemical gradient across cell membranes and exhibit a high degree of structural diversity. They comprise only around 1.3% of the human genome (Venter et al., 2001), but constitute about 13.9% of all drugs approved by regulatory authorities in the US being the second-most frequent targeted gene-family group after G-protein coupled receptors indicating that these channels are attractive drug targets (Overington et al., 2006).

Despite their validation as potential drug targets, only a small fraction out of 406 ion channels found in the human genome is so far targeted by approved drugs (Venter et al., 2001; Imming et al., 2006). The lack of exploitation of this target class is complicated by the inability to assess target occupancy in clinical trials, since adequate biomarkers are missing, which makes the interpretation of negative clinical results difficult (Kaczorowski et al., 2008). Moreover, the modulation of ion channels bears the risk of inducing significant side effects, as they are expressed in many cell types and play a major role in cellular ion homeostasis (Farrugia, 2008).

The fact that up to now low molecular weight (LMW) compounds often do not exhibit sufficient selectivity between ion channel subtypes is obviously unfavorable in terms of drug tolerability (see for instance (reviewed by Yamamoto and Takahara, 2009). In contrast, for some HVA calcium channels selective peptide blockers have been found, as noted in section 1.2.1 (p.19ff). One of them, conotoxin MVIIA (ziconotide), an N-type calcium channel-specific blocker, was successfully approved for treatment of neuropathic pain (Schmidtke et al., 2010). However, other peptidic channel toxins (e.g., ω -agatoxin IVA and IVB) are not suited for clinical development. Reasons for this may include insufficient brain availability (no blood brain barrier penetration), lack of bioavailability and irreversible channel blockage (Adams et al., 1993). Although modifications of peptide toxins have led to somewhat improved biophysical properties (Craik and Adams, 2007), these pitfalls have not yet been overcome. Besides improving drug tolerability by molecular selectivity (towards a specific ion channel), current drug discovery approaches also focus on inducing functional selectivity by identifying state-dependent LMW molecules, as described in section 1.3.3 (p.32ff).

1.3.2 High Throughput Methods

In rational drug discovery, identification and validation of an appropriate (e.g., ion channel) target is followed by large-scale compound screening, identification of (potential) modulators, and subsequent optimization of one or several promising chemical scaffolds (also called lead structures/compounds). Throughout this process many compounds are created, so that biological activity needs to be assessed in a high-throughput manner. Here, a brief overview is given about several existing methods and their respective shortcomings in supporting drug development, which may partially be overcome by automated patch clamp techniques.

Historically, drug development has been hampered by technical constraints, namely the lack of adequate high-throughput methods for identification and validation of novel compounds (Clare, 2010). For functional channel and compound characterization, manual electrophysiology has served as the gold-standard over several decades. This is because of its direct readout of ion channel function via measurement of the current and voltage across the membrane, excellent temporal resolution to resolve fast channel kinetics and high sensitivity due to an exceptional signal-to-noise ratio. However, manual patch-clamp experiments have a low throughput and are labor-intensive, posing a significant bottleneck for ion channel drug development. To this end, there are higher throughput assays available which have been incorporated into drug discovery programs. Among these are methods using fluorescent dyes which are sensitive to the calcium-level (Benjamin et al., 2006) or membrane-potential (Epps et al., 1994; Holevinsky et al., 1994). Furthermore, assays have been established which are fluorescence resonance energy transfer-based (Falconer et al., 2002) or measure ion fluxes (Terstappen, 1999). Unfortunately, these methods lack fast temporal control of voltage, necessary for the precise control of voltage-gated ion channels. In addition, ion-channel activity is only indirectly measured making these assays susceptible to false positives (Tang et al., 2001). Direct measurements of ion fluxes have also been developed (Terstappen, 1999) but lack sufficient sensitivity (Rezazadeh et al., 2004). The limitations of the high throughput assays decrease the correlation of such data with data obtained from more direct electrophysiological methods (reviewed by Dunlop et al., 2008; Terstappen et al., 2010).

During the last decade, higher throughput automated, planar patch clamp systems became commercially available which attempt to bridge this gap. The development of the planar patch clamp technique dates back to early methodological approaches which replaced the patch pipette by a planar surface perforated with a hole mimicking the pipette opening (Krishtal and Pidoplichko, 1975). As reviewed in Behrends and Fertig (2007), this principle has not been further exploited due to technical difficulties in the manufacturing process until solid-state microstructuring technologies became more accessible in the late 1990s. In addition, ion channels have by then received more attention also as a target potentially causing adverse effects, since block of the human ether-à-go-go channel became associated with long QT syndrome which increases the risk for torsades de pointes, a life-threatening ventricular arrhythmia (Curran et al., 1995; Sanguinetti et al., 1995). As a consequence, the planar clamp patch technique has been refined and is nowadays utilized in several commercially available automated patch clamp systems comprising chips either based on polymer substrates (e.g., IonWorks Barracuda from Molecular Devices), silicon (e.g., Qpatch from Sophion, Ballerup, Denmark), or glass microstructuring (e.g., Patchliner from Nanion GmbH, see p.47). In manual electrophysiology electrical access to the cell is obtained through a micropipette, which must first be carefully manipulated by a skilled experimenter into direct vicinity of an (usually) adherent cell (Hamill et al., 1981). By contrast, for automated electrophysiology suspended cells are positioned on a perforated planar surface by suction for subsequent gain of electrical access (Kiss et al., 2003). As this procedure does not require any interaction with the experimenter, several wells can be run in parallel. This, together with shorter preparation times between experiments by omitting fabrication, filling, and positioning of micropipettes, significantly increases the throughput compared to the manual patch clamp technique.

Today, several automated patch clamp systems with different recording properties are available, but generally data quality tends to be higher (due to the direct functional recording of ion channels) and throughput lower compared to the alternative methods introduced above. Therefore, these different methodological approaches are somewhat complementary to each other and will most likely be used in parallel for current and future drug development programs (e.g., Mezler et al., 2012b). Here, we used the Patchliner Platform for automated patch clamping (Farre et al., 2007), which enables medium-throughput (by simultaneous recordings from up

to four cells) and comprises a borosilicate chip surface enabling giga-seal formation. This is a prerequisite for precisely controlling the voltage of the patched cell, which is especially important for accurate measurements of voltage-gated channels.

1.3.3 State-Dependent Channel Modulation

Here, first the concept of tonic and non-tonic, namely use-, state-, and voltage-dependent, channel inhibition is briefly described. Subsequently, the relevance of non-tonic channel block as means of inducing functional selectivity to potentially lower adverse side effects is introduced. Then this is discussed on the example of ongoing drug development activities to identify use- and state-dependent N-type calcium channel blockers for the treatment of neuropathic pain.

On the one hand, pharmacological inhibition of ion channels can be tonic, i.e. irrespective of the channel conformation or factors like membrane potential. On the other hand, channels can also be modulated voltage-, state-, and use-dependently, so that the affinity for the channel depends on the surrounding conditions. By definition, the affinity of a voltage-dependent modulator to its target is sensitive to the surrounding membrane potential. A state-dependent modulator has differential affinities for certain channel states e.g., inactivated states, which can be experimentally assessed by constant (holding potential) or transient (prepulse) depolarization of the membrane potential prior to channel activation. A use-dependent modulator has different affinities due to several (rapid) transitions between states, which can be assessed by repetitive, high frequency channel stimulation. So in theory, a use-dependent blocker is also state-dependent, which in turn (for voltage-gated calcium channels) implies voltage-dependence, but not vice versa.

Increased potency for inactivated states of ion channels is currently believed to aid the therapeutic potential of ion channel blockers by widening the therapeutic window through targeting overactive or pathologically depolarized cells while leaving physiological activity mostly unaltered (Winquist et al., 2005; Kaczorowski et al., 2008). For example, tetrodotoxin (TTX) a highly potent marine biotoxin inhibits open and closed states from most sodium channels in the low nM range (Bocchaccio et al., 1998), thereby tonically suppressing action potential propagation, potentially leading

to pulmonary arrest (Chang et al., 1990). Life-threatening poisoning occurs at plasma concentrations which are above the IC_{50} of TTX to sodium channels, but slight to moderate toxicity, including paralysis of extremities, is already observed at concentrations similar or even below the IC_{50} values (Zimmer, 2010). By contrast, several clinically used sodium channel blockers were found to be state-dependent. For example, lamotrigine, which is effectively used for the treatment of epilepsy, was found to stabilize the inactivated state of the sodium channel thereby suppressing high frequency repetitive firing rates with little or no effects on basal transmission (Xie et al., 1995; Kuo and Lu, 1997). These studies estimated the affinity to inactivated sodium channels to be 12 μ M and 7 μ M, respectively. This is in line with a study of Hirsch et al. (2004) stating that plasma concentrations of about 20 μ M are often efficacious in epilepsy patients, a concentration well tolerated by most patients. These findings support the hypothesis that functional selectivity through state-dependent channel block might decrease adverse effects.

Block of NMDA receptors by memantine was also found to be voltage- and weakly use-dependent (Parsons et al., 1993; Bresink et al., 1996). This along with other properties like NMDA-subunit specificity and fast (un)binding kinetics may underlie the improved tolerability of memantine compared to other NMDA antagonists (reviewed by Rogawski and Wenk, 2003; Lipton, 2006). It needs to be noted, that the contribution of each property (e.g., voltage- vs. use-dependence) to the improved tolerability has not been described.

Several dihydropyridine HVA L-type calcium channel blockers like verapamil, which is used against hypertension and cardiac arrhythmias, have been found to be voltage- and state-dependent as well, preferentially binding to inactivated states (Nawrath and Wegener, 1997). Notably, this effect was described in retrospective to its approval. Another example is the L-type calcium channel antagonist nitrendipine, which is also used to treat hypertension, and was found to preferentially bind to and block channels during voltage-dependent inactivation (Bean, 1984). Furthermore, another dihydropyridine, nimodipine, which is a weakly selective L-type blocker clinically used to treat hypertension (Diochot et al., 1995; Furukawa et al., 2003) also preferentially binds to inactivated channels. Interestingly, nimodipine exhibited antidementive effects in several short-term clinical trials while being well tolerated (reviewed by Birks and López-Arrieta, 2002). As many clinically used L-type calcium

channel blockers are voltage-dependent (Bean, 1984; Sanguinetti et al., 1986; Kamp et al., 1989; Hughes and Wijetunge, 1993; Uneyama et al., 1999) it is tempting to speculate that this property contributes to these drugs' favorable therapeutic window.

As a consequence, current ion channel drug development efforts focus on the discovery of new state-dependent molecules. For example, there is ongoing activity to develop N-type calcium channel blockers against neuropathic pain. The N-type specific compound conotoxin MVIIA (marketed as Prialt) blocks this channel regardless of the channel state, given that there is a physiological membrane potential (Stocker et al., 1997; Feng et al., 2003). As mentioned in the previous section, it is used for the treatment of severe chronic pain not responding to opioid treatment (Miljanich, 2004; Schmidtko et al., 2010). However, despite its efficacy, the clinical benefit of Prialt is greatly limited by two factors. First, due to severe orthostatic hypotension (McGuire et al., 1997) intrathecal instead of systemic application is mandatory. Second, Prialt has a narrow therapeutic window, which is defined as the ratio of the dose inducing toxicity compared to the efficacious dose, of only a factor of 1.5-2.1 in animals and humans (Brose et al., 1997; Mathur, 2000; Staats et al., 2004). Side effects include severe, but reversible CNS impairment, including hallucinations, memory impairments, and speech disorder causing significant drop-out rates of 49% in clinical long-term study (Wallace et al., 2008). The mechanisms of action for these adverse effects are not well understood. However, several factors, like site-specific frequency dependence of neurotransmitter release and differential probability of N-type calcium channels to inactivate, suggest that state-dependent compound properties might ameliorate at least some of the adverse effects (reviewed by Snutch, 2005; Winquist et al., 2005). Abbadie et al. (2010) reported state-dependent N-type calcium channel block by Trox-1, a novel calcium channel blocker in development for treatment of neuropathic pain, which supports this hypothesis. CNS and cardiovascular side effects appeared at 20- to 40-fold higher plasma concentrations compared to the required efficacious plasma concentration for reversing inflammatory-induced hyperalgesia and allodynia induced by nerve injury, underscoring the potential of this state-dependent blocker for systemic tolerability. However, it has to be noted that increasing state-dependent properties to enhance tolerability is only a hypothesis which awaits confirmation from clinical trials.

1.3.4 P/Q-type Calcium Channels as Potential Drug Target

In the following, the involvement of P/Q-type calcium channels in channelopathies is briefly reviewed, which underlines the medical need for development of P/Q-type calcium channel modulators. However, up to now no P/Q-type selective calcium channel blocker is in clinical use. Therefore, possible approaches are mentioned which might aid the development of (selective) compounds.

Mutations in *CACNA1A*, the α_{1A} subunit encoding gene, are associated with three inherited human diseases: familiar hemiplegic migraine, episodic ataxia type 2 (EA2), and autosomal dominant spinocerebellar ataxia type 6 (reviewed by Pietrobon, 2010; Rajakulendran et al., 2012). Most mutations found in patients with familiar hemiplegic migraine, an autosomal-dominant disorder, lead to changes in the primary structure of the pore-forming α_{1A} subunit. In mice these changes facilitate channel function and lower the threshold for cortical spreading depression (van den Maagdenberg et al., 2004; Tottene et al., 2009), which is considered a pathophysiological correlate of migraine aura in humans (Hadjikhani et al., 2001). Specific block of P/Q-type calcium channels might have therapeutic potential in treatment of migraine as this can prevent spreading depression (Kunkler and Kraig, 2004; Tottene et al., 2011). On the contrary, several channel mutations have been reported causing impaired P/Q-type calcium channel function. Some of them lead to a higher susceptibility for absence epilepsy in mice (Fletcher et al., 1996; Ophoff et al., 1998) and humans (Jouveneau et al., 2001). In line with this, P/Q-type calcium channel block was described to inhibit seizure activity in mice (Jackson and Scheideler, 1996). Other channel mutations, which can lead to complete loss of channel function, were identified in episodic ataxia type 2 patients (Guida et al., 2001). Moreover, expansion of the polyglutamine repeat at the C-terminus was found to facilitate P/Q-type calcium channel inactivation in recombinant channels (Toru et al., 2000) and was described to lead to degeneration of Purkinje cells and spinocerebellar ataxia 6 in humans (Zhuchenko et al., 1997). As there are no or only limited medications available for treatment of these disorders and P/Q-type calcium channel might also be involved in AD pathology (see section 1.1.3.3, p.13), the development of P/Q-type calcium channel agonists and antagonists seems promising.

The generation of specific P/Q-type calcium channel blockers, however, is obviously challenging: Only two selective blockers have been identified, ω -agatoxin IVA and

IVB, but this class of toxins does not meet the requirements for clinical development (see section 1.3.1, p.28ff). Nevertheless, development of peptidomimetics with an improved pharmacokinetic profile might overcome these issues, which was at least in part achieved for N-type calcium channel peptides (Menzler et al., 2000; Baell et al., 2004). An alternatively strategy might be to screen LMW compound libraries using a selective ω -agatoxin-based radioligand displacement assay (Nimmrich and Gross, 2012).

This review also provides a comprehensive overview of drugs, which, to some extent, also block P/Q-type calcium channels, but are believed to exert their main therapeutic action via other targets. Examples of these drugs are: calcium channel antagonists and mood stabilizers (e.g., nimodipine; Diochot et al., 1995; Pazzaglia et al., 1998), antipsychotics (e.g., diphenylbutylpiperidines; Sah and Bean, 1994), anticonvulsants (e.g., gabapentin; Gee et al., 1996), anesthetics (e.g., isofluran; Study, 1994), and herbal medications (e.g., α -eudesmol; Horak et al., 2009). Development of novel more selective channel blockers with fewer side effects might benefit from an understanding from the precise off-target profile of these unselective drugs.

As the P/Q-type calcium channel might be involved in AD and other disorders, this PhD work supported drug discovery efforts aimed at identifying novel P/Q-type calcium channel blockers (Mezler et al., 2012b). For this validation of a high throughput assay was supported via electrophysiological methods. In the light of the unselective profile of ion channel blockers in the clinic (see above) and results from previous and current drug discovery efforts on calcium channel blockers (Yamamoto and Takahara, 2009) we could not expect to identify compounds with calcium channel subtype selectivity. Therefore we focused on identification of functional selectivity (here, i.e. state-dependence). This PhD work designed an automated electrophysiological secondary screen to identify novel compounds which block inactivated P/Q-type calcium channels. Finally, state-dependent effects of two novel LMW compounds were quantified by manual electrophysiology.

Aims of the Study

As reviewed in the introduction, AD is accompanied by increased brain levels of soluble A β , and the toxic effects of some A β species may ultimately underlie the cognitive deficits observed in patients (Cleary et al., 2005). A β oligomers have been shown to impair hippocampal synaptic function (Cullen et al., 1997; Selkoe, 2002; Nimmrich et al., 2010), induce presynaptic deficits (reviewed by Nimmrich and Ebert, 2009), and modulate presynaptic HVA calcium channels (Bobich et al., 2004; Nimmrich et al., 2008a). In drug development state-dependency of ion channel modulators is currently believed to improve their tolerability for clinical use. Thus, targeting presynaptic calcium channels with state-dependent blockers may be considered as a promising therapeutic strategy for AD.

The overarching goals of the study were to further elucidate the effect of oligomeric A β on HVA calcium channels, aid the development of novel LMW calcium channel blockers, and to evaluate the therapeutic potential of state-dependent calcium channel block in a hippocampal *in vitro* model of AD. Specifically, this study comprised the following objectives:

1. Characterize calcium channel-dependent effects of oligomeric A β on synaptic transmission.
2. Elucidate effects of oligomeric A β on calcium channel function.
3. Identify novel calcium channel blockers and characterize state-dependent properties.
4. Test whether state-dependent calcium channel block reverses oligomeric A β -induced synaptic deficits.

2 Materials and Methods

2.1 Chemicals and Biologics

The calcium channel reference compounds ω -agatoxin IVA (Alomone Labs, Jerusalem, Israel) and ω -conotoxin MVIIA (Sigma, St. Louis, MO, USA) were dissolved at 0.5 mM and 0.1 mM in water, respectively. Roscovitine (Sigma, St. Louis, MO, USA) was dissolved in dimethylsulfoxide (DMSO) at 10 mM. Stock solutions were immediately stored at -20°C until further use. The polyclonal P/Q-type calcium channel antibody (sc-16228; Santa Cruz Biotechnology, Inc., Santa Cruz, CA, USA) was dialyzed (HiTrap Desalting Column, GE Healthcare Europe GmbH, Freiburg, Germany) against phosphate-buffered saline (PBS; Invitrogen, Darmstadt, Germany) and stored at 160 μ g/mL in water at 4°C.

A β globulomer was prepared (by the lab of Dr. Stefan Barghorn) as described in Barghorn et al. (2005). Synthetic A β ₁₋₄₂ peptide was dissolved in HFIP according to Stine et al. (2003), which was subsequently evaporated in a vacuum concentrator (SA-VC-300H; H. Saur Laborbedarf, Reutlingen, Germany). The peptide was then resuspended in DMSO and PBS containing 0.2% SDS. After 6 h incubation at 37°C the sample was further diluted with three volumes of water, incubated for 18 h at 37°C and centrifuged at 3,000 g for 20 min, concentrated by ultrafiltration (30 kDa cut-off; Millipore, Billerica, MA, USA) and dialyzed against 0.25x PBS-buffer. This was centrifuged at 10,000 g for 10 min and the supernatant containing the 38/48-kDa A β oligomer, termed A β globulomer, aliquoted, and immediately stored at -80°C. The ultrafiltrate (5 kDa cut off; Millipore, Billerica, MA, USA) of A β globulomer, centrifuged at 3,000 g for 1 h, was used as a control for experiments. Synthetic A β ₁₋₄₂ peptide (H-1368; Bachem, Bubendorf, Switzerland) was dissolved in the respective solutions used for patch clamp experiments immediately prior to experiments. The molecular mass of the A β preparations was characterized through SDS-polyacrylamide gel electrophoresis (PAGE) using NuPAGE® 4-12% Bis-Tris gels and NuPAGE® MES SDS running buffers (Invitrogen, Darmstadt, Germany). A β globulomer concentrations are given with respect to the 12-mer complex, e.g., 83 nM of A β globulomer corresponds to a total concentration of 1 μ M of monomeric A β ₁₋₄₂.

2.2 Generation of Cell Lines and High Throughput Screening

In the following, the creation of HEK293 (human embryonic kidney 293) cell lines is described, which stably express the P/Q-type and N-type calcium channel. HEK293 cells were initially derived from transformation of cultured human embryonic kidney cells with the human adenovirus type 5 (Graham et al., 1977; Louis et al., 1997) and, as in this study, have been widely used as a simple heterologous expression system. Interestingly, neuron-specific protein expression was found in HEK293 cells suggesting they might originate from a neuronal cell lineage (Shaw et al., 2002). Stable cell line generation was carried out as described in Mezler et al. (2012b). For this, the respective calcium channel gene constructs were cloned into two expression vectors, which are plasmids used to introduce genes into cells. One vector carries the gene encoding the pore forming subunit of the respective calcium channel and controls its transcription level via a tetracycline sensitive promoter. Thus, functional calcium channels can only be expressed in tetracycline-induced cells. The other vector induces constitutive transcription of the genes encoding the calcium channel subunits. Cloning of the channel subunits, generation of stable HEK293 cell lines and fluorometric imaging plate reader (FLIPR) measurements were carried out by the lab of Dr. Mario Mezler.

In specific, the human $\beta_{1.1}$ subunit hCACNB1 (accession number NM_000723) and $\alpha_{2\delta_1}$ subunit hCACNA2D1 (accession number NM_000722) were amplified by PCR, cloned into the expression vector pBUDCE4.1 (Invitrogen, Darmstadt, Germany), and sequence-verified. The human P/Q-type calcium channel α_{1A} subunit CACNA1A transcript variant 2 (accession number NM_023035) and human N-type calcium channel α_{1B} subunit CACNA1B transcript variant 1 (accession number NM_000718) were each cloned into an inducible vector pcDNA5/FRT/TO (Invitrogen, Darmstadt, Germany) and sequence-verified.

Then, HEK 293 T-Rex cells (Invitrogen, Darmstadt, Germany) were transfected in two subsequent steps with the prepared expression plasmids in a similar fashion as previously described for the rat P/Q channel by Lam et al. (2007). HEK293 T-Rex cells were transfected with the PvuI-linearized pBudCE4.1/hCACNB1.1/hCACNA2D1 plasmid employing Lipofectamine as described by the manufacturer (Invitrogen, Darmstadt, Germany). Briefly, 2.5×10^6 cells were seeded in 10 cm Petri dishes (Greiner Bio One, Frickenhausen, Germany)

with DMEM Glut HG medium (Invitrogen, Darmstadt, Germany) and incubated in a humidified incubator at 37°C, 5% CO₂ overnight. On the following day, 2 µg of the plasmid was dissolved in 100 µL Optimem Glutamax medium, and 12 µL Lipofectamine was dissolved in 100 µL Optimem Glutamax medium. After 5 min incubation at room temperature, the two samples were mixed and incubated for additional 20-30 min at room temperature. Subsequently 0.8 mL Optimem Glutamax medium (Invitrogen Darmstadt, Germany) was added and the mixture used immediately for transfection. For this, the cells in the Petri dishes were first washed twice with Optimem Glutamax medium, and 2 mL medium was added to each petri dish. 1 mL of the Lipofectamine/plasmid mixture was added to each dish and the cells incubated for 5 h at 37°C, 5% CO₂. The medium was changed to DMEM Glut HG medium, changed twice the following day, the cells split (1:5, 1:10, 1:50, 1:100, 1:250, 1:500, 1:1000 and undiluted), and transferred to selection medium containing DMEM Glutamax HG + charcoal-treated and dextran-treated FBS (Thermo Scientific/HyClone, Logan, USA), with 5 µg/mL blasticidin (Invitrogen, Darmstadt, Germany) and 200 µg/mL zeocin (Invitrogen, Darmstadt, Germany). After 14-28 days single cell clones were isolated, expanded, transiently transfected with the human CACNA1A.2 subunit in pcDNA3.1 (Invitrogen, Darmstadt, Germany), tested in FLIPR (see below) for activity, and the most active single cell clones were passed further. Clone K8 demonstrated the most robust calcium signal after transient transfection of the pore forming subunit. Subsequently, the inducible α_{1A} subunit - as a MunI linearized pCDNA5/TO/hCACNA1A.2 plasmid – and the inducible α_{1B} subunit - as a MunI linearized pCDNA5/TO/hCACNA1B plasmid – were transfected into responsive cell clones including K8, as described above. After 14-28 d in selection medium (DMEM Glutamax HG, 10% charcoal and dextran treated FCS, 5 µg/mL blasticidin, 200 µg/mL Zeocin, and 150 µg/mL hygromycin) single cell clones were selected and tested in the FLIPR assay (see below) and by patch clamp electrophysiology. The best clones were chosen, expanded for batch production and cryopreserved with Recovery Cell Culture Freezing (Invitrogen, Darmstadt, Germany) as described by the manufacturer.

For characterization of clones in the FLIPR assay 40,000 cells per well from cell culture or 60,000 cells per well from frozen stock were seeded into 96-well plates (poly-D-Lysine coated BIOCOAT 96-well plates, Becton Dickinson, Heidelberg, Germany) in DMEM Glutamax HG medium, containing charcoal and dextran treated

FCS and 1 µg/mL tetracycline (Sigma, St. Louis, USA), and incubated at 37°C. After 48 h the medium was exchanged for DMEM containing 1 µg/mL tetracycline, but without glutamine or serum. Cells were incubated for additional 2-3 h at 37°C, and loaded with the Calcium 4 Dye (Molecular Devices, Ismaning, Germany), pre-diluted 1:2 in HBSS/HEPES with 12 mM Ca²⁺ and 5 mM Mg²⁺. Activation of the calcium channels was achieved through depolarization of the cells by adding KCl. Measurements were performed in a FLIPR³⁸⁴ device (Molecular Devices, Ismaning, Germany).

For high throughput screening (carried out by the lab of Dr. Sujatha Gopalakrishnan, Abbott Laboratories, Chicago), calcium measurements were performed using FLIPR^{Tetra} (Molecular Devices) and the use of the Calcium 5 Dye (Molecular Devices). Here, cell depolarization and channel activation was obtained by replacing the assay buffer (HBSS with 12 mM Ca²⁺ and 5 mM Mg²⁺, 20 mM HEPES) with a buffer containing a high KCl concentration (final concentration: 5 mM CaCl₂, 60 mM KCl in HBSS without Ca²⁺, Mg²⁺, with 20 mM HEPES).

2.3 Patch Clamp Recordings

The patch clamp technique, which was first described by Neher and Sakmann (1976), enables functional analysis of ion channels (patch clamp technique reviewed by Numberger and Draguhn, 1996) and has been considered as the gold-standard for investigating direct ion channel modulation (Terstappen et al., 2010). Here, data was obtained by whole-cell recordings, which enable electrical access to the entire cell and, thus, record the current flow across multiple ion channels. Cells were patched at room temperature using a manual and an automated 4-channel Patchliner (Nanion GmbH, Munich, Germany) recording setup (see Figure 2.1, p.47).

At least 7 d prior to the electrophysiological experiments, HEK293 T-Rex cells were thawed and cultured in poly-D-Lysine coated flasks (Greiner Bio-One GmbH, Frickenhausen, Germany) at 37°C and 7% CO₂. For passaging twice a week, cells were washed with PBS without calcium and magnesium (Invitrogen, Darmstadt, Germany), incubated with Accutase for 2 min at 37°C (Sigma, St. Louis, MO, USA), lifted of the culture flask by gentle tapping, and diluted in selection medium. Culture density and quality was assessed using the electric-field counting system Casy

(Schärfe Systeme, Reutlingen, Germany) and cells were discarded if the viability fell below 90%. After counting, cells were transferred into new culture flasks containing selection medium. Cells were kept in culture for up to 20 splits post-thaw at an approximate confluency of 50-80%. Channel expression was induced 1-4 d prior to experiments with 1 $\mu\text{g}/\text{mL}$ tetracycline, while the selection antibiotics zeocin and hygromycin were omitted.

2.3.1 Manual Patch Clamp

Prior to manual voltage-clamp and current-clamp experiments, cells were plated in 24-well plates (Costar, Corning, NY, USA) at densities of 2×10^4 cells/well on uncoated, 12 mm diameter glass slides (Menzel, Braunschweig, Germany), which were previously washed with sterile water (Sigma, St. Louis, MO, USA). Prior to recordings, glass slides were washed in the respective external recording solution (see below), put into the manual recording chamber, which was situated within a faraday cage and mounted on a cushioning table (Science Products, Hofheim, Germany). All compounds were applied in a 1:3 fashion to the recording chamber. Pipette tips and cells were visualized by an inverted Olympus IMT-2 microscope (Olympus Deutschland, Hamburg, Germany). Pipette manipulators were electrically controlled by an SM1 control unit (Luigs & Neumann, Ratingen, Germany). Data was acquired and low pass filtered (4-pole Bessel) at 3 kHz with an Axonpatch 200B amplifier (Molecular Devices, Sunnyvale, CA, USA). Data was digitized by a Power1401 analog-digital converter at a sampling rate of 20 kHz, recorded by the Signal 3.14 software (both Cambridge Electronic Design, Cambridge, UK), and stored on a personal computer.

2.3.1.1 Voltage-clamp

After the patch pipette was manipulated onto a cell and a high resistance ($G\Omega$) seal was formed, voltage-clamp whole-cell recordings were obtained by mechanically rupturing the cell surface. This causes the cytosolic solution to be passively replaced with the solution in the patch pipette. Moreover, due to a low series resistance (R_s) (being only about 2-5 times larger than the initial pipette resistance) a good electrical

access to the cell is obtained, which supports fast and accurate voltage control of the cell. Therefore, whole-cell voltage-clamp recordings were used to study the biophysical and pharmacological properties of P/Q-type and N-type calcium channels.

For whole-cell experiments all solutions were filtered with a polyethersulfone 0.22 μm unit (Millipore, Billerica, MA, USA), aliquoted, and stored at -20°C . Pipettes were filled with the following solution (in mM): 110 CsCl, 10 EGTA, 25 HEPES, 4 Mg-ATP, 0.3 Na-GTP; pH 7.3 adjusted with CsCl; 295 mOsmol adjusted with sucrose. During experiments this solution was kept on ice and was again filtered during tip filling by a 0.2 μm nylon filter unit (ThermoScientific, Rochester, NY, USA). The solution surrounding the exterior of the cell (here denoted as *extracellular solution*) was stored at 4°C , used for a maximum of 2 weeks, and comprised (in mM): 130 NaCl, 10 BaCl_2 , 20 glucose, 10 HEPES; pH 7.3 adjusted with NaOH; 305 mOsmol adjusted with sucrose.

Borosilicate pipettes were prepared by a micropipette puller P-97 (Sutter Instrument, Novato, CA, USA) and their resistance of 2-4 $\text{M}\Omega$ was estimated in the recording chamber by application of a 5 mV biphasic square pulse and slight positive pressure within the pipette. Once the pressure was released and the pipette became cell attached the holding potential was switched from 0 to -80 mV which aided giga seal formation. Whole-cell conformation was then obtained through suction, which was immediately relieved after the square pulse-induced transient currents became significantly larger due to the increase in capacitance. Cells were equilibrated for at least 5 min before experiments were started to allow for the passive exchange of cytosolic with the solution of the pipette. After equilibration, voltage-dependent activation was assessed in each cell by generation of a current-voltage (I-V) relationship by measuring peak amplitudes during step depolarization at various potentials (as described in detail in chapter 2.6).

Whole-cell recordings were discarded when series resistance (R_s) exceeded 10 $\text{M}\Omega$ during baseline conditions or 20 $\text{M}\Omega$ anytime during the experiment. R_s was compensated online by $\sim 95\%$. As cells were excluded if seal resistance dropped below 200 $\text{M}\Omega$ anytime during the experiment (in most cases seal resistance remained above 1 $\text{G}\Omega$ throughout the experiment) the resulting ratio $R_{\text{seal}} / R_{\text{series}} \geq 50$

enabled us to neglect the voltage drop caused by the remaining uncompensated R_s . In rare cases experiments were discarded because channel activation occurred in a step-wise or non-exponential fashion during test pulse depolarizations. As this became more pronounced or more frequent when R_s compensation was disabled or interconnected cells were patched, this current shape was most likely due to technical artifacts like lack of temporal and/or spatial voltage control. Therefore, only single, isolated cells were recorded.

Unless otherwise noted, the holding potential was set to -80 and -90 mV for the recombinant P/Q-type and N-type calcium channel, respectively. Different potentials were chosen, because at -80 mV slightly increased run-down was observed for N-type currents and inactivation occurred at more hyperpolarized values for this channel. The test pulse was applied close to a potential inducing the maximum current response, which constitutes 20 and 10 mV for our recombinant P/Q-type and N-type calcium channel, respectively (see results). An intersweep interval of 12 s was used. For analysis of LMW compounds a 3 s prepulse was applied. The prepulse potential was set for each cell individually to induce about 30-70% of current inactivation.

2.3.1.2 Current-clamp

Current-clamp recordings were carried out in perforated whole-cell mode. In this configuration whole-cell access is not obtained by cell rupture but instead by small perforations of the membrane. Here this is obtained by the antibiotic gramicidin D (Sigma, St. Louis, MO, USA). It is supplemented to the solution of the pipette and upon contact with the plasma membrane forms transmembrane channels which are permeable for monovalent cations but not anions and larger cell contents (Kyrozis and Reichling, 1995; Tajima et al., 1996), which largely reduces cell dialysis. Consequently, this technique was applied to estimate the resting membrane potential as well as the potassium-induced depolarization of P/Q-type calcium channel expressing cells under near physiological conditions.

Gramicidin D was dissolved in DMSO at 50 mg/mL and stored at -20°C. Pipettes were filled with solution containing 150 mM KCl and 10 mM HEPES, which was supplemented with 75 µg/mL gramicidin D, thoroughly vortexed, and sonicated for

7 min. Pipette tips were first filled with solution lacking and subsequently backfilled with solution containing the antibiotic. After seal formation, cells were held at -40 mV and R_s was constantly controlled. For $R_s < 200 \text{ M}\Omega$ the patch was considered perforated and the experiment was started. After at least 5 min of baseline recordings, the KCl concentration was increased to 60 mM in the external HBSS solution (containing 10 mM CaCl_2 and 20 mM HEPES; Invitrogen, Darmstadt, Germany) for 3 min before returning to the baseline KCl concentration in the HBSS medium (5.3 mM). After the experiment was finished, cells were excluded if R_s had dropped below 40 $\text{M}\Omega$, which may be indicative of successful whole-cell formation.

2.3.2 Automated Patch Clamp

Voltage clamp whole-cell recordings were also obtained from automated patch clamp experiments. Unlike manual electrophysiology, where electrical access is established through manipulation of a pipette to an adherent cell, the Patchliner automated patch clamp system (Nanion GmbH, Munich, Germany) captures suspended cells through suction onto a small hole. This hole is situated on a planar borosilicate chip surface, which serves as the interface between the *extracellular* and *intracellular compartment* (i.e. having access to the extracellular and intracellular side of the cell, respectively) for whole-cell recordings.

For preparation of automated planar patch clamp recordings, cells were dissociated and isolated with trypsin (Sigma, St. Louis, MO, USA) or Accutase for 2 min, spun for 2 min at 100x g and re-suspended in buffer containing (in mM): 140 NaCl, 4 KCl, 1 MgCl_2 , 2 CaCl_2 , 5 glucose, 10 HEPES; pH 7.4 adjusted with NaOH; 298 mOsmol. Cells were kept in a storage chamber at an approximate density of 1×10^6 cells/mL and were periodically pipetted up and down to maintain viability and dispersion. Planar chips with a resistance of approximately 2-3 $\text{M}\Omega$ were used for recordings. The control of suction to obtain $\text{G}\Omega$ seals and whole-cell configuration between the glass chip and the cell membrane as well as the estimation of R_s , C_{slow} , and C_{fast} values was performed using the PatchControlHT software (Nanion Technologies GmbH, Munich, Germany).

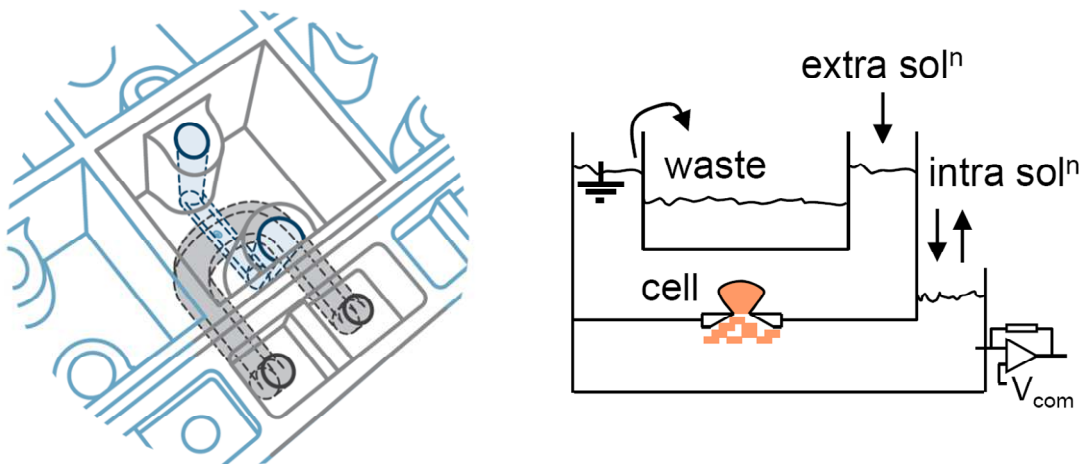


Figure 2.1 The Patchliner – an automated planar patch clamp system (from Nanion GmbH, Munich, Germany). Top: Patch clamp platform including the robotic teflon-coated pipette arm, here positioned above the headstage. Lower left: Three-dimensional illustration of the extracellular (light blue shaded area) and intracellular (dark blue / grey shaded area) compartments from one individual chip. Cells are captured in a small hole at the intersection of these two compartments. The volumes around the openings of the two compartments comprise the respective waste reservoir. Lower right: Two-dimensional scheme of one chip including a cell depicted in whole-cell mode.

Upon start of an experiment, the *intracellular compartment* of the chip was filled with a solution comprising (in mM): 50 CsCl, 10 NaCl, 60 CsF, 2 MgCl₂, 20 EGTA, 5 BAPTA, 5 Mg-ATP, 0.3 Na-GTP, 10 HEPES; pH 7.2 adjusted with CsOH; 290 mOsmol. The *extracellular compartment* of the chip was filled with the following solution used for recordings (in mM): 105 NaCl, 20 TEA-Cl, 20 BaCl₂, 10 mM glucose and 10 HEPES; pH 7.35 adjusted with NaOH; 305 mOsmol. Subsequently, cells were automatically dispensed into the *extracellular compartment* and captured to the

hole of the planar patch clamp chips by suction. For seal enhancement, the *extracellular compartment* was washed with a solution comprising (in mM): 80 NaCl, 3 KCl, 35 CaCl₂, 10 MgCl₂, 10 HEPES; pH 7.4 adjusted with HCl; 298 mOsmol. Whole-cell formation is obtained by transient application of -100 mbar negative pressure, which is increased by steps of -50 mbar (to a maximum of -350 mbar) until $R_s < 40 \text{ M}\Omega$ and $C_{\text{slow}} > 2 \text{ pF}$ is obtained. After successful whole-cell formation, solution of the *extracellular compartment* was again exchanged with the solution used for recordings (see above). Channels with $R_{\text{seal}} < 200 \text{ M}\Omega$ or insufficient whole-cell formation ($R_s > 40 \text{ M}\Omega$ or $C_{\text{slow}} < 2 \text{ pF}$) were excluded from the measurement. R_s was compensated online by 70-90%.

The holding potential was set to -90 mV. Channel opening was elicited by stepping the potential to 20 mV for 20 ms each 12 s. I-V relationships were generated by measuring peak amplitudes during step depolarization to given potentials. For analysis of LMW compounds a 3 s prepulse was applied. The prepulse potential was set for each cell individually to induce about 30-70% of current inactivation. Compounds were dissolved in the recording solution and applied to the *extracellular compartment* by complete exchange of solution. Data acquisition was performed with an EPC10 amplifier and a PatchMaster software package (all HEKA Electronics, Lambrecht/Pfalz, Germany). As recordings were obtained from four independent chips in parallel a HEKA probe Selector (all HEKA Electronics, Lambrecht/Pfalz, Germany) was used to switch the amplifier control between these four independent channels.

2.4 Hippocampal Slice Culture Preparation

As described in the introduction, the hippocampal region has been an intensively investigated cortical structure due its well-structured cytoarchitecture and important physiological function including memory and learning. Hippocampal slice cultures are a well-studied *in vitro* model of the hippocampal region, which have been used to study several aspects of neuronal development or function including synaptic properties under non-pathological (Bonhoeffer et al., 1989) and pathological conditions (Nimmrich et al., 2010). Preparation of hippocampal slice cultures was performed by Tanja Georgi, Siena Kiess, and Michael Bahr.

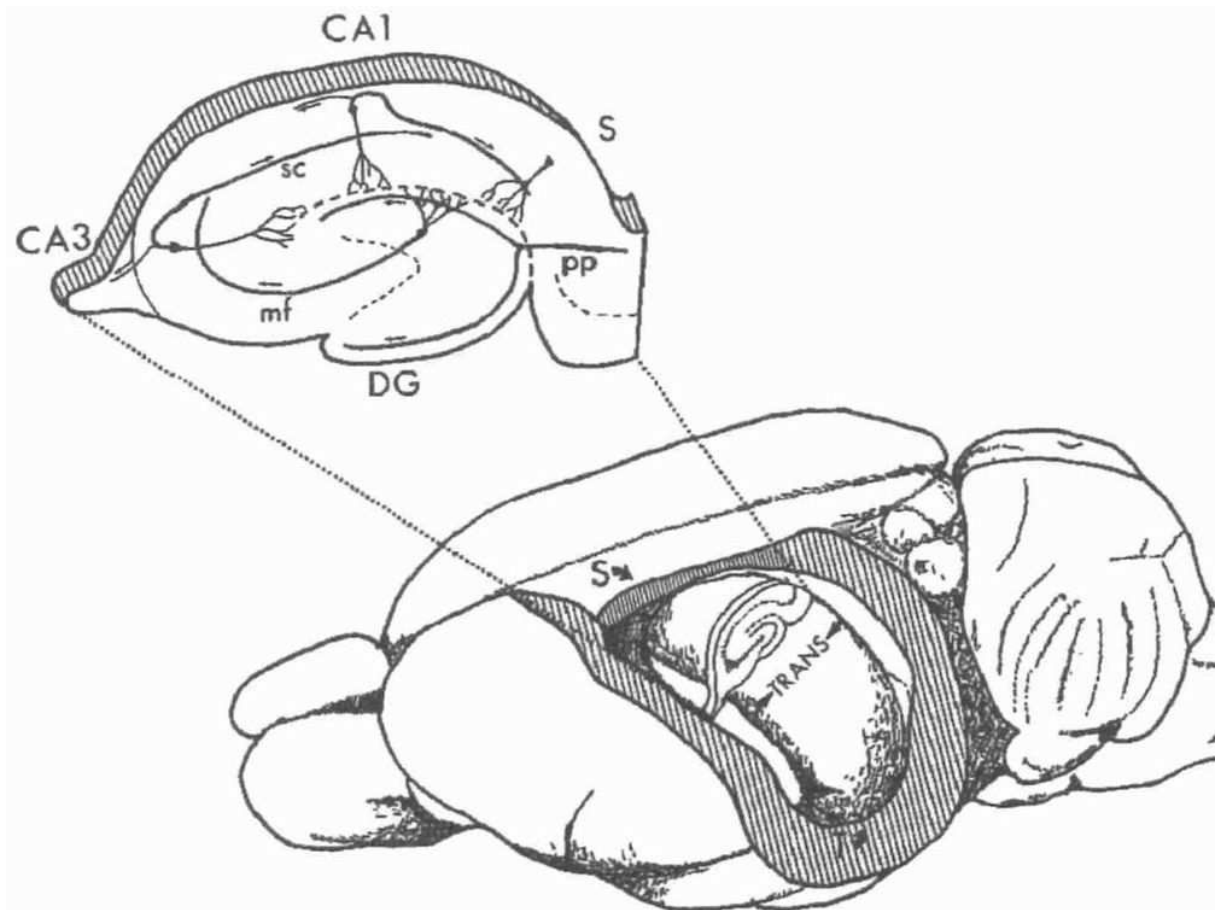


Figure 2.2 The rat hippocampal formation (from Amaral and Witter, 1989). Bottom: Schematic drawing of the location and orientation of the rat hippocampus within the cortex. In this study, isolated hippocampi were chopped along the (orthogonal) transverse axis ("TRANS"). "S" and "T" denote the septo-temporal axis. Top: Scheme of axonal projections (small letters) and histologically defined regions (capital letters) within a transversal hippocampal section. The Schaffer collateral (sc), which was stimulated in this study, transfers information from the hippocampal CA3 to the CA1 region. Abbreviations: DG, dentate gyrus; CA3, CA1, cornu ammonis fields of the hippocampus; S, subiculum; pp, perforant path fibers from entorhinal cortex; mf, mossy fibers from the granule cells.

Organotypic hippocampal slice cultures were prepared as described by Nimmrich et al. (2010) from 9 to 12 day old Wistar rats (Janvier, Genest St.Ile, France), which were decapitated with sharp scissors without anesthesia. Hippocampi were isolated in Gey's balanced salt solution (containing in mM: 138 NaCl, 4.9 KCl, 1.5 CaCl₂, 11 MgCl₂, 333.3 glucose, 0.3 MgSO₄, 0.2 KH₂PO₄, 0.8 NaH₂PO₄, 2.7 NaHCO₃, and 25 HEPES; pH 7.2; all chemicals from Invitrogen, Darmstadt, Germany, except HEPES from Sigma-Aldrich, Steinheim, Germany), which was previously cooled on

ice. Transverse, 400 μm thick hippocampal slices were prepared by using a tissue chopper (Mickle Laboratory Engineering, Gomshall, UK).

Slices were cultured according to Stoppini et al. (1991) on millicell-CM membranes (Millipore, Billerica, MA, USA) in 40% basal medium Eagle (BME) with Earle's salts, 25% horse serum, 25% Earle's balanced salt solution, 1 mM Glutamax I, 28 mM glucose, and 10% 250 mM HEPES in BME (all chemicals, except HEPES, from Invitrogen, Darmstadt, Germany) at 34°C, 5% CO₂. After 3 d media exchange was done with Neurobasal A medium (96.4% Neurobasal A medium, 2% B 27 supplement, 1 mM Glutamax-I; all from Invitrogen Darmstadt, Germany) including 25 mM D-glucose (Sigma-Aldrich, Steinheim, Germany). Media was previously filtered with a 0.2 μm polyethersulfone sterile filter unit (Thermo Scientific, Logan, USA). Hippocampal slices were cultured for 15-25 d before recording.

All animal care and experimental procedures were according to the guidelines of the Association for Assessment and Accreditation of Laboratory Animal Care International (AAALAC) commission, and were approved by the government of Rhineland Platinate (Anzeige 2/92; AZ 889-13).

2.5 Field Potential Recordings

Within the hippocampal region, the Schaffer collateral - CA1 synapse has been widely studied, because of its laminar-organized structure exhibiting functional plasticity which correlates with cognitive measures like learning and memory, as previously noted in the introduction (Morris et al., 1986; Bonhoeffer et al., 1989). After stimulation of the Schaffer collateral in organotypic hippocampal slice cultures, we used the strength of the resulting field excitatory postsynaptic potential (fEPSP) in the CA1 region to assess the functionality of synaptic transmission under several pharmacological conditions.

Specific calcium channel toxins, A β globulomer, test compounds with potential effects on calcium channels and their respective controls were applied to the culture medium of organotypic hippocampal slice cultures 1 d prior recording. As control the corresponding vehicle concentration of water, DMSO, or A β globulomer ultrafiltrate was used. The P/Q antibody was applied 2 h prior to A β globulomer.

Slices were placed on in a Haas-type interface recording chamber (Harvard Apparatus, Hugstetten, Germany), which was supported by a cushioning table (Spindler & Hoyer, Göttingen, Germany). They were continuously perfused with substance-free artificial cerebrospinal fluid (composition in mM: 118 NaCl, 5 KCl, 2 MgSO₄, 2.5 CaCl₂, 1.24 KH₂PO₄, 25.6 NaHCO₃, 10 glucose, pH 7.4; gassed with carbogen (95% O₂, 5% CO₂)) at about 0.7 mL/min driven by a peristaltic Minipuls3 pump (Gilson, Middleton, WI, USA). Slices were allowed to equilibrate in a humidified, carbogen-gassed atmosphere for at least 60 min at 32°C using a TC-10 temperature control unit (npi electronic, Tamm, Germany).

fEPSPs were recorded after stimulation of the Schaffer collateral as described by Nimrich et al. (2010). The Schaffer collateral was stimulated with bipolar pulses (0.1 ms/phase) using a 0.5 MΩ bipolar tungsten electrode (WPI, Sarasota, FL, USA) at an interval of 60 s. Borosilicate glass recording electrodes (Harvard Apparatus, Hugstetten, Germany) were pulled by a vertical patch electrode puller (Ochotzki, Homburg/Saar, Germany) and filled with artificial cerebrospinal fluid. Their resistance was determined at 0.8-1.1 MΩ by a Omega tip-Z MΩ meter (WPI, Sarasota, FL, USA). fEPSPs were recorded from the hippocampal CA1 region (see Figure 2.2 on p.49), after electrode placement by mechanical micromanipulators (Harvard Apparatus, Hugstetten, Germany). Signals were acquired by an Ext 10-2F amplifier (npi electronic, Tamm, Germany), 50 Hz noise reduced by a Hum-Bug (WPI, Sarasota, FL, USA), and digitalized at 10 kHz by a Power1401 (Cambridge Electronic Design, Cambridge, UK). Data was also visualized in parallel by a DL708E oscilloscope (Yokogawa Deutschland, Herrsching, Germany) to control for spontaneous discharges. In case of such discharges slices were excluded from analysis.

2.6 Data Analysis

Data from electrophysiological experiments was exported to Microsoft Excel 2003 (Microsoft, Redmond, WA, USA) for offline analysis. For slice culture experiments input-output curves were created by plotting the fEPSP amplitude over stimulus intensity. For patch clamp experiments, command voltages were corrected offline for the liquid junction potential (Barry, 1994), which was calculated as 5.8 and 4.0 mV for manual and automated patch clamp solutions, respectively. Unless otherwise noted,

figures and calculated results were corrected for this offset, in contrast to the denoted voltage protocols.

For I-V relationships, data was fitted with a combination of a first-order Boltzmann activation function and the Goldman-Hodgkin-Katz (GHK) current-voltage relationship (Kortekaas and Wadman, 1997):

$$I(V) = V \frac{g_{\max}}{1 + \exp\left(\frac{V_h - V}{V_c}\right)} \frac{[Ba^{2+}]_{in} / [Ba^{2+}]_{out} - \exp(-\alpha V)}{1 - \exp(-\alpha V)}$$

with $\alpha = F/RT$ and $g_{\max} = \alpha P_0 [Ba^+]_{out}$, where g_{\max} is the maximal membrane conductance (which is proportional to the maximal permeability), V_h is the potential of half-maximal activation, and V_c is proportional to the slope of the curve at V_h . F represents the Faraday constant, R represents the gas constant, P_0 is the maximal permeability, and T the absolute temperature. For these calculations the intracellular concentration of Ba^{2+} was assumed to be 10 nM. Assuming higher values of up to 10 μ M did not significantly change the results. For some illustrations I-V curves were normalized to the maximal response obtained from recordings in drug-free solution. Activation curves were calculated from $I(V) / I_{\max}(V) = 1 / (1 + \exp((V_h - V) / V_c))$ applying the GHK constants calculated above.

Inactivation curves were obtained by plotting the peak amplitude resulting from a test pulse against the potential of a preceding prepulse. Similar to the activation curves, the voltage dependence of inactivation of the barium current was well described by a first-order Boltzmann function, which normalized the current as follows:

$$N(V) = \frac{I(V)}{I_{\max}}, \text{ where } I(V) = \frac{I_{\max}}{1 + \exp\left(\frac{V_{inact} - V}{V_c}\right)}$$

where $N(V)$ denotes the level of inactivation determined from the current amplitude $I(V)$ normalized to the maximum current I_{\max} , V is the prepulse potential, V_{inact} is the potential of half-maximal inactivation, and V_c is a factor proportional to the slope of the curve at V_{inact} . For very short prepulses (< 1 s), potentials larger than 20 mV were not included in the fit.

For pharmacological patch clamp experiments the last three responses of each incubation period were averaged for analysis and normalized to baseline level, which

was defined as the average of the last three drug-free responses. Unless otherwise noted, test pulses were applied at an interval of 12 s throughout the experiment. The equilibration period after obtaining whole-cell configuration was 5 min and baseline was recorded for another 2-5 min before pharmacological agents were applied. The compound incubation times were chosen to obtain (near) steady-state responses and are denoted in the results section for the respective experiment. Run-down correction was obtained using time-matched vehicle control cells, which resembled the exact application and incubation schemes of compound treated cells. For run-down correction, results from compound treated cells were normalized to time-matched controls: $\overline{cpd}_{corrected} = \overline{cpd} / \overline{control}$. For example, if a given compound application yields 20% of the initial baseline current and its time-matched control 80%, the resulting run-down corrected value was estimated at 25% of baseline level. As time-matched controls also exhibited variation, error propagation needs to be considered, meaning that the relative error of a ratio is given by the sum of the squared relative errors of the dividend and divisor. Here, this translates into $\sigma_{corrected} = \sqrt{(\sigma_{cpd})^2 + (\sigma_{Control})^2}$, where $\sigma_{corrected}$ denotes the run-down corrected relative error, σ_{cpd} and $\sigma_{control}$ denote the relative error of the compound and time-matched control measurements, respectively.

Statistical analysis and data fitting was done using GraphPad Prism 5.03 (GraphPad Software, La Jolla, USA) applying a three-parameter sigmoidal fit for concentration response curves to estimate the IC_{50} and exponential fits for rate and decay constants. Values are represented as average \pm standard error of the mean (S.E.M.). Error bars are not visible if they are smaller than the data point symbol.

2.7 Statistics

For patch clamp experiments, statistical comparisons were made with Student's t-test, one-way ANOVA, or one-way repeated-measure (RM) ANOVA. When applicable, Dunnett's *post hoc* analysis was applied to compare against control application. Input-output relationships in slice cultures were compared using a two-way RM ANOVA with Holm-Sidak *post hoc* analysis to compare all groups. A p value < 0.05 was considered significant.

3 Results

There is converging evidence for the pathological role of A β in AD, as indicated in the introduction. In this study we have, therefore, investigated the effect of a highly stable, oligomeric A β_{1-42} preparation, termed A β globulomer. The corresponding epitope is found in AD patients and inhibits LTP *in vitro*, a physiological correlate of learning and memory (Barghorn et al., 2005).

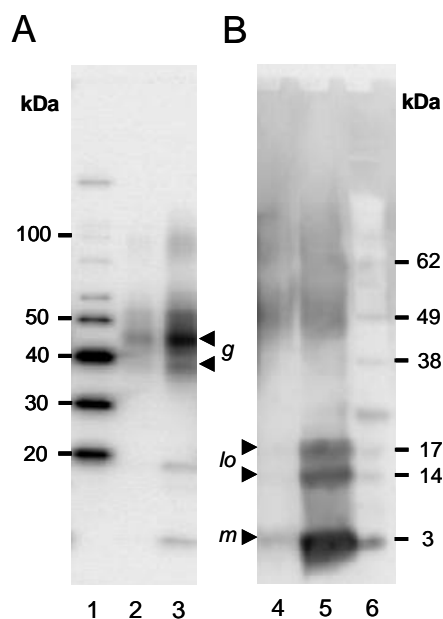


Figure 3.1 Characterization of the A β globulomer preparation. (A) Applying 4-12% Bis-Tris SDS-polyacrylamide gel electrophoresis (PAGE) gels, A β globulomer exhibited strong bands at higher molecular weights corresponding to A β_{1-42} 12-mers ("g") as described in Barghorn et al. (2005). Monomeric and lower order forms were detected at considerably lower intensities. Lanes: 1, MagicMark™ XP marker; 2, A β globulomer (50 pg); 3, A β globulomer (250 pg). (B) Freshly dissolved A β_{1-42} peptide exhibits mainly monomeric ("m") and to a lower extent low order oligomeric fractions ("lo") on the SDS-PAGE gel. Lanes: 4, A β_{1-42} peptide (450 pg); 5, A β_{1-42} peptide (4,500 pg); 6, SeeBlue® Plus2 marker.

Before investigating the functional effects of A β globulomer (synthesized by Dr. Stefan Barghorn), we first validated this preparation by SDS-PAGE (Figure 3.1A). Upon qualitative analysis A β globulomer solution yielded the strongest bands at molecular weights corresponding to the published 38/48 kDa oligomeric complex (12-mer). In addition, at the higher A β globulomer concentration also low levels of ~4 kDa (monomeric) and ~16 kDa (small oligomers) were detected. By contrast, the ~4 kDa fraction was most prominent for the freshly dissolved A β_{1-42} peptide, which also exhibited lower levels of protein around ~16 kDa (Figure 3.1B). A smear was also detected at higher molecular weight levels in this gel, which appeared to be unspecific as it was independent of A β_{1-42} peptide concentration. Fibrillar aggregates, which hardly diffuse through the gel and thus remain adjacent to the gel pockets, were absent for both A β_{1-42} preparations. These results correspond well to the

described A β globulomer preparation published in Barghorn et al. (2005). We therefore used this preparation in our subsequent studies.

3.1 Effects of Oligomeric A β on Synaptic Transmission are Calcium Channel-Dependent

AD leads to progressive worsening of memory formation and retrieval in patients. One of the brain regions earliest affected by AD is the hippocampus (Scoville and Milner, 1957), a brain region necessary for memory and learning. Within the hippocampus, the excitatory, glutamatergic Schaffer collateral-CA1 synapse has been extensively studied. It is involved in activity-dependent plasticity such as short-term and LTP and can be easily studied due to its laminar projections. Because of this, this synapse has served as a classical model for elucidating the basics of learning and memory (Bliss and Collingridge, 1993).

Here it was investigated whether A β oligomer-induced functional deficits could be reversed by blocking calcium channels. To this end we examined extracellular field potentials from evoked synaptic responses in the CA1 region of the hippocampus after stimulation of the Schaffer collateral synapse in rat hippocampal organotypic slice cultures, as previously described by Nimmrich et al. (2010). (Data obtained from hippocampal slice cultures was partly generated by Tanja Georgi and Michaela Müller). Overnight incubation with 83 nM A β globulomer (corresponding to 1 μ M monomeric A β ₁₋₄₂ peptide, see methods) was sufficient to decrease excitatory synaptic transmission compared to control application (Figure 3.2). Specific block of P/Q-type calcium channels with 500 nM ω -agatoxin IVA, a concentration above its IC₅₀ value for P/Q-type calcium channels (Bourinet et al., 1999), successfully prevented synaptic decline (Figure 3.2A; $p < 0.001$, two-way RM ANOVA, Holm-Sidak post hoc; $n = 6-7$ slices per group). By contrast application of 500 nM ω -agatoxin IVA alone did not change synaptic transmission. Next we collected evidence that preventing a direct interaction of A β globulomer with the P/Q-type calcium channel could ameliorate functional deficits in slice cultures. We saturated binding sites at the P/Q-type calcium channels with a polyclonal P/Q antibody for 2 h prior to A β globulomer treatment, which prevented deficits in synaptic transmission (Figure 3.2C; $p < 0.05$; $n = 8-11$ per group). Application of the antibody alone had no

significant effect on synaptic transmission (Figure 3.2D; $p = 0.11$; $n = 10-11$ slices per group). These data indicate that a direct interaction of A β globulomer with the P/Q-type calcium channel causes synaptic impairment.

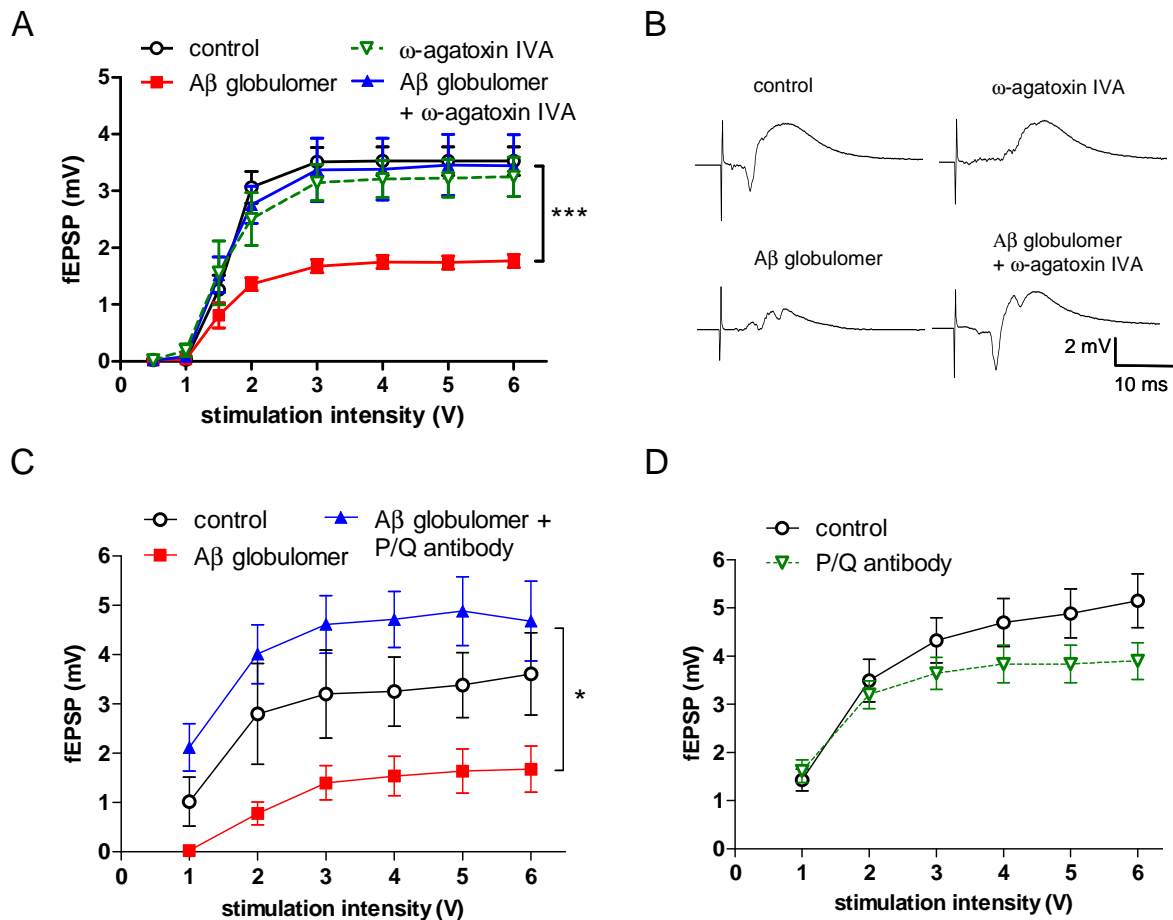


Figure 3.2 Effects of P/Q calcium channel modulation on A β globulomer-induced functional synaptic deficits. Organotypic slice cultures were treated overnight with A β globulomer and compounds. After washout excitatory synaptic transmission was investigated via input-output curves at the Schaffer collateral-CA1 synapse. fEPSP amplitude was decreased after application of 83 nM A β globulomer in A-C, indicating synaptic degeneration. All compounds were applied above their IC₅₀ values. (A) The P/Q-type calcium channel specific blocker ω -agatoxin IVA (500 nM, constituting a concentration above the IC₅₀ value (Bourinet et al., 1999) reverses A β globulomer-induced deficits in excitatory synaptic transmission. This effect was not due to an intrinsic effect of 500 nM ω -agatoxin IVA. (B) Representative current trace examples from A. The stimulation artifact at the beginning of each trace is followed by the resulting fEPSP response, which decreases in amplitude after A β globulomer treatment. (C) Pre-saturation of slice cultures with 2 nM polyclonal P/Q antibody (sc-16228) for 2 h prevents A β globulomer-induced functional deficits in excitatory synaptic transmission. (D) Application of the P/Q antibody alone does not significantly alter neurotransmission. * $p < 0.05$, *** $p < 0.001$, two-way RM ANOVA; Holm-Sidak *post hoc*. (Adapted from Hermann et al. (2013a), submitted)

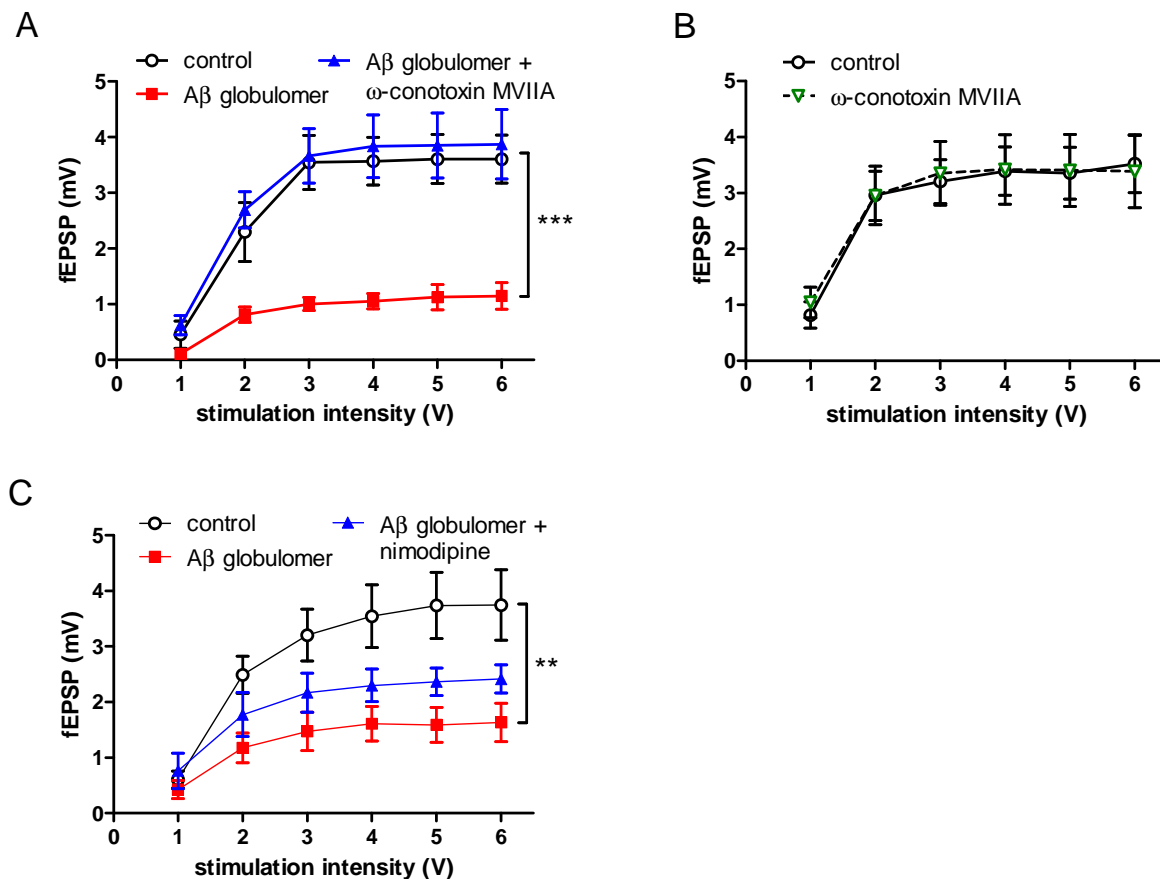


Figure 3.3 Effects of N-type and L-type calcium channel blockers on Aβ globulomer-induced functional deficits in synaptic transmission. (A) Specific N-type calcium channel blockade by 100 nM ω-conotoxin MVIIA protected from Aβ globulomer toxicity. (B) This concentration of ω-conotoxin MVIIA alone left fEPSP amplitude unaltered. (C) In contrast, 10 μM nimodipine, which preferentially blocks L-type calcium channels, did not reverse synaptic deficits induced by 83 nM Aβ globulomer. ** $p < 0.01$, *** $p < 0.001$, two-way RM ANOVA; Holm-Sidak *post hoc*. (Hermann et al. (2013a), submitted).

To test the specificity of this effect we also tested the potential of other calcium channel blockers on restoring synaptic transmission. Specific block of N-type calcium channels with 100 nM ω-conotoxin MVIIA, a concentration above published IC_{50} values (Kaneko et al., 2002), also ameliorated Aβ globulomer-induced deficits in synaptic transmission (Figure 3.3A; $p < 0.001$; $n = 8$ slices per group). This concentration of ω-conotoxin MVIIA did not alter synaptic transmission when applied alone (Figure 3.3B; $n = 8$ slices per group). In contrast, 10 μM nimodipine, did not restore Aβ globulomer-induced deficits (Figure 3.3C; $p = 0.21$; $n = 8$ slices per group). This compound blocks L-type calcium channels at IC_{50} s in the low single digit μM concentrations or below and possibly also other HVA calcium currents at 2-10-fold higher concentrations (Diochot et al., 1995; Xu and Lipscombe, 2001).

In summary, specific block of P/Q-type and N-type calcium channels reversed A β globulomer-induced functional deficits in synaptic transmission, whereas block of L-type calcium channels was ineffective.

3.2 Oligomeric A β Modulates Recombinant Calcium Channels

From these and previous (Nimmrich et al., 2008a) findings, we attempted to further characterize the effect of A β globulomer on P/Q-type and N-type calcium channels. For this, we studied recombinant channels expressed in HEK293 cells. Before testing the effect of acute A β oligomers, we first validated functional channel expression by analysis of their standard biophysical and pharmacological properties applying patch clamp whole-cell analysis.

3.2.1 Biophysical and Pharmacological Validation of Functional Channel Expression

We made use of several cell clones stably transfected with the accessory $\beta_{1.1}$ and $\alpha_{2\delta_1}$ as well as the pore-forming tetracycline-inducible α_{1A} subunit provided by Dr. Mario Mezler. Channel expression was previously tested in a FLIPR-based assay, by Dr. Mario Mezler, measuring intracellular calcium influx, which is triggered by raising the external KCl concentration. The FLIPR assay protocol and inducible channel expression was also functionally characterized by electrophysiological patch clamp recordings.

In order to pre-select cell clones which potentially exhibit functional channel expression, initial screening of 80 single cell clones (carried out by Dr. Mezler) resulted in the identification of cell lines with high and reliable potassium-induced calcium signals (60 mM KCl and 10 mM CaCl₂). Figure 3.4 shows the response of single clones after induction of channel expression with different tetracycline concentrations. For 3 selected cell subclones, K8-11, K1-19, and K1-33, Dr. Mezler evaluated the concentration/response-relation of KCl. These 3 lines were studied under both tetracycline-induced and non-induced conditions (Figure 3.4A; n = 2 per group). The EC₅₀ values after tetracycline induction ranged from 35 to 40 mM for all three subclones. Notably, clones K8-11 and K1-33 responded only weakly to KCl

stimulation under non-induced conditions (maximal signal of 19% and 14% relative to induced response). In contrast the response of the clone K1-19 did not differ between induced and non-induced state (maximal signal 89% relative to induced response) indicating that transfection of the pore forming subunit resulted in loss or a silencing of the tetracycline-on promoter in this clone.

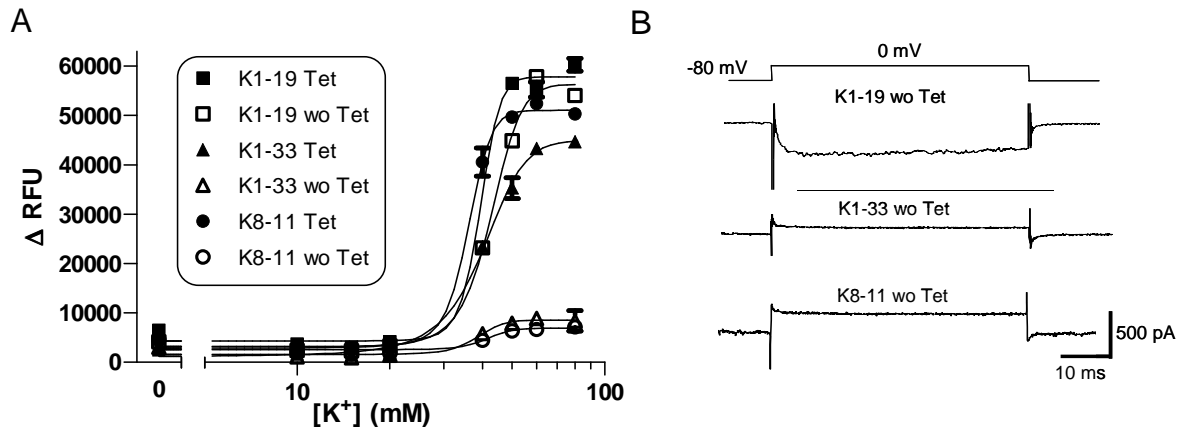


Figure 3.4 Characterization of selected cell lines with inducible P/Q-type calcium channel expression. (A) Concentration-response curve of KCl in three selected cell clones from FLIPR measurements. Tetracycline (Tet) induction is indicated by closed symbols, no induction (wo Tet) by open symbols. Cells were stimulated with buffer containing high potassium (60 mM KCl and 10 mM $CaCl_2$). While cell clone K1-19 responds to KCl depolarization with or without tetracycline induction (\blacksquare ; \square), clones K1-33 (\blacktriangle ; \triangle) and K8-11 (\bullet ; \circ) demonstrate tetracycline-dependent responses. (B) Representative example traces from manual whole-cell recordings of non-tetracycline induced cells. Similar to the results obtained from A, cell clone K1-19 reveals inward currents without previous tetracycline induction unlike K1-33 and K8-11. The corresponding voltage protocol is shown in the upper panel. (A from Mezler et al. (2012b))

As part of this PhD thesis, functional channel expression was further validated by a more direct electrophysiological approach, namely by voltage and current clamp manual patch clamp recordings (Figure 3.4B). Without tetracycline induction clone K1-19 showed significant inward currents, whereas for clone K1-33 and K8-11 ($n = 2$ each) no inward currents were detectable and only passive (leak) currents were measured. As a consequence, electrophysiological and FLIPR-based recordings yielded the similar result that K8-11 and K1-33 were two possible candidate subclones. Here, K8-11 was chosen for all further analysis. K1-33 may function as a backup cell line.

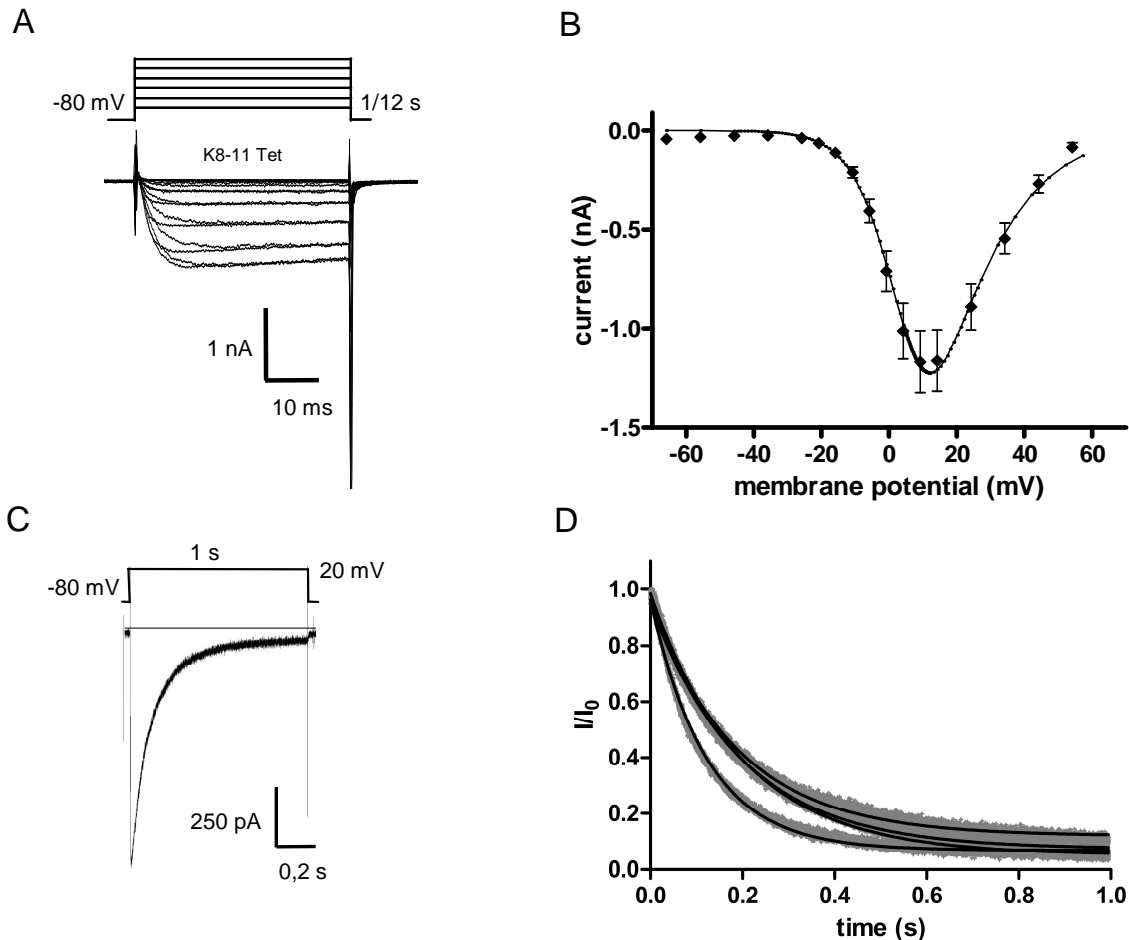


Figure 3.5 Basic biophysical characterization of P/Q-type calcium channels. Steady-state activation and open-state inactivation of P/Q-type calcium channels was recorded from tetracycline-induced HEK293 cells (clone K8-11), recombinantly expressing the full tripartite P/Q-type calcium channel, using manual whole-cell recordings. (A) Voltage protocol (upper inset) and corresponding raw traces applying 50 ms test pulses in voltage-clamp mode. (B) Averaged I-V relationships. The line represents the fit obtained from the GHK-equation. (C) Representative current trace during a 1 s test pulse showing rapid activation and gradual inactivation. Upper inset: Corresponding voltage protocol. (D) Open-state inactivation from four cells plotted as current (normalized to the peak amplitude) vs. depolarization time (grey = raw data, black = exponential fit). (Hermann et al. (2013b))

In order to further validate functional P/Q-type calcium channel expression, we analyzed the voltage-dependence of activation as well as the inactivation during sustained depolarization (open-state inactivation) applying manual whole-cell recordings. The obtained results were subsequently compared to data from previous reports on recombinantly expressed channels. Following tetracycline-induction, cells (clone K8-11) expressed voltage-dependent currents which qualitatively correspond to P/Q-type calcium channel characteristics (Bourinet et al., 1999), including the

expected kinetics of activation and open-state inactivation (Figure 3.5A, C). As shown in Figure 3.4B (p.60) and Figure 3.12A+B (p.78), without tetracycline-induction no inward currents could be recorded serving as negative expression control. I-V relationships from tetracycline-induced cells (Figure 3.5B; $n = 26$) exhibited that for each test pulse potential, the resulting peak current amplitude was reached within 20 ms. The maximum of the I-V relationship was induced at command voltages between 10 and 20 mV (corresponding to 4.2 and 14.2 mV, respectively, after correction for liquid junction potential). In order to obtain a strong current amplitude and, thus, a low signal-to-noise ratio for future recordings, all subsequent experiments utilized depolarizing test pulses to 20 mV (14.2 mV if corrected for liquid junction potential). Prolonged test pulse potentials to 20 mV revealed strong open-state inactivation by $93.7 \pm 1.0\%$ (Figure 3.5D; $n = 4$) of the initial peak amplitude after a depolarization time of 1 s. Current decay followed a single exponential function with an averaged decay time constant $\lambda = 178 \pm 19$ ms, indicative of P/Q-type calcium channel-like state transitions (Hans et al., 1999). These activation and open-state inactivation properties are comparable to previous reports on recombinant P/Q-type calcium channels using a similar splice variant and subunit composition (Bourinet et al., 1999; Hans et al., 1999).

After initial current characterization we carried on with a pharmacological investigation of the recombinant P/Q-type calcium channel, in order to estimate the sensitivity of our calcium channel currents to reference compounds compared to reports from literature. In addition, the specificity of selective calcium channel blockers was tested on our recombinant cell lines. Using a test pulse potential to 20 mV application of the P/Q-type calcium channel specific toxin ω -agatoxin IVA decreased currents with an $IC_{50} = 237$ nM (Figure 3.7A). In contrast, the N-type calcium channel specific blocker ω -conotoxin MVIIA, which blocks N-type currents in the low nanomolar range (Kaneko et al., 2002), did not decrease P/Q-type calcium channel currents up to a concentration of 30 μ M (Figure 3.7A+B). Toxins were applied cumulatively with an 8 min incubation period for each concentration to obtain steady-state block. Currents were normalized to time-matched controls (Figure 3.7A; $n = 5 / 4-6 / 7$ for ω -agatoxin IVA / ω -conotoxin MVIIA / control per concentration).

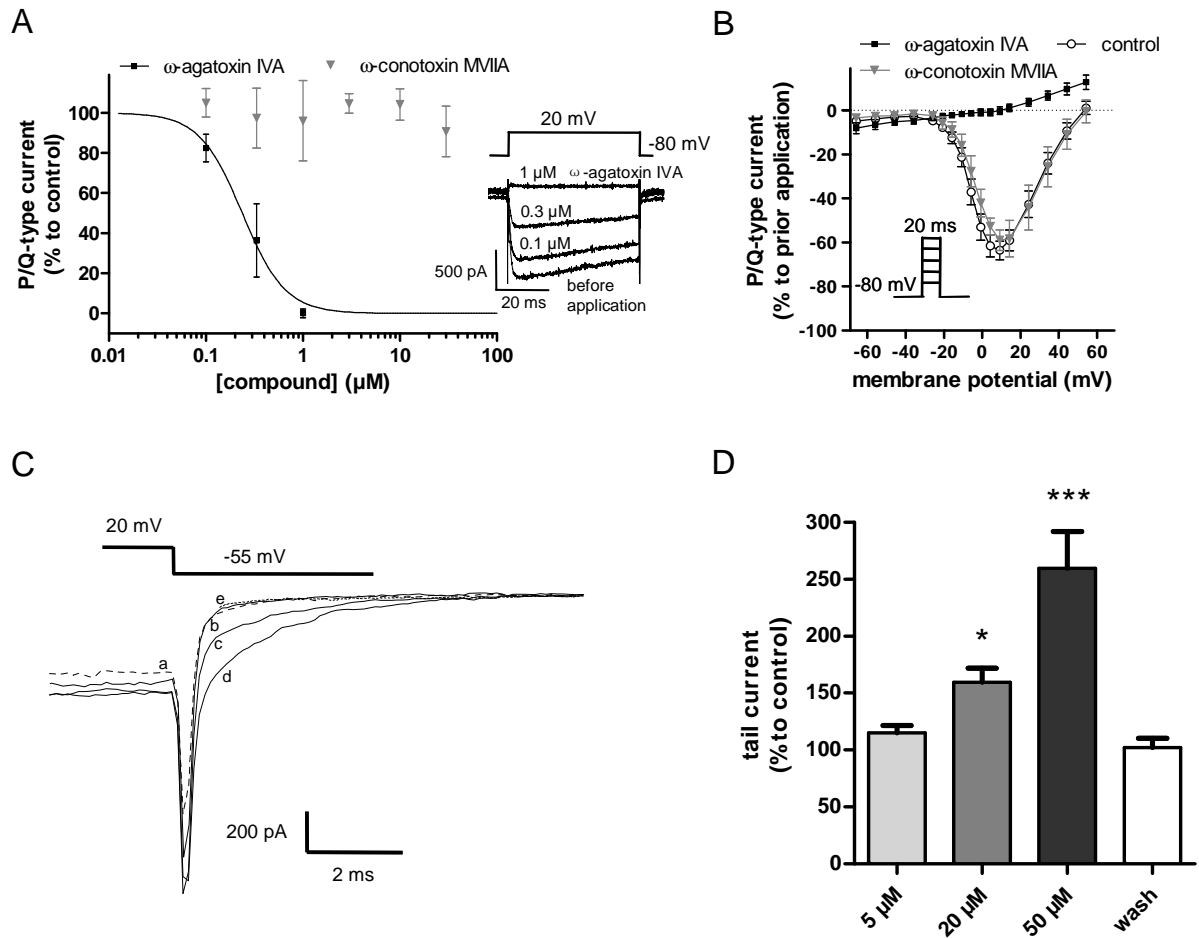


Figure 3.6 Pharmacological validation of P/Q-type calcium channels. (A) Concentration-response curve of ω -agatoxin IVA and ω -conotoxin MVIIA obtained from manual whole-cell recordings on HEK293 cells recombinantly expressing the full tripartite P/Q-type calcium channel. Channels were activated by step depolarizations from -80 to 20 mV for 50 ms. Currents were normalized to time-matched controls under buffer application. Right inset: Representative current response during depolarization to 20 mV of a cell before and after application of cumulative concentrations of ω -agatoxin IVA. (B) Channel activation (I-V relationship) of the recombinant P/Q-type calcium channel was suppressed by ω -agatoxin IVA, but not by ω -conotoxin MVIIA compared to control. Inset: Corresponding voltage protocol. (C) Enhancement of P/Q tail currents by roscovitine is illustrated by superimposed tail current traces from a representative cell induced by hyperpolarization from 20 to -55 mV. Roscovitine was added in a cumulative fashion with the sequence a) control (dotted line), b) 5 μ M roscovitine, c) 20 μ M roscovitine, d) 50 μ M roscovitine, e) washout (dashed line). (D) Quantitative results obtained from C. While 5 μ M roscovitine only tended to increase the tail current, the increases at 20 and 50 μ M were significant. Washout completely reversed the effect. * $p < 0.05$, *** $p < 0.001$, one-way ANOVA, Dunnett's *post hoc*. (A+B from Hermann et al. (2013a, submitted); C+D from Mezler et al. (2012b))

The potency of ω -agatoxin IVA was in the expected range for recombinant P/Q-type calcium channels containing a –NP– sequence at domain IV S3-S4 (Bourinet et al., 1999) indicating that our recombinant cell line exhibits the expected sensitivity to pharmacological modulation by peptide channel toxins. Furthermore, 1 μ M ω -agatoxin IVA fully blocked currents across all voltage steps, while ω -conotoxin MVIIA treatment did not change the I-V relationship at any voltage applied compared to control (Figure 3.6B; n = 5 / 4 / 6 for ω -agatoxin IVA / ω -conotoxin MVIIA / control). This strongly indicates that the current recorded is fully mediated by P/Q-type calcium channels.

In order to test if also LMW compounds affect the recombinant calcium channels properly we applied roscovitine, which has been described to enhance the tail current after quick hyperpolarization from a depolarized potential. This is because channel gating is modulated, including a slowing of the deactivation kinetics of the activated P/Q channel (Buraei et al., 2005). So this compound can provide hints about whether appropriate gating mechanisms are present in our recombinant channels. Roscovitine concentration-dependently enhanced the tail current in our P/Q-type calcium channel expressing cell line. The increase in tail current was significant at 20 μ M and 50 μ M after 2 min of compound application (Figure 3.6D; $159 \pm 13\%^*$ and $260 \pm 33\%^{***}$; *p < 0.05, ***p < 0.001, one-way RM ANOVA, Dunnett's post hoc; n = 13). After a washout of 1 min the tail current returned to baseline ($102 \pm 8\%$). Taken together, we conclude that following tetracycline-induction our P/Q-type calcium channel transfected cells express functional P/Q-type calcium channels, displaying proper characteristics comparable to published data. We therefore considered these cells suitable for investigating the effect of A β oligomers on P/Q-type calcium channels and to search for novel antagonists in drug screening efforts as recently published in Mezler et al. (2012b).

After validation of the P/Q-type calcium channel expressing cell line, we similarly investigated our recombinant N-type calcium channel expressing cell line (Figure 3.7). From FLIPR experiments cell clone 26 was pre-selected (by Dr. Mario Mezler, data not shown), which was used for all subsequent electrophysiological experiments. In order to examine functional channel expression, initial patch clamp experiments characterized channel activation. Upon depolarization, the shape of the raw trace and the resulting I-V relationship appeared qualitatively similar when

compared to the recombinant P/Q-type calcium channel (Figure 3.7A; $n = 11$). However, the maximum peak current of the N-type current occurred at slightly less depolarized values and was obtained around 10 mV step potential (4.2 mV when corrected for liquid junction potential).

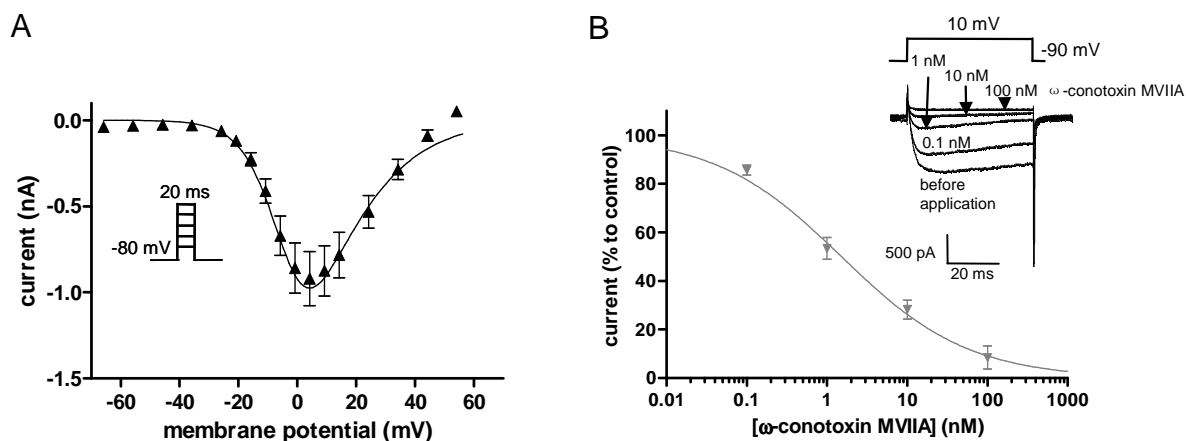


Figure 3.7 Biophysical and pharmacological validation of N-type calcium channel channels. (A) Channel activation of the full tripartite N-type calcium channel recombinantly expressed in HEK293 cells was investigated by I-V relationships using manual whole-cell recordings. The line represents the fit obtained from the GHK-equation. Inset: Corresponding voltage protocol. (B) Concentration-response curve of ω -conotoxin MVIIA on N-type currents. These were blocked by cumulative application (4 min per concentration) of ω -conotoxin MVIIA with an $IC_{50} = 1.5$ nM. N-type currents were evoked by depolarization from -90 to 10 mV for 50 ms and normalized to time-matched controls under buffer application. Inset: Representative peak currents before and after cumulative application of ω -conotoxin MVIIA. (B from Hermann et al. (2013a, submitted))

We then investigated the pharmacological sensitivity of the cell line. As expected, in contrast to the P/Q-type calcium channel expressing cell line, currents in the cell line recombinantly expressing the N-type calcium channel were potently blocked after 4 min application of the N-type specific toxin ω -conotoxin MVIIA with an $IC_{50} = 1.5$ nM, applying a step potential from -90 to 10 mV. Unlike for recordings on P/Q-type calcium channels, a holding potential of -90 mV was applied here, because increased run-down was observed at -80 mV for the recombinant N-type calcium channel currents. Values were normalized to time-matched controls (Figure 3.7B; $n = 3-7 / 4$ for ω -conotoxin MVIIA / control per concentration). These findings compare well to previous findings on similar human N-type calcium channel splice variants (Kaneko et al., 2002) indicating that our recombinant N-type calcium channels are sensitive to

pharmacological modulation and fulfill the main distinguishing feature compared to P/Q-type calcium channels (through sensitivity to ω -conotoxin MVIIA, see chapter 1.2.1). We consequently considered functional channel expression as validated and suitable for analyzing the effect of A β oligomers on N-type calcium channels.

3.2.2 A β Oligomers Facilitate Channel Activation at Intermediate Depolarized Potentials

After validation of functional P/Q-type and N-type calcium channel expression, we investigated whether and how A β globulomer modulates these channels. We revealed that acute, non-cumulative (i.e. one concentration of a pharmacological agent per cell) application of A β globulomer affected voltage-dependent activation but not inactivation of the recombinant P/Q-type calcium channels (Figure 3.8).

The I-V relationship illustrates that the peak current amplitude was altered at some test potentials 10 min after application of 830 nM A β globulomer (corresponding to 10 μ M A β ₁₋₄₂ peptide (see methods); Figure 3.8A; n = 5-7 cells per group). However, the maximum of the I/V relationship occurred at similar membrane voltages for all A β globulomer concentrations. These findings were supported by quantitative analysis using activation parameters obtained from the best fit of the GHK-equation. The voltage at half activation V_h was shifted to more hyperpolarized values for the steady-state activation curve after application of 830 nM A β globulomer (Figure 3.8B+C; for control / 8 nM / 83 nM / 830 nM A β globulomer: $V_h = 6.9 \pm 2.3$ mV / 3.0 ± 1.6 mV / 4.7 ± 2.4 mV / -4.6 ± 2.1 mV^{**}; ^{**}p < 0.01, Student's t-test). This indicates that A β globulomer modulates the voltage-dependence of activation and therefore channel gating of recombinant P/Q-type calcium channels. In contrast, both the maximum conductance g_{max} and the slope of the I-V relationship V_C remained unchanged (Figure 3.8C; for control / 8 nM / 83 nM / 830 nM A β globulomer: $g_{max} = 133 \pm 42$ nS / 148 ± 26 nS / 229 ± 78 nS / 125 ± 36 nS; $V_C = -6.1 \pm 0.2$ mV / -6.4 ± 0.3 mV / -5.9 ± 0.2 mV / -6.2 ± 0.3 mV). This suggests that the conductance of each channel and the voltage range in which channel opening occurs, seen by an unchanged slope of the activation curve in Figure 3.8B, remain unaltered.

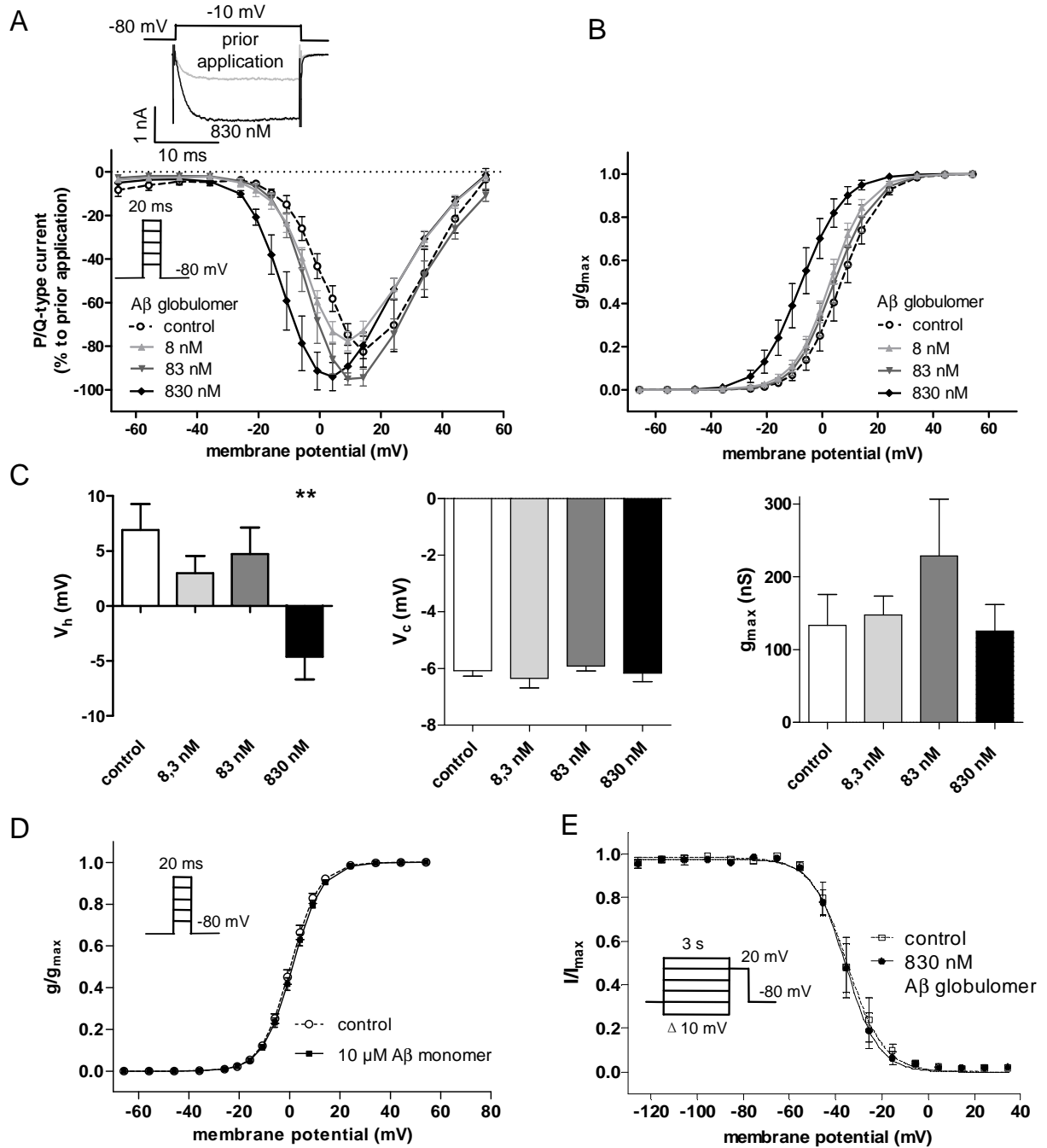


Figure 3.8 Modulation of P/Q-type calcium channels by A β globulomer. (A) The I-V relationship, obtained from manual patch clamp recordings on our P/Q-type calcium channel expressing cell line, was shifted to more hyperpolarized values after 10 min of A β globulomer application. Upper inset: Representative raw trace depolarized from -80 to -10 mV before and after application of 830 nM A β globulomer. Lower inset: Voltage protocol for I-V relationship. Cells were depolarized to the corresponding test potential for 20 ms. Each cell received only a single dose ($n = 5-7$ per concentration). (B) Steady-state activation curve of recombinant P/Q-type calcium channels generated with the parameters derived from the GHK-fit. 830 nM A β globulomer shifts the activation curve to more hyperpolarized potentials. (C) Activation parameters from the GHK-equation yield a difference in the voltage

at half activation V_h after application of 830 nM A β globulomer, but no differences in the maximum conductance g_{max} and the slope of the I-V relationship V_c for all concentrations tested. (D) Steady-state activation curve after 10 min of 10 μ M A β_{1-42} monomer application (corresponding to 830 nM A β globulomer complex). A β_{1-42} monomer does not influence the voltage at half-activation V_h . (E) Steady-state inactivation curve after 10 min of A β globulomer application. Unlike the activation curve, the inactivation curve remained unchanged by 830nM A β globulomer when compared to control. Both the voltage at half inactivation as well as the slope of the inactivation curve was similar between treatments. ** $p < 0.01$, one-way ANOVA, Dunnett's *post hoc* vs. control. (Hermann et al. (2013a, submitted))

The corresponding concentration of freshly dissolved monomeric A β_{1-42} peptide (10 μ M) did not influence the voltage at half activation V_h (Figure 3.8D; for control / A β_{1-42} monomer: $V_h = 0.4 \pm 0.8$ mV / 1.1 ± 0.7 mV; $n = 4 / 5$ per group), the slope of the first-order Boltzmann equation V_c as well as the maximal conductance g_{max} (data not shown). This indicates that the previously observed effects on V_h were specific to A β globulomer and were not caused by the A β peptide per se.

In order to reveal whether A β globulomer also modifies voltage-dependent channel inactivation, we also examined the inactivation curve after application of 830 nM A β globulomer. Inactivation was induced by 3 s prepulses, which is a duration commonly used to inactivate calcium channels (e.g., Nimrich et al., 2008a) and was, here, sufficient to induce full inactivation (see also Figure 3.11, p.75). Prepulses were followed by a short 20 ms test pulse to 20 mV to activate the remaining, non-inactivated channels. As illustrated in Figure 3.8A+B, at this test potential no or very few effects are observed on channel activation, so that the resulting inactivation curve should not be altered due to effects on channel activation. This enabled us to exclusively study possible effects on voltage-dependent inactivation. We found that, unlike the voltage at half-activation V_h , the voltage at half-inactivation V_{inact} remained similar (Figure 3.8E; for control / 830 nM A β globulomer: $V_{inact} = -34.9 \pm 1.0$ mV / -35.7 ± 0.8 mV), suggesting that voltage-dependent inactivation remains unaltered by A β globulomer.

Taken together, this indicates that A β globulomer increases the probability of P/Q-type calcium channel opening at intermediately depolarized potential values (between -30 and 20 mV) without affecting channel inactivation. As A β globulomer

does not uniformly modulate all voltage-dependent properties of these channels unspecifically, these results would support a rather distinct mechanism of action. On a synaptic level, this modulation of P/Q-type calcium channel function would result in facilitated calcium influx upon action potential arrival at the presynapse and may increase neurotransmitter release.

Since block of N-type calcium channels also rescued A β -induced functional synaptic deficits in hippocampal slice cultures illustrated in Figure 3.3 (p.58), we also tested the effect of A β globulomer on the closely homologous N-type calcium channel (Catterall et al., 2005). As noted previously, to minimize run-down for N-type calcium channel recordings a holding potential of -90 instead of -80 mV was applied. After 10 min application of 830 nM A β globulomer, a shift in channel activation was observed as visualized by the I-V relationship and the activation curve (Figure 3.9A+B; n = 5). Quantitative analysis of activation parameters yielded a significant shift of V_h (Figure 3.9C; for control / 830 nM A β globulomer: $V_h = -0.9 \pm 1.0$ mV / -8.4 ± 4.7 mV^{**}; ^{**}p < 0.01, Student's t-test). As for the P/Q-type calcium channel, no difference in the slope of the I-V relationship and the maximal conductance was observed (Figure 3.9C; for control / 830 nM A β globulomer: $V_c = -6.1 \pm 0.1$ mV / -6.4 ± 0.4 mV; $g_{max} = 101 \pm 25$ nS / 106 ± 45 nS). In analogy to the results obtained from recombinant P/Q-type calcium channels, this suggests that voltage-dependent N-type calcium channel opening occurs at more hyperpolarized values. At the same time the relative voltage range in which channel opening can occur and the absolute conductivity of the channels is not affected.

We subsequently investigated inactivation properties of the N-type calcium channel after application of 830 nM A β globulomer by application of 3 s prepulses. To maximize the signal-to-noise ratio a test pulse potential of 10 mV was applied. At this potential only minor effects of A β globulomer on channel activation are expected (Figure 3.9A+B) so that predominately effects of channel inactivation can be analyzed. We found no significant shift of the inactivation curve compared to control (Figure 3.9D; for control / 830 nM A β globulomer: -55.1 ± 0.7 mV / -56.7 ± 0.4 mV; n = 3). This suggests that voltage-dependent inactivation of the N-type calcium channel is not influenced by A β globulomer, as observed for the P/Q-type calcium channel.

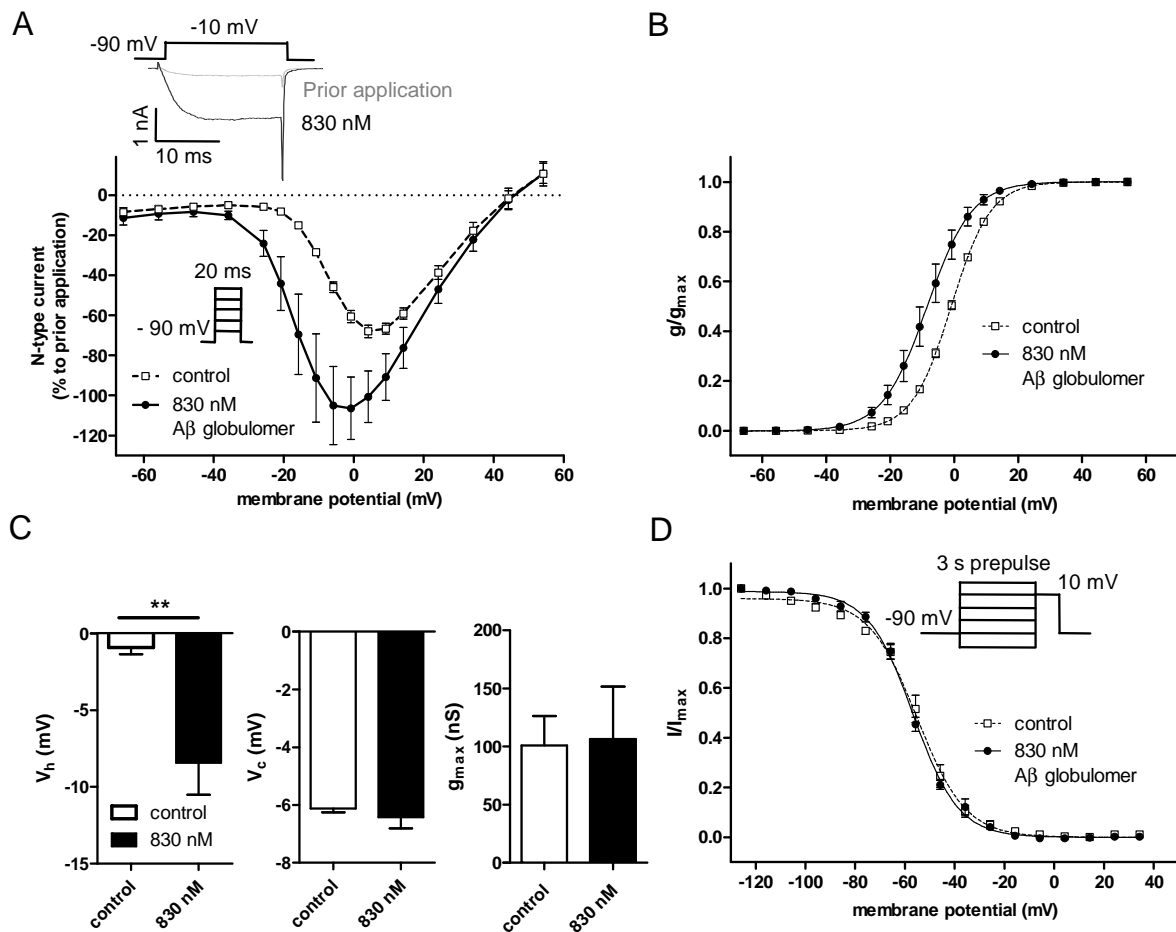


Figure 3.9 Modulation of N-type calcium channels by A β globulomer.

(A) I-V relationship after 10 min of A β globulomer application is shifted to more hyperpolarized potentials as compared to control application using manual whole-cell recordings of our N-type calcium channel expressing cell line. Upper inset: Representative raw trace depolarized to a test potential of -10 mV before and after application of 830 nM A β globulomer. Lower inset: Voltage protocol for I-V relationship. Cells were depolarized to the test potential for 20 ms. (B) Steady-state activation curve of N-type calcium channels calculated from A illustrates a shift to more hyperpolarized potentials after application of 830 nM A β globulomer. (C) Activation parameters derived from A using the GHK-equation yields a left shift in voltage at half activation V_h for 830 nM A β globulomer, but no differences in the maximum conductance g_{max} and the slope of the I-V relationship V_c were found. (D) The inactivation curve remains unaltered by application of 830 nM A β globulomer as compared to control. ** $p < 0.01$, Student's t-test. (Hermann et al. (2013a, submitted))

To conclude, A β globulomer shifted voltage-dependent activation to hyperpolarized values for both the N-type and P/Q-type calcium channel, without altering voltage-dependent inactivation.

3.2.3 Effects of A β Oligomers Appear to be Independent of Channel State

In order to elucidate the effect of A β globulomer on P/Q-type calcium channels in further detail, we examined its time-course and tested for possible state-dependent effects. For this, we compared the effect of A β globulomer application on recombinant P/Q-type calcium channels while giving test pulses either directly from the holding potential of -80 mV (denoted as resting state) or after a depolarizing 3 s prepulse (denoted as inactivated state, Figure 3.10). The prepulse voltage was adjusted for each cell so that about 50% of the channels were inactivated. Test pulses were given at -10 mV, because at this potential a strong current increase can be expected after A β globulomer application (see Figure 3.8A, p.67, and Figure 3.9A, p.70). Here, A β globulomer was applied cumulatively and incubated for only 2 min, as the observed current increase already reached a steady state within one or two sweeps given at a 12 s interval (Figure 3.10A). This, on the one hand, validates that the incubation times for previous patch clamp experiments on A β globulomer were sufficient. On the other hand, the lack of accumulating current increase after subsequent sweeps does not suggest frequency-dependent effects using these intersweep intervals. As expected from the previous experiments, 830 nM A β globulomer significantly increased peak currents. This increase in peak current was similar for resting and inactivated states, regardless of whether the different protocols were compared directly (data not shown) or data was corrected for run-down against the corresponding time-matched control (Figure 3.10A). Likewise, statistical analysis of the peak currents 2 min after cumulative application of A β globulomer resulted in a significant increase at 830 nM, but no significant differences between the two protocols (Figure 3.10B). The increase in current amplitude was reversible upon wash out. Currents already tended to increase at 83 nM for both protocols compared to baseline level without reaching statistical significance using a two-way RM ANOVA (resting / inactivated state protocol (% to control): $I_{8nM} = 102 \pm 3\% / 102 \pm 5\%$; $I_{83nM} = 155 \pm 12\% / 169 \pm 16\%$; $I_{830nM} = 379 \pm 82\%^{***} / 451 \pm 97\%^{***}$; $I_{wash} = 127 \pm 31\% / 154 \pm 43\%$; $^{***}p < 0.001$, two-way RM ANOVA, Dunnett's post hoc vs. control; resting state: $n = 7 / 4$ for A β globulomer / control, inactivation protocol: $n = 7 / 5$ for A β globulomer / control).

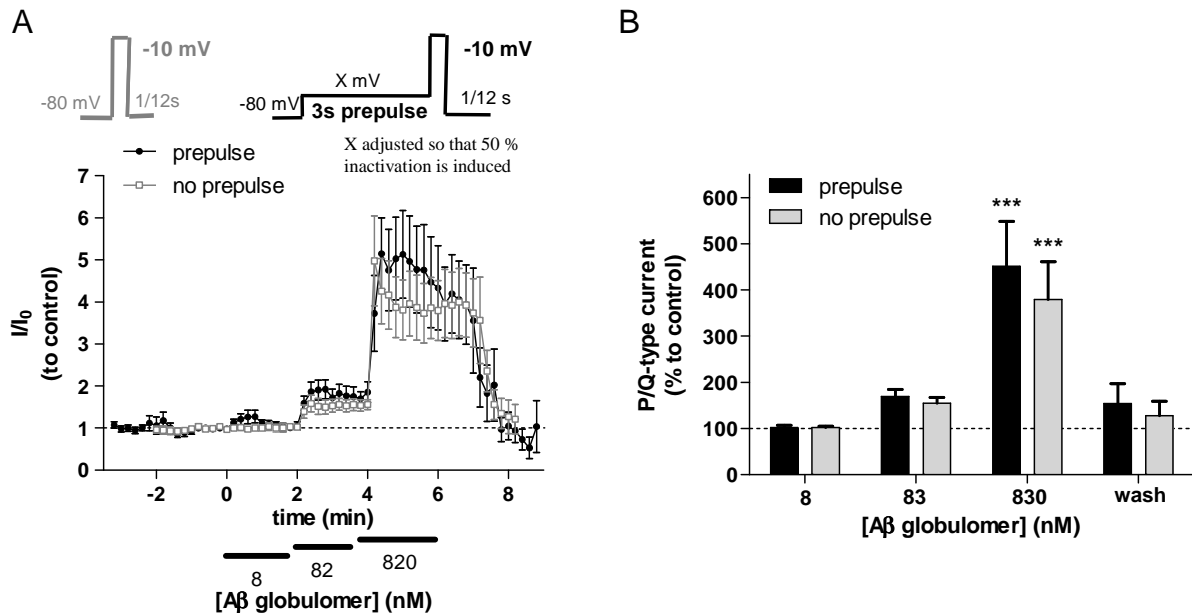


Figure 3.10 Effect of A β globulomer on different P/Q-type calcium channel states.

(A) Time course of the peak current response after stepping from -80 to a test potential of -10 mV during increasing doses of A β globulomer at time points 0, 2, and 4 min. These manual whole-cell recordings were carried out by applying an inactivation protocol (black) and resting state protocol (grey). Data was corrected for the corresponding time-matched control ($n = 5$ and $n = 4$), respectively. Upper inset: Corresponding voltage protocols. Inactivation is induced via a 3 s prepulse at a voltage X, which was set individually for each cell to induce about 50% inactivation. (B) Quantification of current increase at a test potential of -10 mV after A β globulomer application derived from A. The last 3 data points were averaged for each concentration. 830 nM A β globulomer significantly increases P/Q-type currents at a test potential of -10 mV compared to control application for both the resting and the inactivation protocol. *** $p < 0.001$; two-way RM ANOVA, Dunnett's *post hoc* vs. control. (Hermann et al. (2013a, submitted))

Combining all electrophysiological findings, these data indicate that A β globulomer leads to a rapid and state-independent increase of P/Q-type and N-type calcium channel currents at moderately depolarized potentials.

3.3 Identification of Novel State-Dependent P/Q-type Calcium Channel Blockers

After identification that block of presynaptic calcium channels can be synaptoprotective and that oligomeric A β augments presynaptic calcium channel

currents, a primary (FLIPR, Dr. Mario Mezler) and a secondary compound screen (manual and automated patch clamp) was developed to detect, validate, and functionally characterize novel channel blockers. As stated in the introduction, state-dependence is in many cases considered a desirable drug property because it may induce functional selectivity thereby improving the therapeutic window. This may in turn increase the tolerability of the drug and overall success for future clinical trials. Thus, for the development of novel calcium channel blockers, potential compounds should be investigated and ranked by their potency not only on closed and open channels, but also on inactivated channels.

3.3.1 Inactivation of Recombinant Channels Accumulates over Time

As a prerequisite for state-dependent compound evaluation an appropriate screening protocol needs to be chosen, which depends on the inactivation properties of the channel of interest. Upon action potential arrival the amount of presynaptic calcium channels available for opening depends on the fraction of inactivated channels. As HVA calcium channels, given physiological conditions, are mostly present in non-conducting closed states, inactivation from closed states may be of special importance. Therefore, understanding the precise closed-state inactivation properties of heterologously expressed P/Q-type channels serves to optimize functional screening with the aim to identify compounds targeting the inactivated state of the channel.

In order to determine voltage-dependent closed-state inactivation of P/Q-type calcium channels we applied various depolarizing prepulse durations and potentials (Figure 3.11). Varying prepulse potentials were utilized to create inactivation curves, to qualitatively examine the rate of inactivation from open and closed channel states, and to determine the voltage which induces half inactivation, which might be used for state-dependent compound characterization. Through the variation in prepulse duration we attempted to determine if steady-state inactivation was observed, which probably decreases variability between different experiments.

We found that inactivation was dependent on prepulse voltage in a non-trivial manner. Strongest inactivation was reached at intermediate to slightly stronger depolarized potentials between 0 mV and 20 mV whereas even more positive

potentials caused weaker inactivation (Figure 3.11A; $n = 4-8$ per group). The resulting U-shaped inactivation curve suggests preferential inactivation from closed channel states as indicated in previous publications (Patil et al., 1998; Gera and Byerly, 1999). These studies attributed this phenomenon to complex transition kinetics between several closed and inactivated states, which occur at a faster rate than inactivation from open states. Physiologically, this mechanism probably underlies the faster inactivation of HVA calcium channels during trains of action potentials compared to sustained depolarizations; because this mechanism implies that (partial) hyperpolarization between action potentials would result in more channel inactivation compared to a constant sustained depolarization. Detection of this complex and physiologically relevant property indicates that our recombinant P/Q-type calcium channels exhibit proper state transitions.

As V_{inact} , the voltage at half inactivation, was shifted depending on prepulse length in Figure 3.11A, we attempted to find out whether steady-state inactivation could be obtained with longer prepulses. For this, 10 s and 100 s prepulses were applied using an intersweep interval of 120 and 220 s, respectively, to allow for recovery from inactivation between sweeps. Even with these long prepulses, no steady-state inactivation was obtained, which is shown in Figure 3.11B by the linear correlation of V_{inact} with the logarithmic prepulse length ($r^2 = 0.97$; slope = -13.9 ± 1.1). The linearity implies that a 10-fold increase in prepulse duration shifts V_{inact} by about -13.9 mV to more hyperpolarized values and that no steady-state inactivation can be obtained within the range of prepulse durations tested here.

As elaborated in the discussion, for development of AD-related therapeutics we prefer to characterize state-dependent rather than use-dependent compound properties. To this end, it was determined whether the hyperpolarizing period to -80 mV between sweeps was sufficient for recovery from inactivation. Figure 3.11C shows a systematic comparison of inter-sweep intervals of 12 and 120 s in a protocol with prepulses of 3 s duration. The resulting inactivation curves were almost identical ($V_{\text{inact}} = -22.6 \pm 0.7$ mV / -22.1 ± 0.7 mV for 12 / 120 s intersweep interval; $n = 8 / 4$). Thus, intervals of 12 s between depolarizing steps allow full recovery from inactivation at 3 s prepulses. Steady-state inactivation can involve multiple states, affecting the dependence of inactivation from prepulse duration. We therefore tested the degree of inactivation at different prepulse lengths (prepulse potential -30 mV).

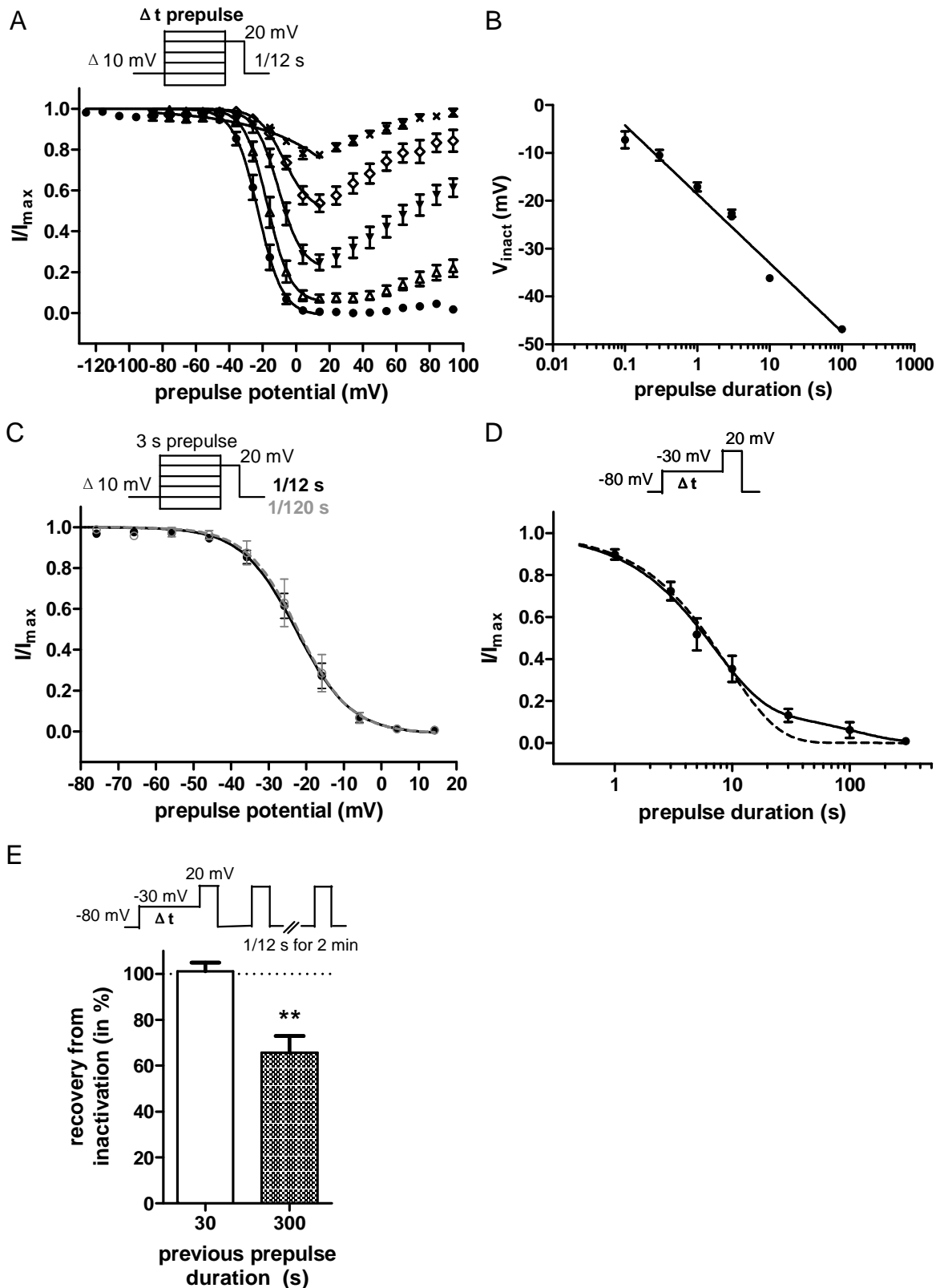


Figure 3.11 Inactivation properties of P/Q-type calcium channels.

(A) Voltage-dependent inactivation of peak currents applying manual whole-cell recordings at different prepulse lengths using test pulses from -80 to 20 mV for 20 ms (see inset). Inactivation curve dependency on prepulse length (in s: ● 3, Δ 1, \blacktriangledown 0.3, \diamond 0.1, x 0.03). Solid lines represent first-order Boltzmann fit of data for prepulses from -80 up to 20 mV. Note

incomplete inactivation for short prepulses ≤ 1 sec and decrease of inactivation at highly depolarized prepulse potentials. (B) Potential of half-maximal inactivation V_{inact} (calculated from A and additional inactivation curves utilizing longer prepulse durations) vs. prepulse length (logarithmic scale). The solid line represents the best linear fit and reveals a strong correlation ($r^2 = 0.97$). (C) Increasing the interpulse interval from 12 (\bullet , black) to 120 s (\circ , grey) does not shift the inactivation curve at a prepulse length of 3 s. Lines represent the first-order Boltzmann fit. Inset: Corresponding voltage protocol. (D) Inactivation vs. prepulse duration (prepulse potential -30 mV, see inset). Increasing prepulse length from 1 to 300 s induced increasing levels of inactivation ($n = 5-7$). Data fit with a double exponential (solid line; $r^2 = 0.89$) and single exponential (dotted line; $r^2 = 0.87$) calculated from data points at prepulse lengths ≤ 10 s. (E) Recovery from inactivation after a 2 min re-polarization phase, same experiments as in D. Inactivation was fully reversible after 30 s prepulses, but not 300 s. Inset: voltage protocol. $**p < 0.01$, Student's t-test. (Hermann et al. (2013b))

Indeed, inactivation at prepulse length >10 s could only be poorly fit by a first order exponential equation (Figure 3.11D, dotted line; $n = 5-7$ per prepulse duration), in contrast to a double exponential equation (solid line). This suggests that inactivation might be mediated by two kinetically different processes, i.e. by fast and slow inactivation (see chapter 1.2.3, p.24ff). In the same experiment, we tested for recovery from prolonged inactivation. P/Q-type currents were inactivated by prepulses of 30 or 300 s duration, respectively. We then re-polarized the cell to -80 mV for 2 min applying test pulses to 20 mV every 12 s (Figure 3.11E). Full recovery of the initial current amplitude was obtained for prepulses lasting 30 s, whereas prolonged prepulses of 300 s duration caused incomplete recovery (current recovery after inactivation: $101.0 \pm 3.9\%$ / $63.5 \pm 7.3\%^{**}$ for 30 s / 300 s prepulse duration; $**p < 0.01$, Student's t-test; $n = 6 / 5$; Figure 3.11E). Thus, prolonged depolarizing prepulses cause lasting inactivation of some fraction of the P/Q-type calcium channel mediated current indistinguishable from run-down. Although time-matched vehicle controls might compensate for that, this decay in current amplitude would nevertheless decrease the signal-to-noise ratio and increase cell-to-cell variability, which would be unfavorable for assay development.

Taken together, our recombinant P/Q-type calcium channels resemble complex inactivation properties, which are a characteristic feature of functional HVA calcium channels (Patil et al., 1998). Moreover, kinetics and recovery of inactivation strongly depend on the choice of voltage- and time-parameters. We therefore decided to

apply 3 s prepulses for future studies, which is sufficient to induce complete but still reversible inactivation,

3.3.2 Channel Activation, but not Inactivation is Similar between Manual and Automated Patch Clamp

On the basis of the previous characterization of the complex inactivation behavior of our recombinant cell line, we aimed to develop a protocol for reproducible and reversible channel inactivation, suited for pharmacological screening purposes. The more pharmacological patch-clamp experiments are carried out the higher the chance becomes to successfully identify novel, potent (state-dependent) compounds. In order to increase the number of functional pharmacological experiments, automated patch clamp is being applied, since manual electrophysiology lacks sufficient throughput. For this purpose we aimed to establish and validate a state-dependent screening protocol for automated patch clamp which mimics manual patch clamp conditions as closely as possible.

We first implemented and validated measurements on recombinant P/Q-type calcium channels on the automated system using voltage clamp analysis. Initially there was a strong rundown observed which was alleviated by addition of 5 mM BAPTA to the internal solution (data not shown). Without induction of P/Q calcium channel expression by tetracycline no appreciable current was obtained at any voltage steps, whereas after tetracycline-induction current traces were observed with a similar shape compared to previous manual patch clamp experiments on P/Q-type calcium channels (Figure 3.12A; middle / lower panel, respectively). This was also true for the I-V relationship, which revealed the maximal peak current at depolarization steps from -80 to 10 or 20 mV (Figure 3.12B, n = 10 / 22 for non-induced / induced cells, respectively).

After establishing the automated recordings from our P/Q-type calcium channel expressing cell line, we compared these measurements with manual patch clamp in detail. At first, we analyzed P/Q-type calcium channel activation by application of the same voltage protocols between the platforms, which yielded identical results for I-V relationships and the resulting activation curves (Figure 3.13A+B; data also shown in Figure 3.5B, p.61, and Figure 3.12B, below). Quantitative parameters were

not significantly different for the two patch-clamp approaches (Figure 3.13C): voltage at half activation (V_h) was 6.1 ± 0.8 mV (manual; $n = 26$) and 7.2 ± 1.0 mV (automatic; $p = 0.39$, Student's t-test; $n = 22$); slope of the I-V relationship (V_c) was -5.8 ± 0.1 mV (manual, $n = 26$) and -6.2 ± 0.2 mV (automatic, $n = 22$; $p = 0.10$); and maximal conductance (g_{max}) yielded 230 ± 33 nS (manual) and 301 ± 32 nS (automatic; $p = 0.14$). This shows that automated patch clamp yields identical results regarding P/Q-type calcium channel activation compared to manual patch clamp and is therefore applicable for investigation of channel activation.

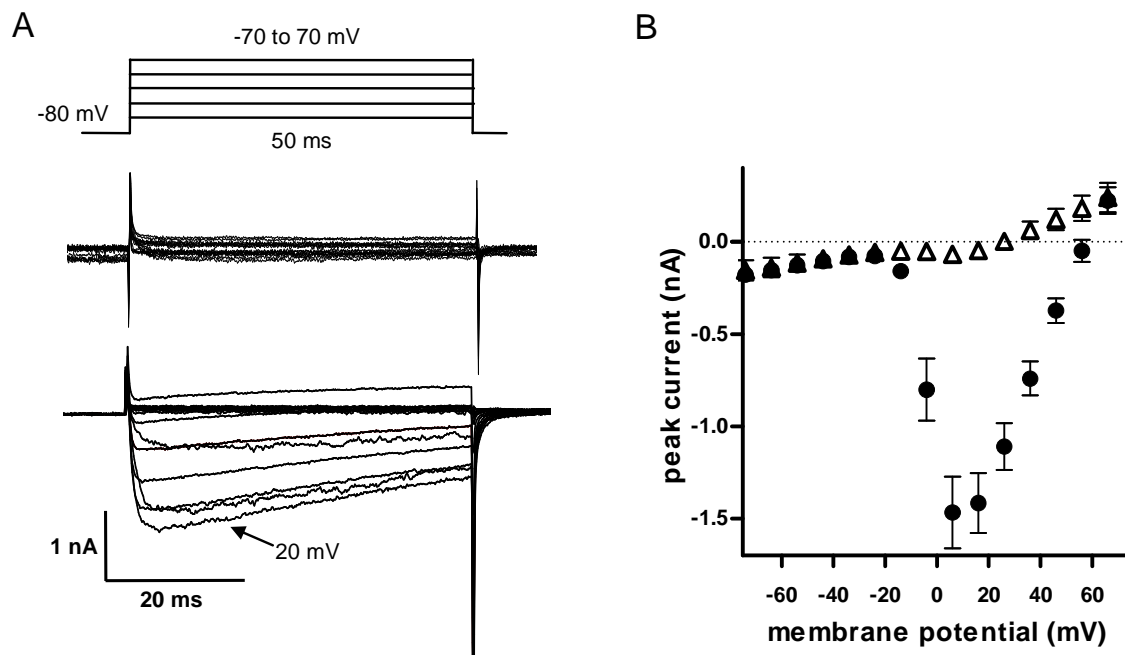


Figure 3.12 Automated electrophysiological recordings from P/Q-type calcium channels. (A) Superimposed current traces from cells without (middle panel) and 48 h after induction with tetracycline (lower panel) obtained from automated whole-cell recordings. Upper panel: Corresponding voltage protocol for I-V relationships during automated whole-cell recordings. (B) Comparison of I-V relationships from non-induced (Δ) and tetracycline-induced cells (\bullet). Only for the latter group inward currents were observed at potentials typical for HVA P/Q-type calcium channels. (Mezler et al. (2012b))

Likewise, inactivation properties were compared between both systems using the 3 s prepulse protocol. In contrast to the activation parameters, voltage at half inactivation (V_{inact}) was significantly more negative in the automatic patch clamp system (Figure 3.13E; manual / automatic: $V_{inact} = -22.5 \pm 1.8$ mV / -33.6 ± 0.9 mV^{***}, ^{***} $p < 0,001$, Student's t-test; $n = 8 / 5$). In order to elucidate the mechanism underlying this difference, we also used the same recording solutions for both systems. However,

this did not abolish or reduce the difference in inactivation curves (Figure 3.13E; V_{inact} remaining at -23.8 ± 1.1 mV; $n = 6$).

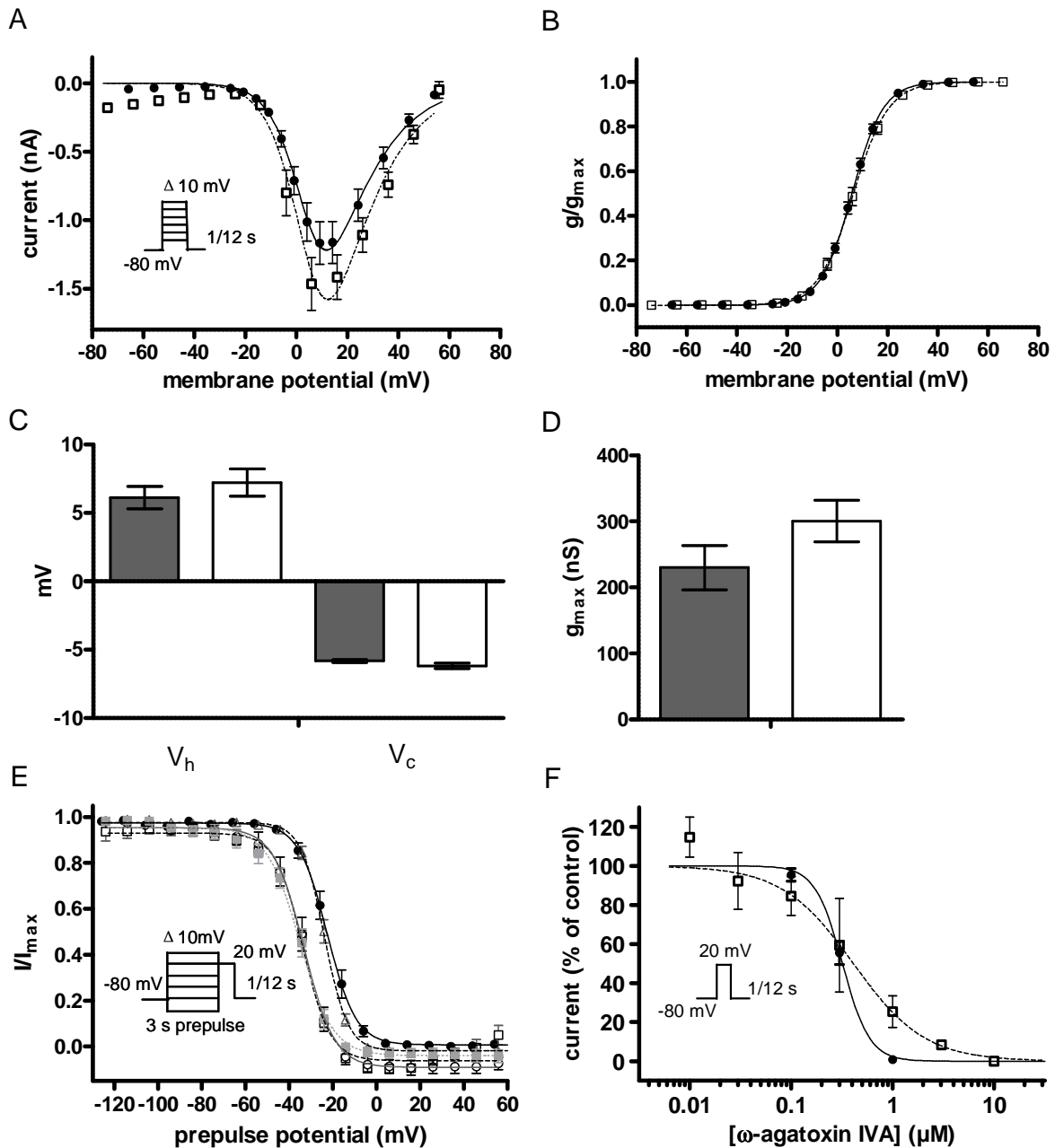


Figure 3.13 Validation of the automated patch clamp recordings for secondary screening on P/Q-type calcium channels. (A) Comparison of the I-V relationship of the manual (\bullet , solid lines, data from Figure 3.5B) and the automated (Patchliner) system (\square , dotted lines, data from Figure 3.12B) yield similar results across all voltage-steps applied. The lines represent the fit obtained from the GHK-equation. Inset: Corresponding voltage protocol. (B) Steady-state activation curves obtained from A. Lines were calculated from a first-order Boltzmann equation. No differences were observed between the systems. (C + D) Activation parameters V_h , V_c , and g_{max} obtained from A. Solid bars: manual patch clamp experiments; open bars: automatic patch clamp experiments. No significant

differences between both systems. (E) Inactivation curves can be different between the systems depending on the cell treatment prior to the experiment. Using the standard procedures (see methods), voltage at half inactivation (V_{inact}) occurs at about 10 mV more hyperpolarized potentials for automatic (\square) as compared to manual (\bullet) patch clamp experiments. Use of “Patchliner solutions” (see methods) in manual experiments does not eliminate this difference (Δ). However, treatment of cells with Accutase (\circ) or trypsin (\blacksquare) prior to manual recordings shifts V_{inact} to values similar to automatic patch clamp experiments. (F) Comparison of pharmacological modulation between both techniques. After 5 min application of the specific P/Q-type calcium channel blocker ω -agatoxin IVA currents were similarly blocked in both systems (\bullet manual / \square automated: $IC_{50} = 320 / 411$ nM). (Hermann et al. (2013b))

We next tested for effects of the protease treatment, which was required to suspend the cells for automatic patch clamp recordings. When cells were dissociated with Accutase prior to manual recordings, V_{inact} was shifted to more hyperpolarized values similar to the results obtained with the automated system ($V_{inact} = -33.6 \pm 1.9$ mV, $n = 4$). A similar treatment of cells with trypsin also shifted inactivation voltage ($V_{inact} = -35.2 \pm 1.5$ mV, $n = 3$) to similar values as observed on the automated patch clamp platform. Thus, protease treatment of cells prior to recording causes a hyperpolarizing shift of about 10 mV in voltage-dependent inactivation properties of recombinant P/Q-type calcium channels. This shows that cell handling is crucial for the function of the P/Q-type calcium channel. These results further indicate that protocols designed to detect state-dependent compounds via induction of voltage-dependent inactivation might need to be adjusted for automated patch clamp experiments

In order to test whether protease cell treatment cells might also interfere with pharmacological modulation, we compared the potency of ω -agatoxin IVA (which binds to an extracellular domain) between manual (non-protease treatment) and automatic (protease treatment) recordings. Both approaches yielded similar concentration-dependent block of P/Q-type currents after 5 min of single-dose application (Figure 3.13F; manual / automated patch: $IC_{50} = 320 \pm 25 / 411 \pm 111$ nM, $n = 4-7 / 4-6$ per concentration). These values are in line with previous studies (Bourinet et al., 1999; Hans et al., 1999). This indicates that sensitivity to pharmacological modulation might not be altered due to protease cell treatment

implying that the automated patch clamp system is suited for pharmacological compound investigation.

3.3.3 Compound Screening Reveals Novel Channel Blockers

For detection of novel P/Q-type calcium channel modulators we established a screening cascade published in Mezler et al. (2012b). It comprises a FLIPR-based primary high throughput screening which identified 3262 validated hits, which inhibited the calcium signal below 10 μM in the respective concentration response evaluation. As part of this PhD thesis, depolarization of P/Q-type calcium channels under FLIPR assay conditions were validated electrophysiologically and following the determination of IC_{50} values by the FLIPR-based assay, an electrophysiological counter screen was established for post-hoc automated patch clamp analysis.

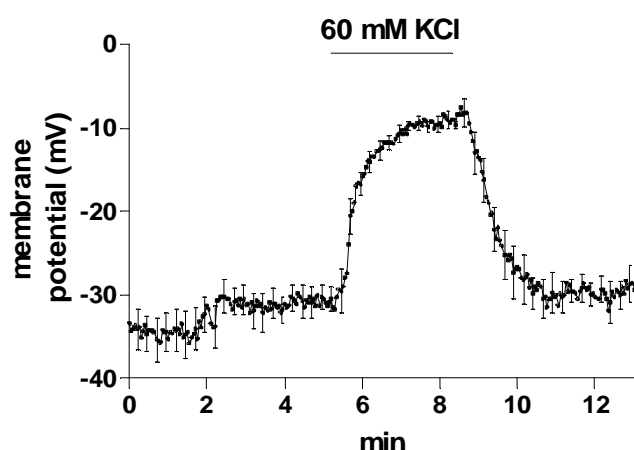


Figure 3.14 Membrane potential of P/Q-type calcium channels during FLIPR assay conditions. Investigation of the membrane potential under varying external KCl concentrations using manual perforated patch clamp recordings. Increasing external KCl concentration of the standard HBSS solution to 60 mM led to profound membrane depolarization, which was reversible upon washout of KCl. (Mezler et al. (2012b))

The recombinant cell line (clone K8-11) was utilized for a FLIPR-based primary screening assay to detect novel LMW P/Q-type calcium channel blockers (performed by Dr. Sujatha Gopalakrishnan). To prepare for this assay, we tested if the respective cell stimulation with KCl results in a sufficient depolarization of the cell for opening of the P/Q-type calcium channels. Thus, we analyzed cells by using the perforated patch-technique in current-clamp mode (Figure 3.14). The baseline potential in external HBSS medium was recorded for at least 5 min after perforation of the membrane was obtained. Increasing the external concentration of KCl from 5.3 mM in the normal HBSS buffer to 60 mM resulted in a fast depolarization, which was fully

reversible upon KCl washout ($V_{\text{mem}} = -30.8 \pm 1.8 \text{ mV} / -7.6 \pm 1.3 \text{ mV}^{***} / -28.77 \pm 1.7 \text{ mV}$ for HBSS / HBSS with 60 mM KCl / HBSS; One way ANOVA with Dunnett's post test, $***p < 0.001$; $n = 6$). Taken together with the voltage-dependence of P/Q-type calcium channel activation (Figure 3.5B, p.61), this demonstrates that the cells sufficiently depolarized for P/Q-type calcium channel opening after KCl-induction under FLIPR-assay conditions. Furthermore, these experiments also show that our cells have a rather depolarized resting membrane potential, typical for HEK293 cells (Thomas and Smart, 2005), before KCl-induction. Considering the voltage-dependence of closed-state inactivation obtained from electrophysiological patch clamp experiments illustrated in Figure 3.11 (p.75), a large fraction of the channels is probably inactivated during FLIPR baseline conditions. This implies that compounds with high affinity to inactivated P/Q-type calcium channels are likely to be detected in the FLIPR assay.

In order to detect compounds that bind to the inactivated state of the channel in a secondary electrophysiological screen, we designed an automated patch assay with inactivating prepulses to allow for the detection of both state-independent and state-dependent compounds. Initial attempts to develop a protocol where inactivation was induced with a constant moderate depolarization (e.g., a depolarizing shift in holding potential) resulted in unstable currents which ran down over time (similar to manual patch clamp recordings; see Figure 3.11D, p.75). A series of experiments determined that a depolarizing prepulse length of 3 s caused channel inactivation while maintaining stable current induction (data not shown). As described in Figure 3.13E (p.79), protease cell treatment, applied to suspend cells prior to automated patch clamp recordings, shifts inactivation to hyperpolarized potentials by about -10 mV. We therefore decided to shift the holding potential from -80 to -90 mV. As the inactivation curve (induced by a single prepulse for each potential) showed no significant inactivation at -80 mV this hyperpolarizing shift to -90 mV might not have been necessary. However, on the one hand, we wanted to avoid any slow accumulating inactivation which would be indistinguishable from run-down as illustrated in Figure 3.11D+E (p.75). On the other hand, it can be speculated that measurements might become more comparable between the methods if the potential difference between holding potential and V_{inact} remain similar. The resulting final screening protocol is depicted in Figure 3.15A. Based on our previous findings illustrated in Figure 3.13A (p.79), test pulses were applied at 20 mV in order to yield

the maximum current amplitude and signal-to-noise ratio. A 12 s interpulse interval was chosen, because at this time no use-dependent inactivation was observed (Figure 3.11C, p.75). A prepulse duration of 3 s was chosen, which can be sufficient to fully inactivate the channel, but at the same time does not induce (a detectable amount of) irreversible slow inactivation or run-down (Figure 3.11A+E, p.75). However, it needs to be noted that this duration does not induce steady-state inactivation (Figure 3.11B, p.75). Individual inactivation of each cell was estimated based on the current amplitudes during the prepulse protocol relative to the currents produced during an initial baseline period where no prepulses were applied. If necessary, the exact prepulse potential was adjusted for each cell individually so that the resulting inactivation was around 50%.

Three control washing steps applying extracellular bath solution were included: the first started 1 min after successful whole-cell formation, the next started 1 min after the first washing was finished and the last 1 min after the start of the prepulse protocol. These steps were implemented because changes in current amplitude were occasionally observed for the first control application (10-20% of cells). In rare cases changes were observed after the second or third control application. In this case, cells were excluded from the analysis (less than 5% of cells, data not shown). Some run-down of current still occurred over time, so time matched control cells were recorded for run-down correction. To further minimize artifacts, we chose to perform single dose experiments, avoiding a cumulative application protocol that is often used for screening purposes.

The stability of the current under different concentrations of DMSO was also examined while continuously applying the prepulse protocol (Figure 3.15B). This was necessary because compound aliquots were dissolved at a concentration of 10 mM in 100% DMSO. We found that run-down remained unchanged after an application of DMSO for 2 min as the current amplitude did not further decrease significantly at any concentration, and only a (non-significant) trend was observed for 0.3% DMSO ($100.3 \pm 5.1\%$ / $98.7 \pm 3.7\%$ / $86.2 \pm 5.4\%$; for 0.01 / 0.1 / 0.3% DMSO; $p = 0.17$; one-way ANOVA; $n = 21 / 51 / 26$). Thus, 0.1% DMSO was used as a control for all compound applications up to 10 μ M. Multiple additions of the same compound on the Patchliner did not significantly increase current block, suggesting that unspecific adsorption did not occur on the Patchliner chips or pipette.

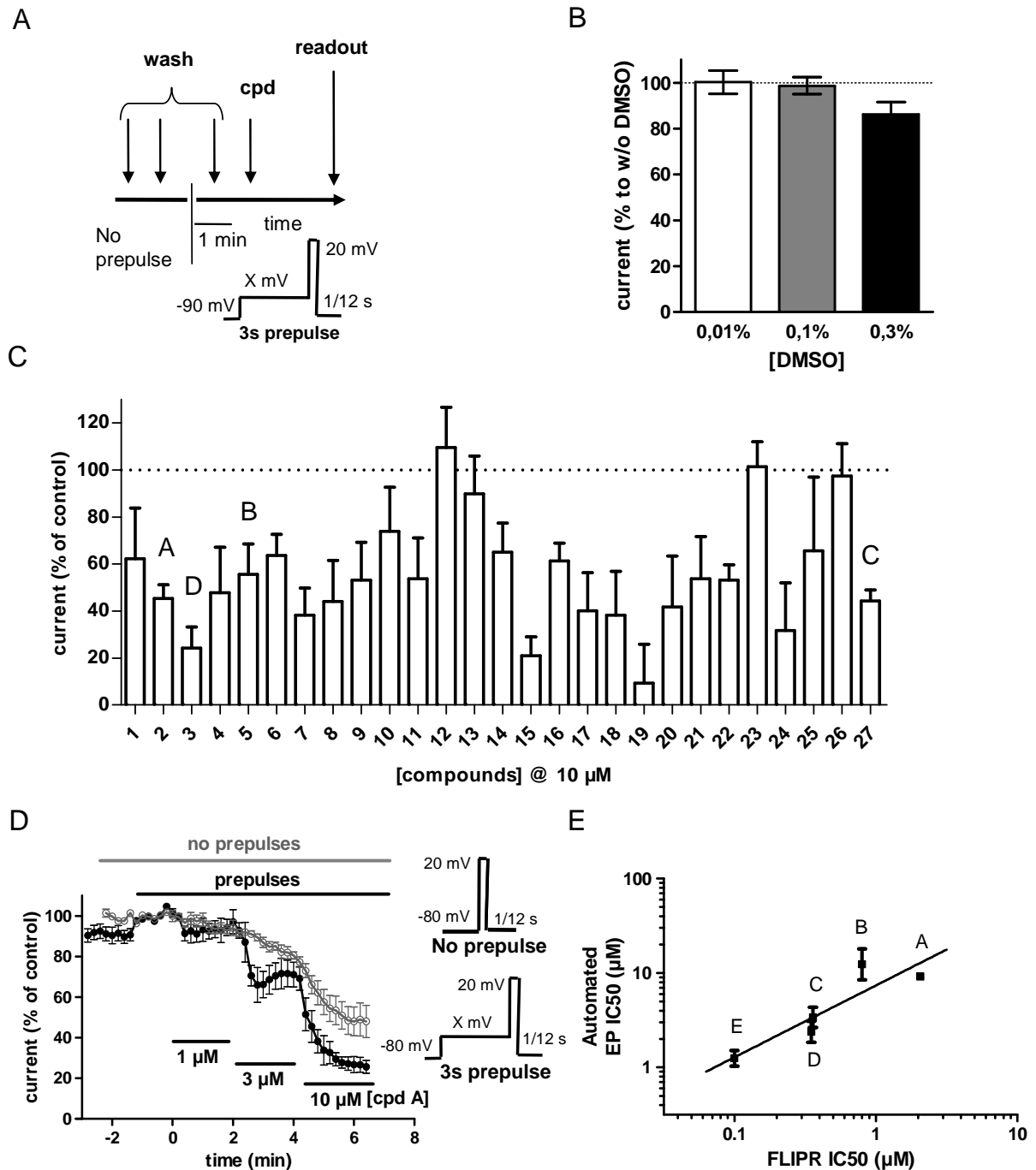


Figure 3.15 Implementation of patch clamp recordings to support the discovery of novel P/Q-type calcium channel blockers. (A) Experimental flow scheme including the voltage protocol for analysis of P/Q-type calcium channel block on the automated system. Washing steps were included to exclude application artifacts. The prepulse potential X was set so that about 30-70% of the current was inactivated and only one concentration was applied per cell. (B) Run-down was only mildly but not significantly affected by increasing concentrations of DMSO and compound concentrations up to 30 μ M could be used in this electrophysiological assay (\square 0.01% DMSO, \blacksquare 0.1% DMSO, \blacksquare 0.3% DMSO). (C) Functional single-dose validation of high throughput screen and hit-to-lead hits on the automated system. Active compounds decrease currents compared to control application. IC₅₀ values

were determined for compounds A-D using automated patch clamp. (D) Evaluation of inhibition of one selected compound (cpd A) by manual patch-clamp. The concentration-dependent block was normalized to time-matched vehicle controls of 0.1% DMSO (● inactivation and ○ resting state protocol). The protocol is shown on the right. In this manual patch clamp experiment holding potential was set to -80 mV (as described in the text). (E) Correlation of IC_{50} values from automated voltage clamp recordings with FLIPR data. The solid line represents the best linear fit to the selected compounds (slope = 0.8 ± 0.2 ; $r^2 = 0.81$). Letters correspond to the compound labels shown in C. (Mezler et al. (2012b))

Using this inactivating prepulse protocol, we investigated a set of 27 compounds on the Patchliner, which were either previously identified as blockers by primary high throughput screening, or were representatives from the subsequent optimization cycles (Figure 3.15C; $n = 3-9$ per compound). Most compounds which blocked calcium influx in the FLIPR assay were active in this functional secondary electrophysiological analysis, which suggests that the calcium FLIPR assay is appropriate for identifying novel P/Q-type calcium channel inhibitors. However, a few compounds (4 out of 27; compound 12, 13, 23, 26), initially identified by the FLIPR screen did not block $\geq 25\%$ of the current amplitude on the Patchliner at 10 μ M. Due to this (arbitrary) cut off, these were considered as false positives from the FLIPR and were excluded from further analysis. To control whether our incubation time would be sufficient for reaching steady-state inhibition, we followed the time course of two compounds by manual patch clamp analysis, which were subsequently chosen for characterization of state-dependent properties. One example (compound A) is shown in Figure 3.15D ($n = 3$ per group) illustrating that a compound incubation time of 2 min turned out to be largely sufficient for reaching steady state inhibition especially when using the inactivated protocol.

In order to validate the relevance of IC_{50} determination in the FLIPR assay, we compared IC_{50} values of compounds detected by the primary FLIPR-based screen with electrophysiologically determined potencies by automated patch clamp. IC_{50} values measured on the automated patch clamp system correlated with the FLIPR results (Figure 3.15E, $r^2 = 0.81$) and thus validated the use of FLIPR for analyzing the large amount of analogues during the hit-to-lead phase. In addition, compounds were more potent in the FLIPR screen compared to automated electrophysiology, which might be caused by different levels of inactivation as described in the discussion.

3.3.4 Characterization of State-Dependency of Selected Compounds

Lead candidates deriving from the chemical compound optimization process were subsequently analyzed for level of state-dependence by manual patch clamp analysis and advanced into the downstream screening cascade. Searching for state-dependent channel blockers requires protocols with high throughput, reliable inactivation, and fast recovery. For characterization of candidate substances, we therefore used prepulses of 3 s duration. Based on the recombinant P/Q-type calcium channel inactivation properties shown previously, this value represents an optimal compromise between full inactivation as well as fast and complete recovery. For assessment of state-dependent properties, we therefore we applied the prepulse and resting protocol illustrated in Figure 3.16A using manual patch clamp.

The prepulse potential was adjusted for individual cells to induce about 50% of current inactivation. Two substances were tested for state-dependent inhibitory potency. They are termed A-1048400 and compound A (denoted as compound 1 and 2 in Figure 3.15C, p.84, respectively) and were originally identified by pharmacological drug discovery on recombinant N-type and P/Q-type calcium channels (Mezler et al., 2012b; Scott et al., 2012). In manual patch clamp experiments, currents of sufficient amplitude were recorded for up to 6 min in drug-free control solution (Figure 3.16B+C). To adjust for run-down, all amplitudes were corrected for the corresponding time-matched vehicle controls ($n = 3$ for each group). In a FLIPR-based screen the compound A-1048400, was found to decrease calcium influx with an $IC_{50} = 1.2 / 2.1 \mu\text{M}$ for recombinant P/Q-type / N-type / T-type calcium channels and compound A with an $IC_{50} = 2.1 / 1.8 / 49 \mu\text{M}$ for recombinant P/Q-type / N-type / T-type calcium channels (data not shown).

In our electrophysiological assessment A-1048400 blocked P/Q-type currents in a state-dependent manner. In resting conditions (without prepulse) and (partially) inactivated conditions the IC_{50} was estimated at $13.1 / 2.7 \mu\text{M}$ (Figure 3.16B; $n = 3$ each) yielding a 5-fold shift in potency. For compound A, the amount of current block was less dependent on the channel state, reaching half-inhibiting concentrations of $IC_{50} = 9.8 / 5.3 \mu\text{M}$ (~ 2-fold difference) for the resting / inactivated state, respectively (Figure 3.16C, $n = 3$ each). For comparison, the clinically used drug verapamil is considered to be state-dependent. After induction of ~ 50% closed-state inactivation as in this study, the state-dependence of verapamil was reported as ~3-4 fold for T-

type calcium channels (Freeze et al., 2006). Data from Nawrath and Wegener (1997), who examined the block of verapamil on the open state including closed-state and open-state inactivation in parallel for the L-type calcium channel, suggests more pronounced state-dependent effects (although not explicitly quantified). Trox-1, a state-dependent calcium blocker currently in development for neuropathic pain, was described as about 6-fold state-dependent by electrophysiological experiments (Abbadie et al., 2010).

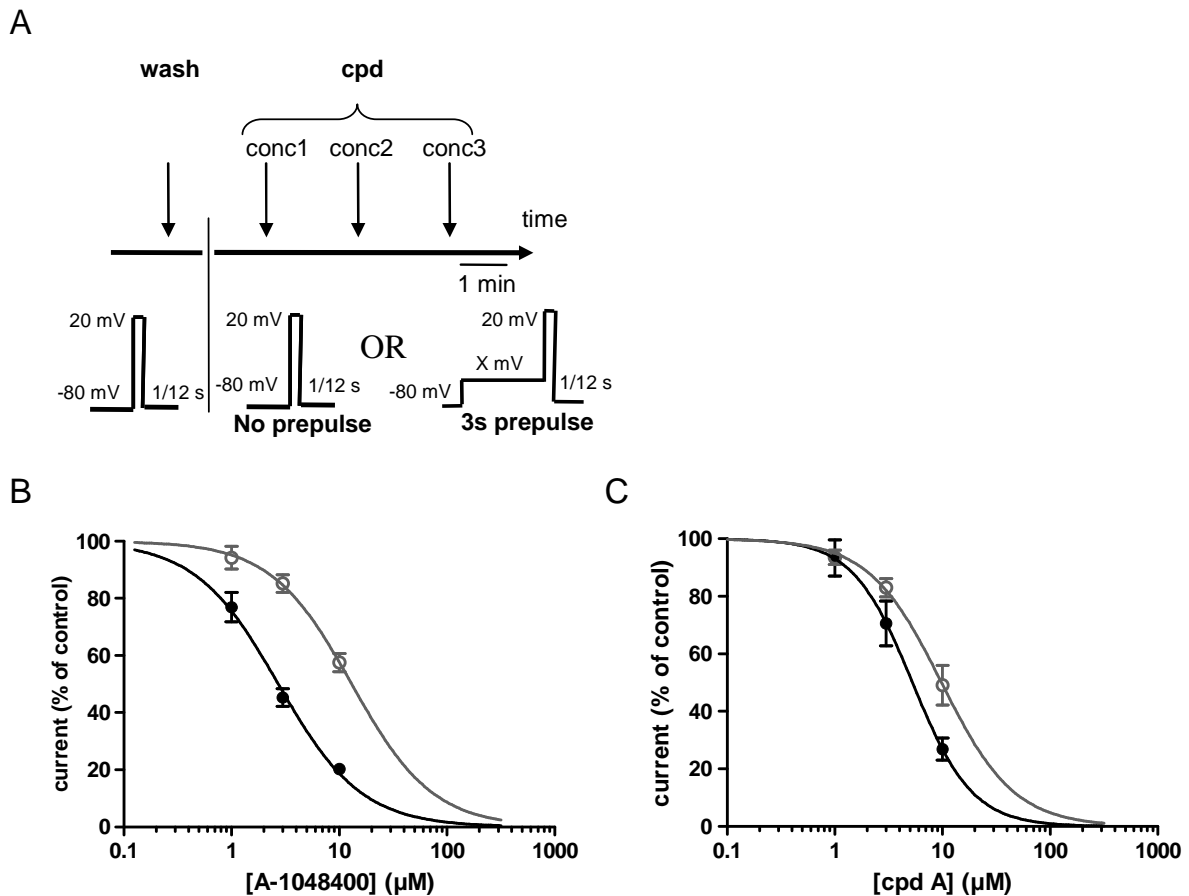


Figure 3.16 Characterization of state-dependent properties of two novel P/Q-type calcium channel blockers. (A) Experimental protocol including cumulative compound applications and pulse protocols. Pre-pulse voltage was adjusted to yield about 30-70% channel inactivation. For analysis of block at resting channel state, prepulses were omitted before stepping to the test potential at 20 mV. (B) The concentration-response curve obtained from manual patch clamp recordings on A-1048400 reveals a 5-fold difference in potency (\circ resting / \bullet inactivation protocol: $IC_{50} = 13 / 2.7 \mu\text{M}$). The concentration dependent block was normalized to the corresponding time-matched vehicle control for both resting and inactivation conditions. (C) Concentration-response curve for compound A reveals a moderate 2-fold shift in potency between the protocols (\circ resting / \bullet inactivation protocol: $IC_{50} = 9.8 / 5.3 \mu\text{M}$). (Hermann et al. (2013b))

Our results indicate that this protocol is suitable to discriminate between P/Q-type calcium channel blockers with different state-dependent potencies. In addition, two state-dependent tool compounds were identified after primary and secondary screening efforts (Mezler et al., 2012b) which can be tested for their potential to reverse A β -induced synaptic deficits in hippocampal synaptic transmission.

3.4 State-Dependent Block of Calcium Channels Prevents Oligomeric A β -induced Synaptic Deficits

Due to automated secondary screening and subsequent manual patch clamp analysis we were able to identify and validate two novel P/Q-type calcium channel blockers and quantify their state-dependent properties. Subsequently, it was addressed whether these compounds could also rescue A β globulomer-induced deficits in synaptic transmission in a similar fashion as the state-independent peptide toxins tested previously.

Considering our previous patch clamp results on recombinant channels (see chapter 3.3.4, p.86ff), we applied concentrations of the compounds slightly below their IC₅₀ for inactivated channel states. Assuming that compound potencies are similar for native channels, a significant fraction of inactivated channels, but only a minor fraction of closed channels should be inhibited in organotypic slice cultures.

We found that 1 μ M of compound A-1048400 and 3 μ M of compound A was sufficient to completely prevent A β -induced functional deficits, respectively (Figure 3.17A+C; n = 8-9 per group each). The observed synaptoprotective effect was similar to the specific state-independent peptide blockers shown in Figure 3.2 (p.57) and Figure 3.3 (p.58). Neither LMW compounds modulated synaptic transmission when applied alone (Figure 3.17B+D; n = 8-9 per group).

In conclusion, A β -induced functional deficits in synaptic transmission can be reversed with state-independent as well as state-dependent calcium channel blockers. Thus, introducing state-dependence, which may represent a more favorable side effect profile, does not impair the synaptoprotective effect of calcium blockers. While maintaining their therapeutic potential, this may reduce unwanted effects on

physiological basal synaptic transmission and might be beneficial for drug development of novel AD drugs, as described in the introduction.

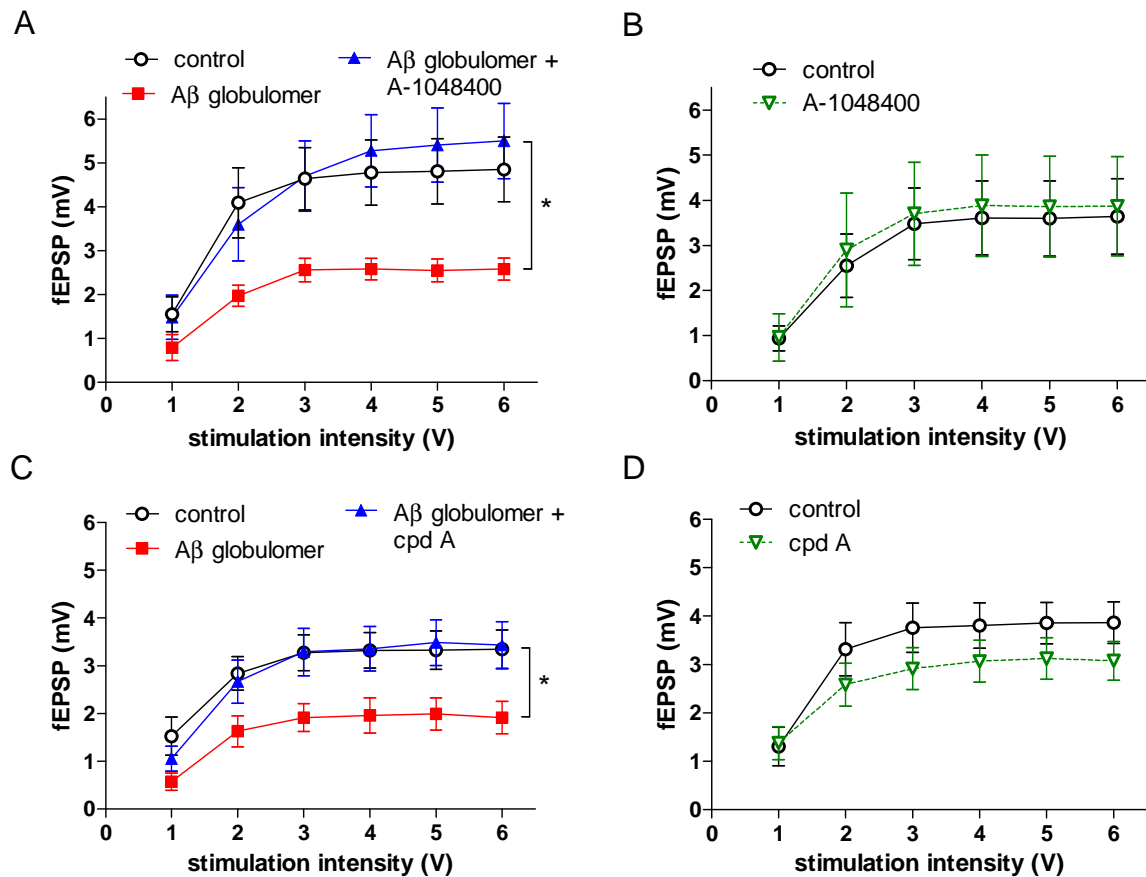


Figure 3.17 State-dependent P/Q-type calcium channel block prevents A β globulomer-induced functional synaptic deficits. (A) Application of 1 μ M compound A-1048400, a LMW compound which was previously identified as 5-fold state-dependent, fully prevents A β globulomer-induced deficits in excitatory synaptic transmission of organotypic hippocampal slice cultures. (B) 1 μ M Compound A-1048400 does not alter synaptic transmission when applied alone. (C) Likewise, 3 μ M compound A, which is only 2-fold state-dependent, also reverses A β globulomer-induced deficits. (D) No intrinsic effects on the input-output curve were detected after application of 3 μ M Compound A. * $p < 0.05$, two-way RM ANOVA, Holm-Sidak *post hoc*. (Hermann et al. (2013a, submitted))

4 Discussion

This study investigated a novel molecular mechanism of AD pathology, namely facilitation of presynaptic calcium channel currents by oligomeric A β . It furthermore showed that functional synaptic deficits can be prevented in nervous tissue by blocking presynaptic ion channels including the P/Q-type calcium channel. As this channel is preferably expressed in the CNS (Luebke et al., 1993; Stea et al., 1994), it would be particularly attractive to target this channel with future therapeutics. We therefore suggest P/Q-type calcium channel blockers as a possible therapeutic strategy for the treatment of AD.

Beyond AD, P/Q-type calcium channels have also been implicated in a number of neurological diseases including migraine (Tottene et al., 2002) and epilepsy (Pietrobon, 2005). Block of P/Q-type calcium channels was also found to decrease seizure activity in mice (Jackson and Scheideler, 1996). At least for AD no effective therapy is available. Thus, this study here describes an electrophysiological secondary screen for the identification of novel P/Q-type calcium channel inhibitors.

State-dependence of modulators, which predominantly bind to inactivated channels, might aid to achieve functional selectivity. This is because they are hypothesized to preferentially bind to pathologically overactivated channels rather than to physiologically activated channels. Therefore this property is believed to enhance the therapeutic potential of a drug candidate (Winqvist et al., 2005). In order to detect state-dependent compounds, an appropriate (screening) protocol needs to be applied. Ideally, this protocol should closely mimic the pathological condition which often includes channel inactivation. This can only be achieved if inactivation of the respective channel complex has been previously characterized under (screening) assay conditions. We found that inactivation may be reversible or irreversible, depending on the applied depolarization protocol. In addition, channel activation was identical for manual and automated patch clamp, whereas voltage-dependent inactivation varied between the systems. Based on these results, we were able to establish a robust inactivation protocol suitable for screening, which in the end proved to be capable of detecting novel state-dependent P/Q-type calcium channel blockers. This functional assay was implemented into the hit-to-lead phase of an

active drug discovery program for the development of P/Q-type calcium channel blockers.

4.1 Overactivation of Presynaptic Calcium Channels as a Potential Molecular Mechanism in AD

Following the first suggestions that oligomeric A β aggregates may cause synaptic deficits in AD, there has been an extensive search for the underlying molecular mechanism (Walsh and Selkoe, 2007). As discussed below, several proteins that are involved in synaptic transmission have been suggested to be modulated in their function.

Oligomeric A β was found to alter presynaptic function by an impairment of vesicle release at axon terminals in hippocampal neurons through depletion of dynamin 1, a protein involved in vesicle recycling (Kelly et al., 2005; Kelly and Ferreira, 2007). This finding was supported by detection of dynamin cleavage in APP-overexpressing mice (Kelly et al., 2005) and AD patients (Yao et al., 2003). This cleavage may in turn be mediated by calpain (Kelly et al., 2005), a protease also associated with neurodegeneration (Nimmrich et al., 2008b).

NMDA receptors may represent another target for A β oligomers, as impaired presynaptic vesicle release can be prevented by NMDA receptor blockers (Kelly and Ferreira, 2006). This may be explained by findings that NMDA receptors are also located presynaptically (Berretta and Jones, 1996; Charton et al., 1999) affecting vesicle release (Woodhall et al., 2001). Moreover, after application of A β oligomers, Shankar et al. (2007) demonstrated an NMDA-mediated decrease in calcium influx into dendritic spines and Lacor et al. (2007) observed a downregulation of NMDA receptors. Furthermore, studies on *Xenopus* oocytes suggest that A β induces calcium influx through NMDA receptors in the absence of glutamate (Texido et al., 2011) but does not facilitate calcium influx when glutamate is present (Mezler et al., 2012a). These effects on NMDA receptor currents may both increase and decrease vesicle release. On the one hand, this might possibly induce vesicle release by a calcium influx even under non-excited conditions (in the absence of glutamate). On the other hand, constantly elevated intracellular calcium levels may decrease the

dynamic range of changes in calcium concentration during arrival of an action potential, which in turn may result in decreased vesicle release. Taken together, A β oligomers may modulate NMDA receptor function, thereby altering presynaptic vesicle release.

The involvement of HVA calcium channels in the pathology of AD was suggested by Sberna et al. (1997). They described that the peptide fragment A β ₂₅₋₃₅ increased activity of acetylcholinesterase by facilitating calcium influx through L-type, but not P/Q-type and N-type calcium channels in embryonal carcinoma cells. In contrast, Bobich et al. (2004) observed an increase in neurotransmitter release probability which they attributed to an A β -mediated increase in N-type rather than P/Q-type and L-type calcium channel currents. In line with this, presynaptic modulation by A β was also reported to increase the release probability at presynaptic terminals leading to an increased network activity and lowered synaptic plasticity (Abramov et al., 2009). In addition, several studies in the past suggested that acute and chronic application of A β peptide influences calcium channel conductance (He et al., 2002). Both presynaptic P/Q-type and N-type (MacManus et al., 2000; Ramsden et al., 2002) as well as postsynaptic L-type voltage-gated calcium channel currents (Ueda et al., 1997; Kim and Rhim, 2011) were reported to be modulated. As noted in the introduction, some of these conflicting results may be caused by the use of different A β fragments and poorly defined A β preparations probably containing a mixture of A β species, which may or may not be relevant in the pathology of AD. We here further investigated the functional relevance of these findings on the network and the cellular level, using A β globulomer, a stable, well-defined, and pathologically relevant oligomeric A β preparation (Barghorn et al., 2005; Gellermann et al., 2008).

4.1.1 Presynaptic Calcium Channel Block Reverses Oligomeric A β -induced Deficits in Synaptic Transmission

On the network level we tested whether block of HVA calcium channels may protect from synaptic deficits induced by oligomeric A β in organotypic hippocampal slice cultures. Previously, Nimmrich et al. (2010) showed that overnight incubation of these slice cultures with A β globulomer causes synaptic decline, as observed by a decrease in evoked glutamatergic transmission. They proposed that such a

functional decline might be a consequence of several detrimental mechanisms including excitotoxicity, which was observed after A β application *in vitro* and *in vivo* (Harkany et al., 2000). Besides other mechanisms, this in turn may potentially be caused by overactivation of HVA calcium channels as observed by Mezler et al. (2012a). Therefore, an initial increase in calcium channel function can in the end lead to decreased excitatory synaptic transmission on the network level. If so, decreasing calcium influx through a specific silencing of overactivated (presynaptic) calcium channels might prevent these functional deficits.

Here we found that specific block of either the presynaptic P/Q-type or N-type calcium channel could in fact prevent oligomeric A β -induced deficits in excitatory synaptic transmission in organotypic hippocampal slice cultures. This indicates that block of these calcium channels may compensate A β oligomer-mediated effects. These may either be specifically mediated via P/Q-type and N-type calcium channels, which are presynaptically expressed at the Schaffer collateral-CA1 synapse (Westenbroek et al., 1992; Westenbroek et al., 1995), or via other (unrelated) mechanisms. The former hypothesis is supported by the observation that pre-application of a P/Q-type calcium channel antibody also prevented A β oligomeric deficits. This beneficial effect might have been mediated by direct channel inhibition or preoccupation of the possible A β globulomer binding site(s). These findings are in line with reports from other groups showing that block of presynaptic calcium channels can prevent functional deficits and neuronal decline. For example, neuroprotective effects of both peptidic and LMW calcium channel blockers have been demonstrated in several models, including neuronal ischemia *in vitro* (Small et al., 1995) and *in vivo* (Valentino et al., 1993) as well as brain injury (Verweij et al., 1997; Berman et al., 2000). Moreover, a common downstream pathway for a wide variety of neurological disorders may be an increased release of excitatory amino acids (Lipton and Rosenberg, 1994), which can be inhibited by P/Q-type calcium channel blockers during neuronal overactivation *in vivo* (Wu et al., 1995). This may explain why P/Q-type calcium channel blockers also protect against several neuronal insults (Jackson and Scheideler, 1996; Asakura et al., 2000) and may also be relevant for AD. This is because diminishing neuronal spike activity by levetiracetam – which also decreases P/Q-type calcium currents – not only reverses synaptic deficits, but also ameliorates learning and memory impairment in APP-transgenic mice (Sanchez et al., 2012).

Next, we tested the effect of nimodipine (10 μ M), which has shown limited efficacy in clinical trials regarding dementia (Birks and López-Arrieta, 2002). This LMW HVA calcium channel blocker was described both as specific (Furakawa et al., 1999) and non-specific (Diochot et al., 1995) for L-type calcium channels, which are predominantly located postsynaptically (Castillo et al., 1994; Wheeler et al., 1994). In contrast to the specific presynaptic calcium channel blockers, this compound did not prevent A β -induced functional deficits in slice cultures. The potency and selectivity of nimodipine greatly varies between previous reports. It has been claimed by Mansvelder et al. (1996) as up to eight orders of magnitude selective for L-type calcium channels in rat pituitary melanotropic cells (L-type IC₅₀ = 3 pM; P/Q-type IC₅₀ = 500 nM). Another study, which observed current block at 10 μ M only for L-type but not other HVA calcium channels on recombinantly expressed channels in *Xenopus* oocytes, also reported nimodipine as selective (Furakawa et al., 1999). However nimodipine may be less selective, because Diochot et al. (1995) reported 1 μ M as IC₅₀ for L-type calcium channels but also a 51% decrease in current amplitude at 10 μ M from dorsal root ganglion neurons containing P/Q-type, N-type, and to a lesser extent L-type calcium channels. This may lead to two alternative interpretations, depending on the specificity of the compound at 10 μ M in our system. Given that nimodipine preferentially blocked L-type calcium channels, this would imply that somato-dendritic intracellular calcium levels do not modulate or participate in the A β -mediated pathology of our *in vitro* model. Assuming that nimodipine unspecifically blocked all HVA calcium channels, this would suggest that additional postsynaptic L-type calcium channel block may dampen the beneficial effect of presynaptic calcium channel block. Testing another, more specific, L-type calcium channel blocker may address which hypothesis holds true in this *in vitro* model of AD. To conclude, based on this data it would be exciting to investigate whether more selective blockers may exceed the clinical efficacy of nimodipine, which could bring about a new generation of antidementive medicine.

4.1.2 Oligomeric A β Augments Presynaptic Calcium Channel Currents

After identification of presynaptic calcium channel block as a protective mechanism in oligomeric A β treated hippocampal slice cultures, this work attempted to elucidate the underlying molecular mechanism. It was recently shown that synthetic A β oligomers

(A β globulomer) increase P/Q-type calcium channel currents, which were expressed in *Xenopus* oocytes (Mezler et al., 2012a), suggesting that enhanced neurotransmitter release may underlie the decline of synaptic function following prolonged exposure to A β oligomers. We confirmed this finding in a stable recombinant expression system using a human-derived cell line (HEK293). We further found that A β oligomers modulate both presynaptic P/Q-type and N-type calcium channels. This implies that synaptic function can be altered in any brain region accessible to soluble oligomeric A β . Compared to the organotypic hippocampal slice culture experiments, significant effects on recombinant channels were only observed at a 10-fold higher concentration of A β (although a trend was observed already at similar concentrations (Figure 3.10, p.72)). The enhanced sensitivity of synaptic transmission to A β globulomer in the slice culture experiments may be, on the one hand, caused by the chronic and thereby longer incubation times. So it may be that already very subtle effects on presynaptic calcium influx will lead overnight to deficits in synaptic transmission. On the other hand, acute effects of A β globulomer might be more potent in native channels, as suggested by previous reports applying extracellular field (Barghorn et al., 2005) and patch clamp recordings (Nimmrich et al., 2008a).

Before studying the effect of A β globulomer on calcium channel kinetics, functional recombinant channel expression was successfully characterized by manual whole cell patch clamp. The currents recorded from the α_{1A} transfected HEK293 cell line after tetracycline-induction were similar to published recombinant P/Q-type calcium channel currents (Hans et al., 1999). Non-induced cells showed no appreciable current after depolarization, indicating that the current obtained in tetracycline-induced cells was generated by charge movements through the recombinant P/Q-type calcium channel. Pharmacological modulation with ω -agatoxin IVA inhibited the depolarization-induced current within the range of published values (Bourinet et al., 1999; Hans et al., 1999). Roscovitine, a less specific channel modulator, slows deactivation kinetics thereby increasing tail currents (Buraei et al., 2007), which could also be reproduced using the α_{1A} transfected cell line. This was taken as a further hint for the appropriate gating of the recombinant channels. Furthermore, the subtype specific blocker ω -conotoxin MVIIA did not block P/Q-type calcium channels but potently inhibited currents from the α_{1B} transfected cell line, which compares well to previous findings on human N-type calcium channels (Kaneko et al., 2002). Taken

together, the currents generated by depolarization steps in our cell lines with inducible α_{1A} and α_{1B} expression are characteristic of P/Q-type and N-type calcium channels, respectively. We therefore considered these cell lines as suitable for analysis of potential effects of oligomeric A β on presynaptic calcium channels.

After validation of proper channel expression, the effect of A β oligomers on presynaptic calcium channels was investigated. It was found that the current amplitude was increased at moderate depolarizations for both the P/Q-type and N-type calcium channels. This was attributed to a shift of the voltage at half-activation V_h to more hyperpolarized values. It needs to be noticed that in this study no evidence was collected that a similar mechanism is existent in patients with Alzheimer's disease. However, this effect may be pathologically relevant as exemplified by P/Q-type calcium channel mutation-induced shifts in V_h which lower the threshold for cortical spreading depression, leading to migraine (Ayata et al., 2000; Tottene et al., 2002). Here, the oligomeric A β -induced increase in P/Q-type calcium channel current amplitude (at depolarizations to -10 mV) was not modulated if part of the channels were previously inactivated. This suggests that the modulatory effect of oligomeric A β appeared to be independent of the previous channel state. Furthermore, it was found that application of oligomeric A β did not change V_{inact} , the voltage inducing half inactivation, for P/Q-type and N-type calcium channels. This implies that voltage-dependent inactivation kinetics are unaffected by application of oligomeric A β . Taken together, A β oligomers may specifically facilitate channel activation without altering other state transition kinetics, which would result in a tonic overactivation of the presynaptic calcium channels.

As a result of this tonic modulation, oligomeric A β will lead to faster activation of presynaptic calcium channels upon arrival of an action potential independent of previous synaptic activity. An overactivation of those channels by oligomeric A β may result in increased calcium levels and some form of synaptic "fatigue" without structural damage like e.g., loss of releasable vesicles (Kelly and Ferreira, 2007). Prolonged exposure to A β oligomers may also lead to retraction of spines and synaptic degradation (Shankar et al., 2007). Harkany et al. (2000) further reported that A β triggered extracellular accumulation of excitatory amino acids *in vivo* with subsequent neuronal loss, which may be a common final mechanism for neurological disorders (Lipton and Rosenberg, 1994). Recent *in vitro* studies by Nimmrich et al.

(2010) show that inhibition of calpain, a group of proteases which promote cell death, prevents NMDA-mediated excitotoxic cell death and restores oligomeric A β -induced functional deficits in synaptic transmission. The present data are compatible with these findings and suggest a possible molecular mechanism of A β -induced pathology in AD via overactivation of presynaptic calcium channels.

Compared to this PhD study, Nimmrich et al. (2008a) observed different functional effects of synthetic oligomeric A β , namely a reduction in P/Q-type, but no effects on N-type calcium channel currents in cultured hippocampal neurons. In both studies the same oligomeric A β preparation and a similar methodology was used. As of today, there is no conclusive explanation concerning this discrepancy of data, but as noted in the introduction (see section 1.1.3.3), bidirectional effects have also been previously observed with other ion channel modulators (Koch et al., 2004). A bidirectional modulation of neuronal physiology has also been shown for A β oligomers. It has been shown that natural A β oligomers can both increase and decrease the frequency of miniature excitatory postsynaptic currents, which could be brought about by a reversal of ion channel regulation (Shankar et al., 2007; Abramov et al., 2009). Similarly, synthetic A β preparations can both increase and decrease LTP (Puzzo et al., 2008).

Possible reasons for such effects may include concentration dependence, state-dependence, or minor changes in the channel conformation. In our study we investigated concentrations ranging three fold in the order of magnitude but have not observed any hint for a possible concentration dependent effect on P/Q-type calcium channels. In addition, in the present study, the modulation of P/Q-type calcium channels by A β globulomer appeared to be tonic and therefore independent of channel state, which does not support the idea of a bidirectional modulation due to different states of the channel. Alternatively, oligomeric A β may have differential effects on native and recombinant channels. However, Rovira et al. (2002) reported that acute application of full length A β to acute hippocampal slices also increases P/Q-type and N-type calcium channel currents. Although this study used a poorly defined oligomeric A β preparation, this suggests that the bidirectional modulation of P/Q-type calcium channels between the studies is not solely caused by principal differences between native and recombinant channel expression. However, Mezler et al. (2012a) have shown that the effect of oligomeric A β on P/Q-type calcium channel

currents, expressed in *Xenopus* oocytes, is mediated by the auxiliary channel subunits. In the absence of these, only an increase in current amplitude, but no shift in channel activation was observed. Introducing the same auxiliary subunits, as used here, also led to a hyperpolarizing shift in channel activation, similarly as observed in this PhD study. This suggests that minor changes in the calcium channel complex, like a different pore forming splice variant or a different subunit composition, may modulate the effect of oligomeric A β . As P/Q-type calcium channels exist in a number of genetic variations (Soong et al., 2002; Tsunemi et al., 2002), the splice variant used in our recombinant systems may not need to be identical to the one(s) in hippocampal neurons. It remains to be shown whether this could actually lead to both a facilitation and depression of the calcium channel currents by A β oligomers and whether bidirectional modulatory effects, induced by a mixture of channel complexes expressed in a single cell, might potentially cancel each other out. A possible approach to address this would be to determine the splice variants and channel subunits of P/Q-type and N-type calcium channels (predominantly) expressed in the cultured hippocampal neurons. Subsequent comparison of the effect of oligomeric A β on these different calcium channel complexes within one study may test this hypothesis.

The relevance of our findings of presynaptic calcium channels as a molecular target for A β oligomers is supported by the fact that oligomers are localized to presynaptic terminals in AD patients (Kokubo et al., 2005b; Noguchi et al., 2009). Immunocytochemical studies indicated that similar A β oligomer forms exist in AD brains. When antibodies were generated against a similar synthetic A β oligomer form, known as amyloid-derived diffusible ligands, oligomers were detected in 70-fold higher concentrations in Alzheimer's disease than in control brains (Gong et al., 2003). Also the A β ₁₋₄₂ globulomer epitope was detected in brain of AD patients (Barghorn et al., 2005). On a functional level, changes in calcium-dependent enzymes – which may be activated after excessive calcium entry – were reported in A β -overexpressing transgenic animals (Kelly et al., 2005) as well as in patients (Green et al., 2007). On a systemic level an increase of presynaptic calcium influx would result in enhanced neuronal excitability. Indeed, Palop et al. (2007) reported elevated neuronal activity and resulting seizure activity in transgenic mice with elevated A β levels. In line with this, increased seizure susceptibility was also detected in sporadic AD (Amatniek et al., 2006) and familiar AD patients (Cabrejo et

al., 2006). It has been recently shown in a mouse model of Alzheimer's disease that prevention of seizure activity by levetiracetam reverses learning and memory deficits (Sanchez et al., 2012). Prolonged exposure to toxic A β inducing such functional effects may ultimately lead to the observed decrease in synaptic spine densities (Lacor et al., 2007; Shankar et al., 2007) and overall excitatory transmission (Hermann et al., 2009), which coincide with learning and memory impairments (Ashe, 2001).

4.2 Development of State-Dependent P/Q-type Calcium Channel Blockers

The data presented in the previous section does not clarify whether blocking presynaptic calcium channels may indeed slow down the progression of synaptic degeneration in AD patients. Yet, from a drug development perspective it may suggest an exciting avenue for novel therapeutics that deserves further testing, e.g., in transgenic animal models. Unfortunately, all available selective presynaptic calcium channel blockers are of natural origin, i.e. toxins of marine snails or other invertebrates. The peptidic nature of these toxins limits drug development efforts, partly because of their limited bioavailability and CNS penetration. Thus, the necessity for improved pharmacokinetics requires the development of LMW ion channel blockers that are readily absorbed and reach sufficient brain levels for achieving the desired effect. Furthermore, under physiological membrane potentials most peptide toxins like ω -agatoxin IVA (McDonough et al., 1997) and ω -conotoxin MVIIA (Feng et al., 2003) do not preferentially bind to inactivated channels and equally or even preferentially bind to closed channels. However, it is now state-of-the-art in ion channel drug discovery to develop state-dependent molecules (see introduction; section 1.3.3), which preferentially target inactivated channel states. These compounds are hypothesized to block tonically overactive sites without altering normal levels of synaptic activity (Winqvist et al., 2005).

Besides a possible relevance for the treatment of AD, P/Q-type calcium channels have been implicated in a number of neurological diseases including migraine and epilepsy. Moreover, some clinically used calcium channel blockers modulate HVA calcium channels, including the P/Q-type calcium channel (Uchitel et al., 2010),

indicating that modulation of this channel is tolerated in humans. For example, gabapentin inhibits channel activity by interacting with the $\alpha_2\delta_1$ and $\alpha_2\delta_2$ subunit (Catterall et al., 2005). Gabapentin might be effective for migraine prevention as suggested by an *in vitro* (Hoffmann et al., 2010) as well as a clinical phase III study (Mathew et al., 2001). Although, to my knowledge, there is no study on pro-cognitive effects in AD patients, gabapentin may increase cognition in non-demented elderly people (Martin et al., 2001). Thus, development of selective P/Q-type calcium channel blockers may find therapeutic application.

It appears that the development of selective calcium channels blockers remains a challenge (reviewed by Yamamoto and Takahara, 2009; Nimmrich and Gross, 2012) due to the sparse information on structure-activity relationships of blockers and the close homology among the HVA calcium channels. Therefore, development of selective compounds may benefit from sophisticated screening (including high throughput electrophysiological methods) as well as counterscreening. Despite these difficulties, due to recent advances in assay development and automated electrophysiological techniques the development of selective calcium channel blockers may be more readily achieved as functional data can now be obtained at a higher throughput supporting investigation of the structure-activity relationship for LMW channel blockers.

The following sections will discuss the generation and results of our electrophysiological secondary screen (following a FLIPR-based primary screen) for the identification of novel P/Q-type calcium channel inhibitors. Moreover, it is discussed that effective development of an electrophysiological secondary screening assay benefits from theoretical considerations of the targeted pathophysiology as well as from detailed analysis of inactivation kinetics. It is subsequently described that recombinant channel inactivation may be reversible or irreversible, depending on the applied depolarization protocol. In addition, despite identical channel activation, P/Q-type calcium channel inactivation varies between manual and automated patch clamp, so that a screening protocol for inactivated channels needs to be adjusted between systems. Based on these results a robust inactivation protocol suitable for screening was established, which allowed the detection of both state-independent and state-dependent novel P/Q-type calcium channel blockers, as validated by manual electrophysiology. This electrophysiological screen was implemented into the

hit-to-lead cycle of a drug development plan. The final part of this section discusses the effect of these novel LMW compounds on preventing A β oligomer-induced synaptic deficits.

4.2.1 Appropriate Screening Protocol Selection Depends on Disease- and Channel-Specific Properties

In recent years a number of different protocols have been suggested for the detection of state-dependent ion channel blockers (Dai et al., 2008; Belardetti et al., 2009; Finley et al., 2010). Ideally, the appropriate protocol should be designed to reflect the pathophysiology of the disease of interest as well as the physiological function and the inactivation kinetics of the therapeutic target.

Pain is hypothesized to be mediated by excessive firing of dorsal root ganglion neurons (Nordin et al., 1984). For development of pain therapeutics it may therefore be beneficial that the respective screening protocol reflects the repetitive activity of neurons by implementation of a use-dependent protocol (Winquist et al., 2005). Indeed, previous and current drug discovery efforts for pain therapeutics have included high-frequency stimulation protocols, inducing rapid changes in channel states where the on- and off-kinetics of compounds can have a greater influence (Finley et al., 2010; Swensen et al., 2012). In contrast, several P/Q-type calcium channel-related diseases exhibit a pathophysiology that involves a more sustained depolarization of neurons. For example, the underlying mechanism of some familiar migraines is a gain-of-function of the P/Q-channel, leading to cortical spreading depression (Tottene et al., 2009). This phenomenon is marked by a tonic depolarization of neurons that propagates through the cortex. Furthermore, we suggest here that AD is marked by presynaptic accumulation of soluble A β oligomers that might also tonically enhance P/Q-type calcium currents, potentially leading to increased neurotransmitter release and excitotoxic cell death discussed in previous publications (Lipton and Rosenberg, 1994; Harkany et al., 2000; Nimmrich et al., 2010). For the development of P/Q-type calcium channel blockers we therefore decided to use a sustained prepulse which may be more relevant to the pathophysiology of A β -mediated effects than rapid changes in membrane potential as e.g., during seizure activity.

Moreover, the P/Q-type calcium channel is expressed preferably in the CNS, which is composed of multiple types of neurons. Some of these, like fast spiking interneurons, exhibit high-frequency firing. Their signaling might be silenced by use-dependent P/Q-type calcium channel block, leading to disinhibition at the network level. Similarly, synaptic plasticity in pyramidal neurons may involve spiking coupled to oscillations like theta rhythms (O'Keefe and Recce, 1993; Buzsáki, 2002). One may speculate that an interruption of such a process can disturb the delicate process of memory formation in the brain. To potentially avoid such adverse effects, we confirmed that our prepulse protocol did not induce any use-dependent accumulation of inactivation. It needs to be noted that these analogies are largely hypothetical, especially as the recombinant test system is not identical to native neuronal cells which express a variety of splicing variants and subunit compositions (Soong et al., 2002; Liao et al., 2009).

In any case, precise knowledge of the biophysical inactivation properties of the channel is necessary for the design of an appropriate prepulse paradigm. State-dependent compounds can be detected with a variety of protocols since inactivation can be induced either by short prepulses or by sustained depolarizations, as applied in Dai et al. (2008). In order to obtain a sensitive, robust screening assay, possibly resembling a pathological AD-like channel state, we examined whether a sustained inactivation protocol was best applicable for identification of novel P/Q-type calcium channel blockers. Thus, we studied the properties of voltage-dependent inactivation of the recombinant P/Q-type calcium channel in detail using manual electrophysiology.

Steady-state inactivation of the recombinant P/Q-type calcium channel was not achieved under any prepulse condition (up to 5 min). With increasing prepulse lengths channel inactivation progressively shifted to more hyperpolarized values. However, the decay in current amplitude could only be fitted with a two-exponential relationship suggesting the existence of more than one molecular mechanism of inactivation. It may be that additional slow inactivated states of the channels become effective with longer prepulse durations. Slow inactivation kinetics of recombinant calcium channels have also been observed in previous studies. Bezprozvanny et al. (1995) reported slow inactivation of recombinant N-type and Q-type calcium channels, especially in the presence of syntaxin, a membrane protein triggering

vesicle fusion. Here, probably in the absence of such intracellular modulators, we also observed that the current amplitude keeps decaying even for long prepulses hinting at a very slow transition rate. In line with our findings, several biophysical studies on voltage-gated calcium channels reported the presence of several inactivated states including fast and slow transition rates (Patil et al., 1998; Degtiar et al., 2000). Which of these are most relevant for drug discovery has not been elucidated yet, but this may depend on the pathology of interest (see above).

Furthermore, we found that inactivation induced by depolarizations of several minutes was no longer reversible. This might be explained by extremely slowly reversing inactivated states or, alternatively, by inactivation-unrelated effects, e.g., channel desensitization, phosphorylation, or internalization. Vortherms et al. (2011) described an automated patch clamp assay for the N-type calcium channel using prolonged depolarizations to induce inactivation. Attempts were made to reproduce this protocol for our P/Q-type cell line but currents were less stable over time when prepulse duration significantly exceeded 3 s. Although prolonged depolarizations may be present in AD, a favorable screening protocol for state-dependent P/Q-type calcium channel blockers should also be designed to deliver reproducible, robust results at an acceptable throughput. Therefore, a protocol was established using 3 s prepulses inducing approximately 50% inactivation represented the best balance between strong, reversible inactivation and non-saturating slow inactivation or run down. Although this inactivation protocol probably increases the potency of state-dependent compounds, state-independent blockers can also be detected. In fact, using this protocol for automated patch clamp and subsequent manual patch clamp analysis, both state-dependent and state-independent blockers were detected (see results section 3.3.3 and 3.3.4).

It should be noted that assays using short to moderate (up to several seconds long) depolarization prepulses may underestimate compound potency. This is because channel inhibition would either need to occur within the allotted prepulse time or be maintained sufficiently between test pulses to allow for accumulation of block. The protocol used here might especially underestimate the potency of molecules with very slow binding kinetics to the inactivated state. Thus, protocols utilizing longer depolarizations could be more sensitive to slow-binding state-dependent molecules and potentially detect more, and for some pathological states (e.g., migraine) also

more relevant channel modulators. However, prepulses over several minutes or constant depolarizations might be less favorable for state-dependent screening of P/Q-type calcium channel blockers. As observed here, this may induce effects precluding the reversal of inactivation (e.g., run-down, channel internalization), and may thus be unspecific.

To conclude, multiple aspects should be considered when designing electrophysiological assays for identification and validation of calcium channel blockers. The electrophysiological protocol should be chosen adequately for the disease area of interest as well as take into account the inactivation kinetics of the recombinant channel.

4.2.2 Compound Screening Reveals Novel Channel Blockers

For initial detection of novel channel blockers, the P/Q-type calcium channel cell line was applied to a FLIPR-based high-throughput screen as published in Mezler et al. (2012b). For this method cells are loaded with a calcium sensitive fluorescent dye, which can be stimulated with an argon laser. Thus, the emitted fluorescent signal detected by the system is proportional to the intracellular calcium concentration. The signal could be transiently increased upon addition of KCl to the media surrounding the tetracycline-induced P/Q-type calcium channel transfected cells. A subset of potential channel blockers, identified by the high throughput screen, was subsequently validated by secondary screening using automated patch clamp recordings.

Validation of the FLIPR calcium assay was supported in this PhD study by perforated whole-cell analysis in current-clamp mode. Depolarized resting membrane potentials (approximately -30 mV) were observed, which corresponds to published values for HEK293 cells (Thomas and Smart, 2005). This implies that during FLIPR-based compound screening a large fraction of channels is inactivated as demonstrated by the electrophysiologically determined inactivation curves. This may facilitate the detection of state-dependent inhibitors. However, these results are only accurate for the specific solution applied to the patch pipette (here: 150 mM KCl and 10 mM HEPES). In order to obtain a more exact estimation of the resting potential, intracellular recordings applying sharp electrodes are necessary which do

not (or at most hardly) alter ionic concentrations of the cytosol. The current-clamp experiments further revealed that an extracellular increase in KCl concentration to 60 mM (as applied in the FLIPR calcium assay) sufficiently depolarizes the cells to induce P/Q-type calcium channel opening. Taken together, this suggests that the resting membrane potential seemed to be depolarized enough to induce channel inactivation during compound incubation in the FLIPR assay. However, the membrane potential was still sufficiently hyperpolarized that upon depolarization enough channels were available for opening, as observed by a robust increase in intracellular calcium concentration during FLIPR measurements. As a consequence, additional methods for adjusting the membrane potential, like pharmacological modulation or co-transfection with an inward rectifier, were not necessary (Dai et al., 2008). Indeed, in that study assessment of inactivated state block for HVA calcium channels was carried out at resting membrane potentials which were similar to our values. It should, however, be noted that other calcium channel assays might require adjusted methods, such as the use of gramicidin for better control of the membrane potential, to produce adequately robust calcium signals for analysis (Belardetti et al., 2009).

In turn, a chemically diverse subset of Abbott's compound library was screened at AbbVie and a large number of hits identified (about 2% of the screening set, corresponding to 3,262 validated hits of 150,000 compounds - with an IC_{50} between 8 nM and 10 μ M), which is comparable to analogous ion channel programs. For instance, 115,320 compounds were screened in a N-type calcium channel high throughput screen, resulting in 3,600 confirmed hits with >60% inhibition at 5 μ M (Lubin et al., 2006).

Subsequently, in order to exclude unspecific effects on intracellular calcium levels (possibly detected by the FLIPR-based assay) and to show functional activity on the P/Q-type calcium channel, several confirmed hits were validated electrophysiologically in this PhD study. In order to obtain higher throughput automated planar patch clamp recordings from a 4-channel Patchliner system were established and compared to manual patch clamp data.

Here, this Patchliner system increased the throughput by roughly 3- to 5-fold compared to manual patch clamp. This is because usually two to three automated experiments could be successfully run in parallel. Definition of a successful

experiment included cell capture at the hole of the planar chip and establishment of a whole-cell configuration ($R_{\text{seal}} \geq 200 \text{ M}\Omega$; $C_s > 2 \text{ pF}$; $R_s \leq 20 \text{ M}\Omega$). The additional increase in throughput was obtained by shortened preparation times between experiments, as noted in the introduction (section 1.3.2). Characterization of recombinant P/Q-type calcium channel activation and pharmacological sensitivity to ω -agatoxin IVA yielded identical results between the manual and automated Patchliner set up. Our values also compared well to previous reports of recombinant (Hans et al., 1999) and native channels (Mintz et al., 1992). This indicates that our cell line in combination with automated patch clamp is well suited for pharmacological analysis.

However, for the automated system a hyperpolarizing shift in channel inactivation was observed. This was dependent on the protease treatment by trypsin or Accutase prior to automated experiments, as this shift could be reproduced in manual patch clamp recordings if cells were freshly dissociated prior to the measurements. In the process of cell dissociation, channel function may be altered through partial digestion of channel proteins or even simply by the loss of cell adhesion.

Since protease treatment with either accutase or trypsin might be causal to the observed shift in voltage-dependence, alternative cell dissociation methods could be evaluated. Ideally, such methods would allow achieving an identical voltage-dependence of inactivation compared to manual patch clamp (lacking prior protease cell treatment). Combination formulations, like the proteolytic, collagenolytic, and DNase enzyme combination FACSmax, Detachin, or similar preparations could be used. Further, it may be worth testing whether preparation of cell suspensions required for the automated setup might be done by ethylenediaminetetraacetic (EDTA) treatment alone or even by simple mechanical dislocation of the cells. As the cell line used here is HEK293, also these more gentle methods could be successful. If the shift in the inactivation curve is due to the suspension of the cells and their loss of cellular adhesion, then alternative enzymatic or mechanic treatment would not change the outcome of the electrophysiological measurements. Importantly however, since the difference in inactivation kinetics can be accounted for by adjusting the screening protocol, further exploration of these methods was not mandatory for this study. In our case this was obtained by shifting the holding and prepulse potential by -10 mV to more hyperpolarized values in the automated system. Taken together, it

can be concluded that automated patch clamp is a valuable option for higher throughput compound analysis, given that shifts in inactivation kinetics are corrected between the manual and automated patch clamp system.

The automated electrophysiological secondary screen was performed at a single concentration (applying 3 s prepulses) to assess the functional activity of a larger number of structures in order to adequately support the throughput needed within the hit-to-lead drug discovery phase. This phase attempts to identify - from the numerous compounds after screening - chemical scaffolds, which may be suitable for further optimization by medicinal chemistry. Out of 27 compounds tested in this secondary screening assay, 23 compounds confirmed appreciable P/Q-type calcium channel inhibition.

The reason for the lack of P/Q-type calcium channel inhibition of the four compounds was not further investigated, but may arise from non channel-related lowering of cytosolic calcium levels detected in the FLIPR-based assay. This might be caused by compound-dye interactions (Wolff et al., 2003), calcium uptake from intracellular organelles, or effects on e.g., calcium transporters (Tang et al., 2001; Terstappen, 2005). Electrophysiologically validated hits were transferred back to medicinal chemistry hit-to-lead program and potential lead structure candidates were examined for their level of state-dependence by manual patch clamp analysis and advanced into the downstream screening cascade. This secondary analysis further confirmed the ability of the FLIPR-based high throughput screen to detect novel P/Q-type calcium channel inhibitors.

The depolarized resting membrane potential of the HEK293 cells could, on the one hand, explain why most compounds blocked P/Q-type calcium channels also in the secondary screen. This suggests that these compounds (also) block inactivated calcium channels, although this was not explicitly tested (for this the channel block would also need to be assessed omitting the depolarizing prepulse). On the other hand, compounds tended to be more potent in the FLIPR assay as compared to the electrophysiological recordings. This could partially be caused by the fact that cells were constantly depolarized during the 3 min incubation time in the FLIPR compared to a transient 3 s depolarization (at a 12 s interval) during the 2 min incubation in the automated patch clamp assay. Therefore, channel inactivation was most likely more pronounced and sustained in the FLIPR assay. This could explain the increased

potency in the FLIPR assay especially for slow binding and state-dependent modulators.

4.2.3 State-Dependent Calcium Channel Block Ameliorates Oligomeric A β -induced Deficits in Synaptic Transmission

As noted in the introduction, state-dependent molecules are believed to have a beneficial safety profile by leaving physiological resting state activity largely unaltered. However, if this is the case only inactivated channels are fully blocked whereas channels in other states are blocked only to a lesser extent. Therefore, the overall block of channel currents decreases, which might compromise the therapeutic efficacy. Therefore, the synaptoprotective potential of the two previously characterized mixed P/Q-type and N-type calcium channel blockers was tested. One compound hardly distinguishes between resting and inactivated channels; the other preferentially blocks inactivated channels at 5-fold lower IC₅₀ compared to the resting channels.

Based on the potencies determined by electrophysiological and FLIPR measurements, compounds were applied to hippocampal slice cultures at concentrations below or close to the IC₅₀ determined for inactivated P/Q-type calcium channels. For the 5-fold state-dependent compound this concentration is expected to induce little block at presynaptic P/Q-type and N-type channels at resting state and no block at L-type calcium channels (Scott et al., 2012). We were able to show that both (state-independent and state-dependent) LMW blockers completely reversed A β globulomer-induced deficits in synaptic transmission. Indeed, the effect of both compounds was comparable to the rather state-independent toxins, which were even applied at concentrations (slightly) above their IC₅₀. It can therefore be concluded that state-dependence of compounds does not compromise the therapeutic effect in this *in vitro* model of AD. However, it might coincide with a lower side effect profile as observed for the sodium channel blocker like lamotrigine (Xie et al., 1995) compared to TTX (Zimmer, 2010), for example.

4.3 Conclusion and Outlook

This study revealed that block of presynaptic calcium channels by selective peptides protects against oligomeric A β -induced functional decline in synaptic transmission in organotypic hippocampal slice cultures. This might be brought about by inhibiting excessive neurotransmitter release and possibly decreasing synapse loss (Shankar et al., 2007). We further report that oligomeric A β increases calcium currents from recombinant P/Q-type and N-type calcium channels by shifting voltage activation to more hyperpolarized values in a state-independent manner. This probably promotes facilitated neurotransmitter release and functional synaptic decline, which may potentially lead to excitotoxicity.

Moreover, an automated electrophysiological secondary screen was established to identify novel calcium channel blockers, which has not been described previously for the P/Q-type calcium channel. Proper functional assay development requires the complex analysis of biophysical inactivation properties of the recombinant ion channel. The design and optimization of an inactivation protocol for routine automated patch clamp recordings is reported by this thesis, based on an intensive study of voltage-dependent inactivation of the recombinant P/Q-type calcium channel. This protocol is appropriate for the detection and validation of P/Q-type calcium channel blockers and was successfully implemented into the hit-to-lead phase of an electrophysiological secondary screen of a drug development program (Mezler et al., 2012b). One out of two validated calcium channel blockers, which were subsequently analyzed by manual patch clamp, was identified as state-dependent. The discovery and further optimization of state-dependent P/Q-type calcium channel blockers may also lead to the development of new medications for a range of neurological disease indications beyond AD, like migraine and epilepsy.

Finally, both LMW calcium channel blockers were able to reverse oligomeric A β -induced deficits in synaptic transmission. Thus, state-dependent P/Q-type and N-type calcium channel block may antagonize functional synaptic deficits in *in vitro* models of AD. It is unclear whether this *in vitro* data can be extrapolated to patients suffering from AD. It now needs to be shown whether such calcium channel block may alleviate synaptic loss and neurodegeneration in animal models of AD.

Publications

Development and validation of a fluorescence-based high throughput screen assay for the identification of P/Q-type calcium channel blockers

Mezler M*, Hermann D*, Swensen AM, Draguhn A, Terstappen GC, Gross G, Schoemaker H, Freiberg G, Pratt S, Gopalakrishnan SM, Nimmrich V

Combinatorial Chemistry and High Throughput Screening 2012 Jun. 1; 15(5):372-86

* Both authors contributed equally to the work.

Establishment of a Secondary Screening Assay for P/Q-type Calcium Channel Blockers

Hermann D*, Mezler M*, Swensen AM, Bruehl C, Obergroßberger A, Wicke K, Schoemaker H, Gross G, Draguhn A, Nimmrich V

Combinatorial Chemistry & High Throughput Screening, 2013, 16; In Press

* Both authors contributed equally to the work

Synthetic A β oligomers (A β ₁₋₄₂ globulomer) modulate presynaptic calcium currents: Prevention of A β -induced synaptic deficits by calcium channel blockers

Hermann D, Mezler M, Müller MK, Wicke K, Gross G, Draguhn A, Bruehl C, Nimmrich V

Submitted

Bibliography

- Abbadie C, McManus OB, Sun SY, Bugianesi RM, Dai G, Haedo RJ, Herrington JB, Kaczorowski GJ, Smith MM, Swensen AM, Warren VA, Williams B, Arneric SP, Eduljee C, Snutch TP, Tringham EW, Jochnowitz N, Liang A, Euan MacIntyre D, McGowan E, Mistry S, White VV, Hoyt SB, London C, Lyons KA, Bunting PB, Volksdorf S, Duffy JL (2010) Analgesic effects of a substituted N-triazole oxindole (TROX-1), a state-dependent, voltage-gated calcium channel 2 blocker. *J Pharmacol Exp Ther* 334:545-555.
- Abramov E, Dolev I, Fogel H, Ciccotosto GD, Ruff E, Slutsky I (2009) Amyloid- β as a positive endogenous regulator of release probability at hippocampal synapses. *Nat Neurosci* 12:1567-1576.
- Adams ME, Mintz IM, Reily MD, Thanabal V, Bean BP (1993) Structure and properties of ω -agatoxin IVB, a new antagonist of P-type calcium channels. *Mol Pharmacol* 44:681-688.
- Alzheimer A (1907) Über eine eigenartige Erkrankung der Hirnrinde. *Allg Z Psychiatr-Gerichtl Med* 64:146-147.
- Amaral DG, Witter MP (1989) The three-dimensional organization of the hippocampal formation: a review of anatomical data. *Neuroscience* 31:571-591.
- Amatniek JC, Hauser WA, DelCastillo-Castaneda C, Jacobs DM, Marder K, Bell K, Albert M, Brandt J, Stern Y (2006) Incidence and predictors of seizures in patients with Alzheimer's disease. *Epilepsia* 47:867-872.
- Armstrong CM, Bezanilla F (1973) Currents related to movement of the gating particles of the sodium channels. *Nature* 242:459-461.
- Asakura K, Kanemasa T, Minagawa K, Kagawa K, Yagami T, Nakajima M, Ninomiya M (2000) α -eudesmol, a P/Q-type Ca(2+) channel blocker, inhibits neurogenic vasodilation and extravasation following electrical stimulation of trigeminal ganglion. *Brain Res* 873:94-101.
- Ashe KH (2001) Learning and memory in transgenic mice modeling Alzheimer's disease. *Learn Mem* 8:301-308.
- Atwood CS, Obrenovich ME, Liu T, Chan H, Perry G, Smith MA, Martins RN (2003) Amyloid- β : a chameleon walking in two worlds: a review of the trophic and toxic properties of amyloid- β . *Brain Res Brain Res Rev* 43:1-16.
- Ayata C, Shimizu-Sasamata M, Lo EH, Noebels JL, Moskowitz MA (2000) Impaired neurotransmitter release and elevated threshold for cortical spreading depression in mice with mutations in the α_{1A} subunit of P/Q type calcium channels. *Neuroscience* 95:639-645.
- Bachurin S, Bukatina E, Lermontova N, Tkachenko S, Afanasiev A, Grigoriev V, Grigorieva I, Ivanov YU, Sablin S, Zefirov N (2001) Antihistamine agent Dimebon as a novel neuroprotector and a cognition enhancer. *Ann N Y Acad Sci* 939:425-435.
- Bachurin SO, Shevtsova EP, Kireeva EG, Oxenkrug GF, Sablin SO (2003) Mitochondria as a target for neurotoxins and neuroprotective agents. *Ann N Y Acad Sci* 993:334-344.
- Baell JB, Duggan PJ, Forsyth SA, Lewis RJ, Lok YP, Schroeder CI (2004) Synthesis and biological evaluation of nonpeptide mimetics of ω -conotoxin GVIA. *Bioorg Med Chem* 12:4025-4037.
- Barghorn S, Nimmrich V, Striebinger A, Krantz C, Keller P, Janson B, Bahr M, Schmidt M, Bitner RS, Harlan J, Barlow E, Ebert U, Hillen H (2005) Globular amyloid β -peptide₁₋₄₂

- oligomer - a homogenous and stable neuropathological protein in Alzheimer's disease. *J Neurochem* 95:834-847.
- Barnes CA, Danysz W, Parsons CG (1996) Effects of the uncompetitive NMDA receptor antagonist memantine on hippocampal long-term potentiation, short-term exploratory modulation and spatial memory in awake, freely moving rats. *Eur J Neurosci* 8:565-571.
- Barry P (1994) JPCalc, a software package for calculating liquid junction potential corrections in patch-clamp, intracellular, epithelial and bilayer measurements and for correcting junction potential measurements. *J Neurosci Methods* 51:107-116.
- Bartus RT, Dean RL, 3rd, Beer B, Lippa AS (1982) The cholinergic hypothesis of geriatric memory dysfunction. *Science* 217:408-414.
- Bauer CS, Nieto-Rostro M, Rahman W, Tran-Van-Minh A, Ferron L, Douglas L, Kadurin I, Sri Ranjan Y, Fernandez-Alacid L, Millar NS, Dickenson AH, Lujan R, Dolphin AC (2009) The increased trafficking of the calcium channel subunit $\alpha_2\delta$ -1 to presynaptic terminals in neuropathic pain is inhibited by the $\alpha_2\delta$ ligand pregabalin. *J Neurosci* 29:4076-4088.
- Bean BP (1984) Nitrendipine block of cardiac calcium channels: high-affinity binding to the inactivated state. *Proc Natl Acad Sci U S A* 81:6388-6392.
- Behrends JC, Fertig N (2007) Planar patch clamping. *Neuromethods* 38:411-433.
- Belardetti F, Tringham E, Eduljee C, Jiang X, Dong H, Hendricson A, Shimizu Y, Janke DL, Parker D, Mezeyova J, Khawaja A, Pajouhesh H, Fraser RA, Arneric SP, Snutch TP (2009) A fluorescence-based high-throughput screening assay for the identification of T-type calcium channel blockers. *Assay Drug Dev Technol* 7:266-280.
- Benilova I, Karran E, De Strooper B (2012) The toxic A β oligomer and Alzheimer's disease: an emperor in need of clothes. *Nat Neurosci* 15:349-357.
- Benjamin ER, Pruthi F, Olanrewaju S, Ilyin VI, Crumley G, Kutlina E, Valenzano KJ, Woodward RM (2006) State-dependent compound inhibition of Na $_v$ 1.2 sodium channels using the FLIPR V $_m$ dye: on-target and off-target effects of diverse pharmacological agents. *J Biomol Screen* 11:29-39.
- Berman RF, Verweij BH, Muizelaar JP (2000) Neurobehavioral protection by the neuronal calcium channel blocker ziconotide in a model of traumatic diffuse brain injury in rats. *J Neurosurg* 93:821-828.
- Berretta N, Jones RSG (1996) Tonic facilitation of glutamate release by presynaptic N-methyl-d-aspartate autoreceptors in the entorhinal cortex. *Neuroscience* 75:339-344.
- Bezánilla F (2002) Voltage sensor movements. *J Gen Physiol* 120:465-473.
- Bezprozvanny I, Scheller RH, Tsien RW (1995) Functional impact of syntaxin on gating of N-type and Q-type calcium channels. *Nature* 378:623-626.
- Birks J (2006) Cholinesterase inhibitors for Alzheimer's disease. *Cochrane Database Syst Rev* CD005593.
- Birks J, López-Arrieta J (2002) Nimodipine for primary degenerative, mixed and vascular dementia. *Cochrane Database Syst Rev* CD000147.
- Blennow K, Bogdanovic N, Alafuzoff I, Ekman R, Davidsson P (1996) Synaptic pathology in Alzheimer's disease: Relation to severity of dementia, but not to senile plaques, neurofibrillary tangles, or the ApoE4 allele. *J Neural Transm* 103:603-618.
- Bliss TV, Collingridge GL (1993) A synaptic model of memory: long-term potentiation in the hippocampus. *Nature* 361:31-39.

- Bliss TV, Lomo T (1973) Long-lasting potentiation of synaptic transmission in the dentate area of the anaesthetized rabbit following stimulation of the perforant path. *J Physiol* 232:331-356.
- Bobich JA, Zheng Q, Campbell A (2004) Incubation of nerve endings with a physiological concentration of $A\beta_{1-42}$ activates CaV2.2(N-Type)-voltage operated calcium channels and acutely increases glutamate and noradrenaline release. *J Alzheimers Dis* 6:243-255.
- Boccaccio A, Moran O, Conti F (1998) Calcium dependent shifts of Na^+ channel activation correlated with the state dependence of calcium-binding to the pore. *Eur Biophys J* 27:558-566.
- Bonhoeffer T, Staiger V, Aertsen A (1989) Synaptic plasticity in rat hippocampal slice cultures: local "Hebbian" conjunction of pre- and postsynaptic stimulation leads to distributed synaptic enhancement. *Proc Natl Acad Sci U S A* 86:8113-8117.
- Borst JGG, Sakmann B (1998) Facilitation of presynaptic calcium currents in the rat brainstem. *J Physiol* 513:149-155.
- Bouras C, Hof PR, Giannakopoulos P, Michel JP, Morrison JH (1994) Regional distribution of neurofibrillary tangles and senile plaques in the cerebral cortex of elderly patients: a quantitative evaluation of a one-year autopsy population from a geriatric hospital. *Cereb Cortex* 4:138-150.
- Bourinet E, Soong TW, Sutton K, Slaymaker S, Mathews E, Monteil A, Zamponi GW, Nargeot J, Snutch TP (1999) Splicing of α_{1A} subunit gene generates phenotypic variants of P- and Q-type calcium channels. *Nat Neurosci* 2:407-415.
- Bowen DM, Benton JS, Spillane JA, Smith CCT, Allen SJ (1982) Choline acetyltransferase activity and histopathology of frontal neocortex from biopsies of demented patients. *J Neurol Sci* 57:191-202.
- Bowen DM, Smith CB, White P, Davison AN (1976) Neurotransmitter-related enzymes and indices of hypoxia in senile dementia and other abiotrophies. *Brain* 99:459-496.
- Braak H, Braak E, Bohl J (1993) Staging of Alzheimer-related cortical destruction. *Eur Neurol* 33:403-408.
- Branchaw JL, Banks MI, Jackson MB (1997) Ca^{2+} - and voltage-dependent inactivation of Ca^{2+} channels in nerve terminals of the neurohypophysis. *J Neurosci* 17:5772-5781.
- Bresink I, Benke TA, Collett VJ, Seal AJ, Parsons CG, Henley JM, Collingridge GL (1996) Effects of memantine on recombinant rat NMDA receptors expressed in HEK 293 cells. *Br J Pharmacol* 119:195-204.
- Brose WG, Gutlove DP, Luther RR, Bowersox SS, McGuire D (1997) Use of intrathecal SNX-111, a novel, N-type, voltage-sensitive, calcium channel blocker, in the management of intractable brachial plexus avulsion pain. *Clin J Pain* 13:256-259.
- Brunnstrom HR, Englund EM (2009) Cause of death in patients with dementia disorders. *Eur J Neurol* 16:488-492.
- Buhl EH, Szilagyi T, Halasy K, Somogyi P (1996) Physiological properties of anatomically identified basket and bistratified cells in the CA1 area of the rat hippocampus in vitro. *Hippocampus* 6:294-305.
- Buraei Z, Anghelescu M, Elmslie KS (2005) Slowed N-type calcium channel (CaV2.2) deactivation by the cyclin-dependent kinase inhibitor roscovitine. *Biophys J* 89:1681-1691.
- Buraei Z, Elmslie KS (2008) The separation of antagonist from agonist effects of trisubstituted purines on CaV2.2 (N-type) channels. *J Neurochem* 105:1450-1461.

- Buraei Z, Schofield G, Elmslie KS (2007) Roscovitine differentially affects CaV2 and Kv channels by binding to the open state. *Neuropharmacology* 52:883-894.
- Buraei Z, Yang J (2010) The β subunit of voltage-gated Ca²⁺ channels. *Physiol Rev* 90:1461-1506.
- Butterfield DA, Pocernich CB (2003) The glutamatergic system and Alzheimer's disease: therapeutic implications. *CNS Drugs* 17:641-652.
- Buzsáki G (1984) Feed-forward inhibition in the hippocampal formation. *Prog Neurobiol* 22:131-153.
- Buzsáki G (2002) Theta oscillations in the hippocampus. *Neuron* 33:325-340.
- Cabrejo L, Guyant-Marechal L, Laquerriere A, Vercelletto M, De la Fourniere F, Thomas-Anterion C, Verny C, Letournel F, Pasquier F, Vital A, Checler F, Frebourg T, Campion D, Hannequin D (2006) Phenotype associated with APP duplication in five families. *Brain* 129:2966-2976.
- Campion D, Dumanchin C, Hannequin D, Dubois B, Belliard S, Puel M, Thomas-Anterion C, Michon A, Martin C, Charbonnier F, Raux G, Camuzat A, Penet C, Mesnage V, Martinez M, Clerget-Darpoux F, Brice A, Frebourg T (1999) Early-onset autosomal dominant Alzheimer disease: prevalence, genetic heterogeneity, and mutation spectrum. *Am J Hum Genet* 65:664-670.
- Canti C, Bogdanov Y, Dolphin AC (2000) Interaction between G proteins and accessory β subunits in the regulation of α 1B calcium channels in *Xenopus* oocytes. *J Physiol* 527:419-432.
- Castillo PE, Weisskopf MG, Nicoll RA (1994) The role of Ca²⁺ channels in hippocampal mossy fiber synaptic transmission and long-term potentiation. *Neuron* 12:261-269.
- Catterall WA, Few AP (2008) Calcium channel regulation and presynaptic plasticity. *Neuron* 59:882-901.
- Catterall WA, Perez-Reyes E, Snutch TP, Striessnig J (2005) International Union of Pharmacology. XLVIII. Nomenclature and structure-function relationships of voltage-gated calcium channels. *Pharmacol Rev* 57:411-425.
- Cerella C, Diederich M, Ghibelli L (2010) The dual role of calcium as messenger and stressor in cell damage, death, and survival. *Int J Cell Biol* 2010:546163.
- Chang FC, Benton BJ, Salyer JL, Foster RE, Franz DR (1990) Respiratory and cardiovascular effects of tetrodotoxin in urethane-anesthetized guinea pigs. *Brain Res* 528:259-268.
- Chartier-Harlin MC, Crawford F, Houlden H, Warren A, Hughes D, Fidani L, Goate A, Rossor M, Roques P, Hardy J, Mullan M (1991) Early-onset Alzheimer's disease caused by mutations at codon 717 of the β -amyloid precursor protein gene. *Nature* 353:844-846.
- Charton JP, Herkert M, Becker C-M, Schröder H (1999) Cellular and subcellular localization of the 2B-subunit of the NMDA receptor in the adult rat telencephalon. *Brain Res* 816:609-617.
- Choi DW (1988) Calcium-mediated neurotoxicity: relationship to specific channel types and role in ischemic damage. *Trends Neurosci* 11:465-469.
- Citron M, Oltersdorf T, Haass C, McConlogue L, Hung AY, Seubert P, Vigo-Pelfrey C, Lieberburg I, Selkoe DJ (1992) Mutation of the β -amyloid precursor protein in familial Alzheimer's disease increases β -protein production. *Nature* 360:672-674.
- Citron M, Westaway D, Xia W, Carlson G, Diehl T, Levesque G, Johnson-wood K, Lee M, Seubert P, Davis A, Kholodenko D, Motter R, Sherrington R, Perry B, Yao H, Strome R, Lieberburg I, Rommens J, Kim S, Schenk D, Fraser P, St George Hyslop P, Selkoe DJ (1997) Mutant presenilins of Alzheimer's disease increase production of 42-

- residue amyloid β -protein in both transfected cells and transgenic mice. *Nat Med* 3:67-72.
- Clare JJ (2010) Targeting ion channels for drug discovery. *Discov Med* 9:253-260.
- Cleary JP, Walsh DM, Hofmeister JJ, Shankar GM, Kuskowski MA, Selkoe DJ, Ashe KH (2005) Natural oligomers of the amyloid- β protein specifically disrupt cognitive function. *Nat Neurosci* 8:79-84.
- Corder E, Saunders A, Strittmatter W, Schmechel D, Gaskell P, Small G, Roses A, Haines J, Pericak-Vance M (1993) Gene dose of apolipoprotein E type 4 allele and the risk of Alzheimer's disease in late onset families. *Science* 261:921-923.
- Coric V, van Dyck CH, Salloway S, Andreasen N, Brody M, Richter RW, Soininen H, Thein S, Shiovitz T, Pilcher G, Colby S, Rollin L, Dockens R, Pachai C, Portelius E, Andreasson U, Blennow K, Soares H, Albright C, Feldman HH, Berman RM (2012) Safety and tolerability of the γ -secretase inhibitor avagacestat in a phase 2 study of mild to moderate Alzheimer disease. *Arch Neurol* 1-12.
- Courtney C, Farrell D, Gray R, Hills R, Lynch L, Sellwood E, Edwards S, Hardyman W, Raftery J, Crome P, Lendon C, Shaw H, Bentham P (2004) Long-term donepezil treatment in 565 patients with Alzheimer's disease (AD2000): randomised double-blind trial. *Lancet* 363:2105-2115.
- Craik DJ, Adams DJ (2007) Chemical modification of conotoxins to improve stability and activity. *ACS Chem Biol* 2:457-468.
- Cuijpers P (2005) Depressive disorders in caregivers of dementia patients: a systematic review. *Aging Ment Health* 9:325-330.
- Cullen WK, Suh YH, Anwyl R, Rowan MJ (1997) Block of LTP in rat hippocampus in vivo by β -amyloid precursor protein fragments. *Neuroreport* 8:3213-3217.
- Curran ME, Splawski I, Timothy KW, Vincent GM, Green ED, Keating MT (1995) A molecular basis for cardiac arrhythmia: HERG mutations cause long QT syndrome. *Cell* 80:795-803.
- Cuttle MF, Tsujimoto T, Forsythe ID, Takahashi T (1998) Facilitation of the presynaptic calcium current at an auditory synapse in rat brainstem. *J Physiol* 512:723-729.
- Dai G, Haedo RJ, Warren VA, Ratliff KS, Bugianesi RM, Rush A, Williams ME, Herrington J, Smith MM, McManus OB, Swensen AM (2008) A high-throughput assay for evaluating state dependence and subtype selectivity of Cav2 calcium channel inhibitors. *Assay Drug Dev Technol* 6:195-212.
- Danysz W, Parsons CG (2003) The NMDA receptor antagonist memantine as a symptomatological and neuroprotective treatment for Alzheimer's disease: preclinical evidence. *Int J Geriatr Psychiatry* 18:S23-32.
- Davies A, Hendrich J, Van Minh AT, Wratten J, Douglas L, Dolphin AC (2007) Functional biology of the $\alpha_2\delta$ subunits of voltage-gated calcium channels. *Trends Pharmacol Sci* 28:220-228.
- Davies A, Kadurin I, Alvarez-Laviada A, Douglas L, Nieto-Rostro M, Bauer CS, Pratt WS, Dolphin AC (2010) The $\alpha_2\delta$ subunits of voltage-gated calcium channels form GPI-anchored proteins, a posttranslational modification essential for function. *Proc Natl Acad Sci U S A* 107:1654-1659.
- Davies P, Maloney AJ (1976) Selective loss of central cholinergic neurons in Alzheimer's disease. *Lancet* 2:1403.
- De Strooper B, Saftig P, Craessaerts K, Vanderstichele H, Guhde G, Annaert W, Von Figura K, Van Leuven F (1998) Deficiency of presenilin-1 inhibits the normal cleavage of amyloid precursor protein. *Nature* 391:387-390.

- Degtiar VE, Scheller RH, Tsien RW (2000) Syntaxin modulation of slow inactivation of N-type calcium channels. *J Neurosci* 20:4355-4367.
- DeKosky ST, Scheff SW (1990) Synapse loss in frontal cortex biopsies in Alzheimer's disease: correlation with cognitive severity. *Ann Neurol* 27:457-464.
- DeKosky ST, Scheff SW, Styren SD (1996) Structural correlates of cognition in dementia: quantification and assessment of synapse change. *Neurodegeneration* 5:417-421.
- Demuro A, Parker I, Stutzmann GE (2010) Calcium signaling and amyloid toxicity in Alzheimer disease. *J Biol Chem* 285:12463-12468.
- Dietrich D, Kirschstein T, Kukley M, Pereverzev A, von der Brelie C, Schneider T, Beck H (2003) Functional specialization of presynaptic Ca_v2.3 Ca²⁺ channels. *Neuron* 39:483-496.
- Diochot S, Richard S, Baldy-Moulinier M, Nargeot J, Valmier J (1995) Dihydropyridines, phenylalkylamines and benzothiazepines block N-, P/Q- and R-type calcium currents. *Pflugers Arch* 431:10-19.
- Disterhoft JF, Moyer JR, Jr., Thompson LT (1994) The calcium rationale in aging and Alzheimer's disease. Evidence from an animal model of normal aging. *Ann N Y Acad Sci* 747:382-406.
- Dodel R, Neff F, Noelker C, Pul R, Du Y, Bacher M, Oertel W (2010) Intravenous immunoglobulins as a treatment for Alzheimer's disease: rationale and current evidence. *Drugs* 70:513-528.
- Dodge HH, Shen C, Pandav R, DeKosky ST, Ganguli M (2003) Functional transitions and active life expectancy associated with Alzheimer disease. *Arch Neurol* 60:253-259.
- Dolmetsch RE, Pajvani U, Fife K, Spotts JM, Greenberg ME (2001) Signaling to the nucleus by an L-type calcium channel-calmodulin complex through the MAP kinase pathway. *Science* 294:333-339.
- Dolphin AC (2012) Calcium channel auxiliary α_2 and β subunits: trafficking and one step beyond. *Nat Rev Neurosci* 13:542-555.
- Doody RS, Gavrilova SI, Sano M, Thomas RG, Aisen PS, Bachurin SO, Seely L, Hung D (2008) Effect of dimebon on cognition, activities of daily living, behaviour, and global function in patients with mild-to-moderate Alzheimer's disease: a randomised, double-blind, placebo-controlled study. *Lancet* 372:207-215.
- Drachman DA, Leavitt J (1974) Human memory and the cholinergic system. A relationship to aging? *Arch Neurol* 30:113-121.
- Duff K, Eckman C, Zehr C, Yu X, Prada CM, Perez-tur J, Hutton M, Buee L, Harigaya Y, Yager D, Morgan D, Gordon MN, Holcomb L, Refolo L, Zenk B, Hardy J, Younkin S (1996) Increased amyloid- β 42(43) in brains of mice expressing mutant presenilin 1. *Nature* 383:710-713.
- Dunlop J, Bowlby M, Peri R, Vasilyev D, Arias R (2008) High-throughput electrophysiology: an emerging paradigm for ion-channel screening and physiology. *Nat Rev Drug Discov* 7:358-368.
- Dutar P, Rascol O, Lamour Y (1989) ω -Conotoxin GVIA blocks synaptic transmission in the CA1 field of the hippocampus. *Eur J Pharmacol* 174:261-266.
- Engert F, Bonhoeffer T (1999) Dendritic spine changes associated with hippocampal long-term synaptic plasticity. *Nature* 399:66-70.
- Epps DE, Wolfe ML, Groppi V (1994) Characterization of the steady-state and dynamic fluorescence properties of the potential-sensitive dye bis-(1,3-dibutylbarbituric acid)trimethine oxonol (Dibac₄(3)) in model systems and cells. *Chem Phys Lipids* 69:137-150.

- Falconer M, Smith F, Surah-Narwal S, Congrave G, Liu Z, Hayter P, Ciaramella G, Keighley W, Haddock P, Waldron G, Sewing A (2002) High-throughput screening for ion channel modulators. *J Biomol Screen* 7:460-465.
- Farre C, Stoelzle S, Haarmann C, George M, Bruggemann A, Fertig N (2007) Automated ion channel screening: patch clamping made easy. *Expert Opin Ther Targets* 11:557-565.
- Farrugia G (2008) Ion channels as targets for treatment of gastrointestinal motility disorders. *Eur Rev Med Pharmacol Sci* 12:135.
- Feng ZP, Doering CJ, Winkfein RJ, Beedle AM, Spafford JD, Zamponi GW (2003) Determinants of inhibition of transiently expressed voltage-gated calcium channels by ω -conotoxins GVIA and MVIIA. *J Biol Chem* 278:20171-20178.
- Ferri CP, Sousa KM, Albanese E, Riberio W, Honyashiki M (2009) World Alzheimer Report 2009. <http://www.alz.co.uk/research/files/WorldAlzheimerReport.pdf>: Alzheimer's Disease International.
- Fink K, Dooley DJ, Meder WP, Suman-Chauhan N, Duffy S, Clusmann H, Göthert M (2002) Inhibition of neuronal Ca^{2+} influx by gabapentin and pregabalin in the human neocortex. *Neuropharmacology* 42:229-236.
- Finley MF, Lubin ML, Neeper MP, Beck E, Liu Y, Flores CM, Qin N (2010) An integrated multiassay approach to the discovery of small-molecule N-type voltage-gated calcium channel antagonists. *Assay Drug Dev Technol* 8:685-694.
- Fitzjohn SM, Doherty AJ, Collingridge GL (2008) The use of the hippocampal slice preparation in the study of Alzheimer's disease. *Eur J Pharmacol* 585:50-59.
- Fletcher CF, Lutz CM, O'Sullivan TN, Shaughnessy JD, Hawkes R, Frankel WN, Copeland NG, Jenkins NA (1996) Absence epilepsy in tottering mutant mice is associated with calcium channel defects. *Cell* 87:607-617.
- Förstl H, Kurz A (1999) Clinical features of Alzheimer's disease. *Eur Arch Psychiatry Clin Neurosci* 249:288-290.
- Forsythe ID, Tsujimoto T, Barnes-Davies M, Cuttle MF, Takahashi T (1998) Inactivation of presynaptic calcium current contributes to synaptic depression at a fast central synapse. *Neuron* 20:797-807.
- Freeze BS, McNulty MM, Hanck DA (2006) State-dependent verapamil block of the cloned human $Ca_v3.1$ T-type Ca^{2+} channel. *Mol Pharmacol* 70:718-726.
- Frotscher M, Heimrich B, Deller T (1997) Sprouting in the hippocampus is layer-specific. *Trends Neurosci* 20:218-223.
- Frotscher M, Heimrich B, Deller T, Nitsch R (1995) Understanding the cortex through the hippocampus: lamina-specific connections of the rat hippocampal neurons. *J Anat* 187:539-545.
- Furakawa T, Yamakawa T, Midera T, Sagawa T, Mori Y, Nukada T (1999) Selectivities of dihydropyridine derivatives in blocking Ca^{2+} channel subtypes expressed in *Xenopus* oocytes. *JPET* 291:464-473.
- Furukawa K, Wang Y, Yao PJ, Fu W, Mattson MP, Itoyama Y, Onodera H, D'Souza I, Poorkaj PH, Bird TD, Schellenberg GD (2003) Alteration in calcium channel properties is responsible for the neurotoxic action of a familial frontotemporal dementia tau mutation. *J Neurochem* 87:427-436.
- Galasko DR, Peskind E, Clark CM, Quinn JF, Ringman JM, Jicha GA, Cotman C, Cottrell B, Montine TJ, Thomas RG, Aisen P (2012) Antioxidants for Alzheimer disease: a randomized clinical trial with cerebrospinal fluid biomarker measures. *Arch Neurol* 69:836-841.

- Gaugler JE, Duval S, Anderson KA, Kane RL (2007) Predicting nursing home admission in the U.S: a meta-analysis. *BMC Geriatr* 7:13.
- Gee NS, Brown JP, Dissanayake VUK, Offord J, Thurlow R, Woodruff GN (1996) The novel anticonvulsant drug, gabapentin (Neurontin), binds to the $\alpha 2\delta$ subunit of a calcium channel. *J Biol Chem* 271:5768-5776.
- Geib S, Sandoz G, Cornet V, Mabrouk K, Fund-Saunier O, Bichet D, Villaz M, Hoshi T, Sabatier JM, De Waard M (2002) The interaction between the I-II loop and the III-IV loop of $Ca_v2.1$ contributes to voltage-dependent inactivation in a β -dependent manner. *J Biol Chem* 277:10003-10013.
- Gellermann GP, Byrnes H, Striebinger A, Ullrich K, Mueller R, Hillen H, Barghorn S (2008) A β -globulomers are formed independently of the fibril pathway. *Neurobiol Dis* 30:212-220.
- Gera S, Byerly L (1999) Measurement of calcium channel inactivation is dependent upon the test pulse potential. *Biophys J* 76:3076–3088.
- Gilman S, Koller M, Black RS, Jenkins L, Griffith SG, Fox NC, Eisner L, Kirby L, Rovira MB, Forette F, Orgogozo JM (2005) Clinical effects of A β immunization (AN1792) in patients with AD in an interrupted trial. *Neurology* 64:1553-1562.
- Giuffrida ML, Caraci F, Pignataro B, Cataldo S, De Bona P, Bruno V, Molinaro G, Pappalardo G, Messina A, Palmigiano A, Garozzo D, Nicoletti F, Rizzarelli E, Copani A (2009) β -amyloid monomers are neuroprotective. *J Neurosci* 29:10582-10587.
- Glenner GG, Wong CW (1984) Alzheimer's disease and Down's syndrome: Sharing of a unique cerebrovascular amyloid fibril protein. *Biochemical and Biophysical Research Communications* 122:1131-1135.
- Gloeckner SF, Meyne F, Wagner F, Heinemann U, Krasnianski A, Meissner B, Zerr I (2008) Quantitative analysis of transthyretin, tau and amyloid- β in patients with dementia. *J Alzheimers Dis* 14:17-25.
- Goate A, Chartier-Harlin MC, Mullan M, Brown J, Crawford F, Fidani L, Giuffra L, Haynes A, Irving N, James L, Mant R, Newton P, Rooke K, Roques P, Talbot C, Pericak-Vance M, Roses A, Williamson R, Rossor M, Owen M, Hardy J (1991) Segregation of a missense mutation in the amyloid precursor protein gene with familial Alzheimer's disease. *Nature* 349:704-706.
- Golde TE, Schneider LS, Koo EH (2011) Anti-a β therapeutics in Alzheimer's disease: the need for a paradigm shift. *Neuron* 69:203-213.
- Gómez-Isla T, Price JL, McKeel DW, Morris JC, Growdon JH, Hyman BT (1996) Profound loss of layer II entorhinal cortex neurons occurs in very mild Alzheimer's disease. *J Neurosci* 16:4491-4500.
- Gong Y, Chang L, Viola KL, Lacor PN, Lambert MP, Finch CE, Krafft GA, Klein WL (2003) Alzheimer's disease-affected brain: presence of oligomeric A beta ligands (ADDLs) suggests a molecular basis for reversible memory loss. *Proc Natl Acad Sci U S A* 100:10417-10422.
- Gosche KM, Mortimer JA, Smith CD, Markesbery WR, Snowdon DA (2002) Hippocampal volume as an index of Alzheimer neuropathology: Findings from the Nun Study. *Neurology* 58:1476-1482.
- Graham FL, Smiley J, Russell WC, Nairn R (1977) Characteristics of a human cell line transformed by DNA from human adenovirus type 5. *J Gen Virol* 36:59-72.
- Green KN, Smith IF, Laferla FM (2007) Role of calcium in the pathogenesis of Alzheimer's disease and transgenic models. *Subcell Biochem* 45:507-521.

- Green RC, Schneider LS, Amato DA, Beelen AP, Wilcock G, Swabb EA, Zavitz KH (2009) Effect of tarenflurbil on cognitive decline and activities of daily living in patients with mild Alzheimer disease: a randomized controlled trial. *JAMA* 302:2557-2564.
- Greenamyre JT, Penney JB, D'Amato CJ, Young AB (1987) Dementia of the Alzheimer's type: Changes in hippocampal L-[3H]glutamate binding. *J Neurochem* 48:543-551.
- Greenamyre JT, Young AB (1989) Excitatory amino acids and Alzheimer's disease. *Neurobiol Aging* 10:593-602.
- Guida S, Trettel F, Pagnutti S, Mantuano E, Tottene A, Veneziano L, Fellin T, Spadaro M, Stauderman K, Williams M, Volsen S, Ophoff R, Frants R, Jodice C, Frontali M, Pietrobon D (2001) Complete loss of P/Q calcium channel activity caused by a CACNA1A missense mutation carried by patients with episodic ataxia type 2. *Am J Hum Genet* 68:759-764.
- Haass C, Selkoe DJ (2007) Soluble protein oligomers in neurodegeneration: lessons from the Alzheimer's amyloid β -peptide. *Nat Rev Mol Cell Biol* 8:101-112.
- Hadjikhani N, Sanchez Del Rio M, Wu O, Schwartz D, Bakker D, Fischl B, Kwong KK, Cutrer FM, Rosen BR, Tootell RB, Sorensen AG, Moskowitz MA (2001) Mechanisms of migraine aura revealed by functional MRI in human visual cortex. *Proc Natl Acad Sci U S A* 98:4687-4692.
- Halasy K, Buhl EH, Lörinczi Z, Tamas G, Somogyi P (1996) Synaptic target selectivity and input of GABAergic basket and bistratified interneurons in the CA1 area of the rat hippocampus. *Hippocampus* 6:306-329.
- Hamill OP, Marty A, Neher E, Sakmann B, Sigworth FJ (1981) Improved patch-clamp techniques for high-resolution current recording from cells and cell-free membrane patches. *Pflugers Arch* 391:85-100.
- Hempel H, Blennow K, Shaw LM, Hoessler YC, Zetterberg H, Trojanowski JQ (2010) Total and phosphorylated tau protein as biological markers of Alzheimer's disease. *Exp Gerontol* 45:30-40.
- Hans M, Urrutia A, Deal C, Brust F, Stauderman K, Ellis SB, Harpold MM, Johnson EC, Williams ME (1999) Structural elements in domain IV that influence biophysical and pharmacological properties of human α_{1A} -containing high-voltage-activated calcium channels. *Biophys J* 76:1384-1400.
- Hardy J, Allsop D (1991) Amyloid deposition as the central event in the aetiology of Alzheimer's disease. *Trends Pharmacol Sci* 12:383-388.
- Hardy J, Selkoe DJ (2002) The amyloid hypothesis of Alzheimer's disease: progress and problems on the road to therapeutics. *Science* 297:353-356.
- Harkany T, Abraham I, Timmerman W, Laskay G, Toth B, Sasvari M, Konya C, Sebens JB, Korf J, Nyakas C, Zarandi M, Soos K, Penke B, Luiten PGM (2000) β -Amyloid neurotoxicity is mediated by a glutamate-triggered excitotoxic cascade in rat nucleus basalis. *Eur J Neurosci* 12:2735-2745.
- Harvey RJ, Skelton-Robinson M, Rossor MN (2003) The prevalence and causes of dementia in people under the age of 65 years. *J Neurol Neurosurg Psychiatry* 74:1206-1209.
- He LM, Chen LY, Lou XL, Qu AL, Zhou Z, Xu T (2002) Evaluation of beta-amyloid peptide 25-35 on calcium homeostasis in cultured rat dorsal root ganglion neurons. *Brain Res* 939:65-75.
- Hebb DO (1949) *The Organization of Behavior - A neuropsychological Theory*: John Wiley & Sons, Inc.
- Hell JW, Westenbroek RE, Warner C, Ahljianian MK, Prystay W, Gilbert MM, Snutch TP, Catterall WA (1993) Identification and differential subcellular localization of the

- neuronal class C and class D L-type calcium channel $\alpha 1$ subunits. *J Cell Biol* 123:949-962.
- Hepler RW, Grimm KM, Nahas DD, Breese R, Dodson EC, Acton P, Keller PM, Yeager M, Wang H, Shughrue P, Kinney G, Joyce JG (2006) Solution state characterization of amyloid β -derived diffusible ligands. *Biochemistry* 45:15157-15167.
- Hermann D, Both M, Ebert U, Gross G, Schoemaker H, Draguhn A, Wicke K, Nimrich V (2009) Synaptic transmission is impaired prior to plaque formation in amyloid precursor protein-overexpressing mice without altering behaviorally-correlated sharp wave-ripple complexes. *Neuroscience* 162:1081-1090.
- Hermann D, Mezler M, Müller MK, Wicke K, Gross G, Draguhn A, Bruehl C, Nimrich V (2013a) Submitted: Synthetic A β oligomers (A β_{1-42} globulomer) modulate presynaptic calcium currents: Prevention of A β -induced synaptic deficits by calcium channel blockers.
- Hermann D, Mezler M, Swensen AM, Bruehl C, Obergrußberger A, Wicke K, Schoemaker H, Gross G, Draguhn A, Nimrich V (2013b) Establishment of a secondary screening assay for P/Q-type calcium channel blockers. *Comb Chem High Throughput Screen* (Epub ahead of print).
- Hess P, Lansman JB, Tsien RW (1986) Calcium channel selectivity for divalent and monovalent cations. Voltage and concentration dependence of single channel current in ventricular heart cells. *J Gen Physiol* 88:293-319.
- Hillen H, Barghorn S, Striebinger A, Labkovsky B, Muller R, Nimrich V, Nolte MW, Perez-Cruz C, van der Auwera I, van Leuven F, van Gaalen M, Bessalov AY, Schoemaker H, Sullivan JP, Ebert U (2010) Generation and therapeutic efficacy of highly oligomer-specific β -amyloid antibodies. *J Neurosci* 30:10369-10379.
- Hilt DC, Gawryl M, Koenig G, Dgetluck N, Loewen G, Harrison J, Moebius HJ, Group E--S (2012) EVP-6124, a selective $\alpha 7$ partial agonist, has positive effects on cognition and clinical function in mild to moderate Alzheimer's disease patients. In: Alzheimer's Association International Conference Vancouver, British Columbia, Canada.
- Hirsch LJ, Weintraub D, Du Y, Buchsbaum R, Spencer HT, Hager M, Straka T, Bazil CW, Adams DJ, Resor SR, Morrell MJ (2004) Correlating lamotrigine serum concentrations with tolerability in patients with epilepsy. *Neurology* 63:1022-1026.
- Hockerman GH, Dilmac N, Scheuer T, Catterall WA (2000) Molecular determinants of diltiazem block in domains IIS6 and IVS6 of L-type Ca^{2+} channels. *Mol Pharmacol* 58:1264-1270.
- Hoffmann U, Dilekoz E, Kudo C, Ayata C (2010) Gabapentin suppresses cortical spreading depression susceptibility. *J Cereb Blood Flow Metab* 30:1588-1592.
- Holevinsky KO, Fan Z, Frame M, Makielski JC, Groppi V, Nelson DJ (1994) ATP-sensitive K^+ channel opener acts as a potent Cl^- channel inhibitor in vascular smooth muscle cells. *J Membr Biol* 137.
- Holmes C, Boche D, Wilkinson D, Yadegarfar G, Hopkins V, Bayer A, Jones RW, Bullock R, Love S, Neal JW, Zotova E, Nicoll JAR (2008) Long-term effects of A β_{42} immunisation in Alzheimer's disease: follow-up of a randomised, placebo-controlled phase I trial. *Lancet* 372:216-223.
- Hoppa MB, Lana B, Margas W, Dolphin AC, Ryan TA (2012) $\alpha 2\delta$ expression sets presynaptic calcium channel abundance and release probability. *Nature* 486:122-125.
- Horak S, Koschak A, Stuppner H, Striessnig J (2009) Use-dependent block of voltage-gated $\text{Ca}_v2.1$ Ca^{2+} channels by petasins and eudesmol isomers. *J Pharmacol Exp Ther* 330:220-226.

- Hoshi T, Zagotta W, Aldrich R (1990) Biophysical and molecular mechanisms of Shaker potassium channel inactivation. *Science* 250:533-538.
- Hughes AD, Wijetunge S (1993) The action of amlodipine on voltage-operated calcium channels in vascular smooth muscle. *Br J Pharmacol* 109:120-125.
- Hyman B, Van Hoesen G, Damasio A, Barnes C (1984) Alzheimer's disease: cell-specific pathology isolates the hippocampal formation. *Science* 225:1168-1170.
- Imming P, Sinning C, Meyer A (2006) Drugs, their targets and the nature and number of drug targets. *Nat Rev Drug Discov* 5:821-834.
- Imredy J (1994) Mechanism of Ca²⁺-sensitive inactivation of L-type Ca²⁺ channels. *Neuron* 12:1301-1318.
- Innocent N, Evans N, Hille C, Wonnacott S (2010) Oligomerisation differentially affects the acute and chronic actions of amyloid-beta in vitro. *Neuropharmacology* 59:343-352.
- Ishibashi H, Yatani A, Akaike N (1995) Block of P-type Ca²⁺ channels in freshly dissociated rat cerebellar Purkinje neurons by diltiazem and verapamil. *Brain Res* 695:88-91.
- Ishibashi K, Tomiyama T, Nishitsuji K, Hara M, Mori H (2006) Absence of synaptophysin near cortical neurons containing oligomer A β in Alzheimer's disease brain. *J Neurosci Res* 84:632-636.
- Isom LL, De Jongh KS, Catterall WA (1994) Auxiliary subunits of voltage-gated ion channels. *Neuron* 12:1183-1194.
- Jackson HC, Scheideler MA (1996) Behavioural and anticonvulsant effects of Ca²⁺ channel toxins in DBA/2 mice. *Psychopharmacology (Berl)* 126:85-90.
- Jaturapatporn D, Isaac MG, McCleery J, Tabet N (2012) Aspirin, steroidal and non-steroidal anti-inflammatory drugs for the treatment of Alzheimer's disease. *Cochrane Database Syst Rev* 2:CD006378.
- Jellinger KA (2006) Clinicopathological analysis of dementia disorders in the elderly--an update. *J Alzheimers Dis* 9:61-70.
- Johnson&Johnson (2012) Johnson & Johnson announces discontinuation of phase 3 development of bapineuzumab intravenous (IV) in mild-to-moderate Alzheimer's disease. <http://www.jnj.com/connect/news/all/johnson-and-johnson-announces-discontinuation-of-phase-3-development-of-bapineuzumab-intravenous-iv-in-mild-to-moderate-alzheimers-disease>.
- Jones O, Kunze D, Angelides K (1989) Localization and mobility of ω -conotoxin-sensitive Ca²⁺ channels in hippocampal CA1 neurons. *Science* 244:1189-1193.
- Jones RW (2010) Dimebon disappointment. *Alzheimers Res Ther* 2:25.
- Jouveneau A, Eunson LH, Spauschus A, Ramesh V, Zuberi SM, Kullmann DM, Hanna MG (2001) Human epilepsy associated with dysfunction of the brain P/Q-type calcium channel. *Lancet* 358:801-807.
- Kaczorowski GJ, McManus OB, Priest BT, Garcia ML (2008) Ion channels as drug targets: the next GPCRs. *J Gen Physiol* 131:399-405.
- Kadurin I, Alvarez-Laviada A, Ng SF, Walker-Gray R, D'Arco M, Fadel MG, Pratt WS, Dolphin AC (2012) Calcium currents are enhanced by $\alpha_2\delta$ -1 lacking its membrane anchor. *J Biol Chem* 287.
- Kamp TJ, Sanguinetti MC, Miller RJ (1989) Voltage- and use-dependent modulation of cardiac calcium channels by the dihydropyridine (+)-202-791. *Circ Res* 64:338-351.
- Kaneko I, Morimoto K, Kubo T (2001) Drastic neuronal loss in vivo by β -amyloid racemized at Ser²⁶ residue: conversion of non-toxic [D-Ser²⁶] β -amyloid 1-40 to toxic and proteinase-resistant fragments. *Neuroscience* 104:1003-1011.

- Kaneko S, Cooper CB, Nishioka N, Yamasaki H, Suzuki A, Jarvis SE, Akaike A, Satoh M, Zamponi GW (2002) Identification and characterization of novel human Ca_v2.2 (α_{1B}) calcium channel variants lacking the synaptic protein interaction site. *J Neurosci* 22:82-92.
- Kass RS (1987) Voltage-dependent modulation of cardiac calcium channel current by optical isomers of Bay K 8644: implications for channel gating. *Circ Res* 61:11-5.
- Kelly BL, Ferreira A (2006) β -Amyloid-induced dynamin 1 degradation is mediated by N-methyl-D-aspartate receptors in hippocampal neurons. *J Biol Chem* 281:28079-28089.
- Kelly BL, Ferreira A (2007) A β disrupted synaptic vesicle endocytosis in cultured hippocampal neurons. *Neuroscience* 147:60-70.
- Kelly BL, Vassar R, Ferreira A (2005) β -amyloid-induced dynamin 1 depletion in hippocampal neurons. A potential mechanism for early cognitive decline in Alzheimer disease. *J Biol Chem* 280:31746-31753.
- Kim JH, Anwyl R, Suh YH, Djamgoz MB, Rowan MJ (2001) Use-dependent effects of amyloidogenic fragments of β -amyloid precursor protein on synaptic plasticity in rat hippocampus in vivo. *J Neurosci* 21:1327-1333.
- Kim S, Rhim H (2011) Effects of amyloid-beta peptides on voltage-gated L-type Ca_v1.2 and Ca_v1.3 Ca²⁺ channels. *Mol Cells* 32:289-294.
- Kiss L, Bennett PB, Uebele VN, Koblan KS, Kane SA, Neagle B, Schroeder K (2003) High throughput ion-channel pharmacology: planar-array-based voltage clamp. *Assay Drug Dev Technol* 1:127-135.
- Klugbauer N, Lacinova L, Marais E, Hobom M, Hofmann F (1999) Molecular diversity of the calcium channel $\alpha_2\delta$ subunit. *J Neurosci* 19:684-691.
- Klyubin I, Betts V, Welzel AT, Blennow K, Zetterberg H, Wallin A, Lemere CA, Cullen WK, Peng Y, Wisniewski T, Selkoe DJ, Anwyl R, Walsh DM, Rowan MJ (2008) Amyloid β protein dimer-containing human CSF disrupts synaptic plasticity: prevention by systemic passive immunization. *J Neurosci* 28:4231-4237.
- Knopman DS, DeKosky ST, Cummings JL, Chui H, Corey-Bloom J, Relkin N, Small GW, Miller B, Stevens JC (2001) Practice parameter: Diagnosis of dementia (an evidence-based review). *Neurology* 56:1143-1153.
- Koch ED, Olivera BM, Terlau H, Conti F (2004) The binding of κ -conotoxin PVIIA and fast C-Type inactivation of shaker K⁺ channels are mutually exclusive. *Biophys J* 86:191-209.
- Kokubo H, Kaye R, Glabe CG, Saido TC, Iwata N, Helms JB, Yamaguchi H (2005a) Oligomeric proteins ultrastructurally localize to cell processes, especially to axon terminals with higher density, but not to lipid rafts in Tg2576 mouse brain. *Brain Res* 1045:224-228.
- Kokubo H, Kaye R, Glabe CG, Yamaguchi H (2005b) Soluble A β oligomers ultrastructurally localize to cell processes and might be related to synaptic dysfunction in Alzheimer's disease brain. *Brain Res* 1031:222-228.
- Kornhuber J, Weller M (1997) Psychotogenicity and N-methyl-D-aspartate receptor antagonism: Implications for neuroprotective pharmacotherapy. *Biological Psychiatry* 41:135-144.
- Kortekaas P, Wadman WJ (1997) Development of HVA and LVA calcium currents in pyramidal CA1 neurons in the hippocampus of the rat. *Brain Res Dev Brain Res* 101:139-147.

- Kraus RL, Sinnegger MJ, Koschak A, Glossmann H, Stenirri S, Carrera P, Striessnig J (2000) Three new familial hemiplegic migraine mutants affect P/Q-type Ca^{2+} channel kinetics. *J Biol Chem* 275:9239-9243.
- Krishtal OA, Pidoplichko VI (1975) Intracellular perfusion of giant snail neurons. *Neirofiziologija* 7:327-329.
- Kristian T, Siesjö BK (1998) Calcium in ischemic cell death. *Stroke* 29:705-718.
- Krystal JH, Karper LP, Seibyl JP, Freeman GK, Delaney R, Bremner JD, Heninger GR, Bowers MB, Jr., Charney DS (1994) Subanesthetic effects of the noncompetitive NMDA antagonist, ketamine, in humans. Psychotomimetic, perceptual, cognitive, and neuroendocrine responses. *Arch Gen Psychiatry* 51:199-214.
- Kunkler PE, Kraig RP (2004) P/Q Ca^{2+} channel blockade stops spreading depression and related pyramidal neuronal Ca^{2+} rise in hippocampal organ culture. *Hippocampus* 14:356-367.
- Kuo CC, Lu L (1997) Characterization of lamotrigine inhibition of Na^+ channels in rat hippocampal neurones. *Br J Pharmacol* 121:1231-1238.
- Kuperstein I, Broersen K, Benilova I, Rozenski J, Jonckheere W, Debulpaep M, Vandersteen A, Segers-Nolten I, Van Der Werf K, Subramaniam V, Braeken D, Callewaert G, Bartic C, D'Hooge R, Martins IC, Rousseau F, Schymkowitz J, De Strooper B (2010) Neurotoxicity of Alzheimer's disease $\text{A}\beta$ peptides is induced by small changes in the $\text{A}\beta_{42}$ to $\text{A}\beta_{40}$ ratio. *EMBO J* 29:3408-3420.
- Kyrozis A, Reichling DB (1995) Perforated-patch recording with gramicidin avoids artifactual changes in intracellular chloride concentration. *J Neurosci Methods* 57:27-35.
- Lacor PN, Buniel MC, Furlow PW, Clemente AS, Velasco PT, Wood M, Viola KL, Klein WL (2007) $\text{A}\beta$ oligomer-induced aberrations in synapse composition, shape, and density provide a molecular basis for loss of connectivity in Alzheimer's disease. *J Neurosci* 27:796-807.
- Lam JK, Jiang X, Hendricson A, Tringham E, Belardetti F, Areneric SP, Snutch TP, Parker DB (2007) Rat Cav2.1 stable cell line expression in HEK 293 cells. In: SBS 13th Annual Conference 2007 (Advancing the Science of Drug Discovery: Bridging Research & Development), Montréal, Canada.
- Lambert M, Barlow A, Chromy B, Edwards C, Freed R, Liosatos M, Morgan T, Rozovsky I, Trommer B, Viola K (1998) Diffusible, nonfibrillar ligands derived from $\text{A}\beta_{1-42}$ are potent central nervous system neurotoxins. *Proc Natl Acad Sci USA* 95:6448.
- Lanctot KL, Herrmann N, Yau KK, Khan LR, Liu BA, LouLou MM, Einarson TR (2003) Efficacy and safety of cholinesterase inhibitors in Alzheimer's disease: a meta-analysis. *CMAJ* 169:557-564.
- Lashuel HA, Hartley DM, Balakhaneh D, Aggarwal A, Teichberg S, Callaway DJ (2002) New class of inhibitors of amyloid- β fibril formation. Implications for the mechanism of pathogenesis in Alzheimer's disease. *J Biol Chem* 277:42881-42890.
- Lazarov O, Lee M, Peterson DA, Sisodia SS (2002) Evidence that synaptically released β -amyloid accumulates as extracellular deposits in the hippocampus of transgenic mice. *J Neurosci* 22:9785-9793.
- Lee A, Scheuer T, Catterall WA (2000) Ca^{2+} /calmodulin-dependent facilitation and inactivation of P/Q-type Ca^{2+} channels. *J Neurosci* 20:6830-6838.
- Lee A, Wong ST, Gallagher D, Li B, Storm DR, Scheuer T, Catterall WA (1999) Ca^{2+} /calmodulin binds to and modulates P/Q-type calcium channels. *Nature* 399:155-159.

- Lee J, Culyba EK, Powers ET, Kelly JW (2011) Amyloid- β forms fibrils by nucleated conformational conversion of oligomers. *Nat Chem Biol* 7:602-609.
- Lesne S, Koh MT, Kotilinek L, Kaye R, Glabe CG, Yang A, Gallagher M, Ashe KH (2006) A specific amyloid- β protein assembly in the brain impairs memory. *Nature* 440:352-357.
- Leveque C, el Far O, Martin-Moutot N, Sato K, Kato R, Takahashi M, Seagar MJ (1994) Purification of the N-type calcium channel associated with syntaxin and synaptotagmin. *J Biol Chem* 269:6306-6312.
- Lewis J, Dickson DW, Lin WL, Chisholm L, Corral A, Jones G, Yen SH, Sahara N, Skipper L, Yager D, Eckman C, Hardy J, Hutton M, McGowan E (2001) Enhanced neurofibrillary degeneration in transgenic mice expressing mutant tau and APP. *Science* 293:1487-1491.
- Liao P, Zhang HY, Soong TW (2009) Alternative splicing of voltage-gated calcium channels: from molecular biology to disease. *Pflugers Arch* 458:481-487.
- Lilly (2010) Lilly halts development of semagacestat for Alzheimer's disease based on preliminary results of phase III clinical trials. <http://newsroom.lilly.com/releasedetail.cfm?releaseid=499794>: Eli Lilly and Company.
- Lilly (2012) Eli Lilly and Company announces top-line results on solanezumab phase 3 clinical trials in patients with Alzheimer's disease. <https://investor.lilly.com/releaseDetail.cfm?ReleaseID=702211>: Eli Lilly and Company.
- Lipton SA (2006) Paradigm shift in neuroprotection by NMDA receptor blockade: memantine and beyond. *Nat Rev Drug Discov* 5:160-170.
- Lipton SA, Rosenberg PA (1994) Excitatory amino acids as a final common pathway for neurologic disorders. *N Engl J Med* 330:613-622.
- Lott IT, Head E (2005) Alzheimer disease and Down syndrome: factors in pathogenesis. *Neurobiol Aging* 26:383-389.
- Louis N, Eveleigh C, Graham FL (1997) Cloning and sequencing of the cellular-viral junctions from the human adenovirus type 5 transformed 293 cell line. *Virology* 233:423-429.
- Lubin ML, Reitz TL, Todd MJ, Flores CM, Qin N, Xin H (2006) A nonadherent cell-based HTS assay for N-type calcium channel using calcium 3 dye. *Assay Drug Dev Technol* 4:689-694.
- Lue LF, Kuo YM, Roher AE, Brachova L, Shen Y, Sue L, Beach T, Kurth JH, Rydel RE, Rogers J (1999) Soluble amyloid β peptide concentration as a predictor of synaptic change in Alzheimer's disease. *Am J Pathol* 155:853.
- Luebke JI, Dunlap K, Turner TJ (1993) Multiple calcium channel types control glutamatergic synaptic transmission in the hippocampus. *Neuron* 11:895-902.
- Lundbeck (2012) Lundbeck's Lu AE58054 meets primary endpoint in large placebo-controlled clinical proof of concept study in people with Alzheimer's disease. vol. 2012 <http://investor.lundbeck.com/releasedetail.cfm?ReleaseID=677436>.
- MacManus A, Ramsden M, Murray M, Henderson Z, Pearson HA, Campbell VA (2000) Enhancement of $^{45}\text{Ca}^{2+}$ influx and voltage-dependent Ca^{2+} channel activity by β -amyloid-(1-40) in rat cortical synaptosomes and cultured cortical neurons. *J Biol Chem* 275:4713-4718.
- Maher-Edwards G, Dixon R, Hunter J, Gold M, Hopton G, Jacobs G, Williams P (2011) SB-742457 and donepezil in Alzheimer disease: a randomized, placebo-controlled study. *Int J Geriatr Psychiatry* 26:536-544.

- Maher-Edwards G, Zvartau-Hind M, Hunter AJ, Gold M, Hopton G, Jacobs G, Davy M, Williams P (2010) Double-blind, controlled phase II study of a 5-HT₆ receptor antagonist, SB-742457, in Alzheimer's disease. *Curr Alzheimer Res* 7:374-385.
- Mangialasche F, Solomon A, Winblad B, Mecocci P, Kivipelto M (2010) Alzheimer's disease: clinical trials and drug development. *Lancet Neurol* 9:702-716.
- Mansvelder HD, Stoof JC, Kits KS (1996) Dihydropyridine block of ω -agatoxin IVA and ω -conotoxin GVIA-sensitive Ca²⁺ channels in rat pituitary melanotropic cells. *Eur J Pharmacol* 311:293-304.
- Maragos WF, Greenamyre JT, Penney JB, Young AB (1987) Glutamate dysfunction in Alzheimer's disease: an hypothesis. *Trends Neurosci* 10:65-68.
- Martin R, Meador K, Turrentine L, Faught E, Sinclair K, Kuzniecky R, Gilliam F (2001) Comparative cognitive effects of carbamazepine and gabapentin in healthy senior adults. *Epilepsia* 42:764-771.
- Masliah E, Terry RD, Mallory M, Alford M, Hansen LA (1990) Diffuse plaques do not accentuate synapse loss in Alzheimer's disease. *Am J Pathol* 137:1293.
- Masters CL, Simms G, Weinman NA, Multhaup G, McDonald BL, Beyreuther K (1985) Amyloid plaque core protein in Alzheimer disease and Down syndrome. *Proc Natl Acad Sci U S A* 82:4245-4249.
- Mathew NT, Rapoport A, Saper J, Magnus L, Klapper J, Ramadan N, Stacey B, Tepper S (2001) Efficacy of gabapentin in migraine prophylaxis. *Headache* 41:119-128.
- Mathur VS (2000) Ziconotide: A new pharmacological class of drug for the management of pain. *Semin Anesth Periop Med Pain* 19:67-75.
- Matsuyama Z, Wakamori M, Mori Y, Kawakami H, Nakamura S, Imoto K (1999) Direct alteration of the P/Q-type Ca²⁺ channel property by polyglutamine expansion in spinocerebellar ataxia 6. *J Neurosci* 19:RC14.
- Matsuzaki M, Honkura N, Ellis-Davies GC, Kasai H (2004) Structural basis of long-term potentiation in single dendritic spines. *Nature* 429:761-766.
- Mattson MP (2004) Pathways towards and away from Alzheimer's disease. *Nature* 430:631-639.
- Mattson MP, Cheng B, Davis D, Bryant K, Lieberburg I, Rydel RE (1992) β -Amyloid peptides destabilize calcium homeostasis and render human cortical neurons vulnerable to excitotoxicity. *J Neurosci* 12:376-389.
- Mc Donald JM, Savva GM, Brayne C, Welzel AT, Forster G, Shankar GM, Selkoe DJ, Ince PG, Walsh DM (2010) The presence of sodium dodecyl sulphate-stable A β dimers is strongly associated with Alzheimer-type dementia. *Brain* 133:1328-1341.
- McDonough SI, Mintz IM, Bean BP (1997) Alteration of P-type calcium channel gating by the spider toxin omega-Aga-IVA. *Biophysical Journal* 72:2117-2128.
- McGowan E, Eriksen J, Hutton M (2006) A decade of modeling Alzheimer's disease in transgenic mice. *Trends Genet* 22:281-289.
- McGuire D, Bowersox S, Fellmann JD, Luther RR (1997) Sympatholysis after neuron-specific, N-type, voltage-sensitive calcium channel blockade: first demonstration of N-channel function in humans. *J Cardiovasc Pharmacol* 30:400-403.
- McKhann G, Drachman D, Folstein M, Katzman R, Price D, Stadlan EM (1984) Clinical diagnosis of Alzheimer's disease. *Neurology* 34:939-939.
- McKhann GM, Knopman DS, Chertkow H, Hyman BT, Jack CR, Jr., Kawas CH, Klunk WE, Koroshetz WJ, Manly JJ, Mayeux R, Mohs RC, Morris JC, Rossor MN, Scheltens P,

- Carrillo MC, Thies B, Weintraub S, Phelps CH (2011) The diagnosis of dementia due to Alzheimer's disease. *Alzheimers Dement* 7:263-269.
- McLaurin J, Cecal R, Kierstead ME, Tian X, Phinney AL, Manea M, French JE, Lambermon MH, Darabie AA, Brown ME, Janus C, Chishti MA, Horne P, Westaway D, Fraser PE, Mount HT, Przybylski M, St George-Hyslop P (2002) Therapeutically effective antibodies against amyloid-beta peptide target amyloid-beta residues 4-10 and inhibit cytotoxicity and fibrillogenesis. *Nat Med* 8:1263-1269.
- McLean CA, Cherny RA, Fraser FW, Fuller SJ, Smith MJ, Konrad V, Bush AI, Masters CL (1999) Soluble pool of A β amyloid as a determinant of severity of neurodegeneration in Alzheimer's disease. *Annals of neurology* 46:860-866.
- Menzler S, Bikker JA, Suman-Chauhan N, Horwell DC (2000) Design and biological evaluation of non-peptide analogues of ω -conotoxin MVIIA. *Bioorg Med Chem Lett* 10:345-347.
- Mezler M, Barghorn S, Schoemaker H, Gross G, Nimmrich V (2012a) A β -amyloid oligomer directly modulates P/Q-type calcium currents in *Xenopus* oocytes. *Br J Pharmacol* 165:1572-1583.
- Mezler M, Hermann D, Swensen AM, Draguhn A, Terstappen GC, Gross G, Schoemaker H, Freiberg G, Pratt S, Gopalakrishnan SM, Nimmrich V (2012b) Development and validation of a fluorescence-based HTS assay for the identification of P/Q-type calcium channel blockers. *Comb Chem High Throughput Screen* 15:372-385.
- Miljanich GP (2004) Ziconotide: neuronal calcium channel blocker for treating severe chronic pain. *Curr Med Chem* 11:3029-3040.
- Millucci L, Ghezzi L, Bernardini G, Santucci A (2010) Conformations and biological activities of amyloid beta peptide 25-35. *Curr Protein Pept Sci* 11:54-67.
- Milstein AD, Nicoll RA (2008) Regulation of AMPA receptor gating and pharmacology by TARP auxiliary subunits. *Trends Pharmacol Sci* 29:333-339.
- Mintz IM, Adams ME, Bean BP (1992) P-type calcium channels in rat central and peripheral neurons. *Neuron* 9:85-95.
- Mori Y, Friedrich T, Kim MS, Mikami A, Nakai J, Ruth P, Bosse E, Hofmann F, Flockerzi V, Furuichi T, Mikoshiba K, Imoto K, Tanabe T, Numa S (1991) Primary structure and functional expression from complementary DNA of a brain calcium channel. *Nature* 350:398-402.
- Morris RG, Anderson E, Lynch GS, Baudry M (1986) Selective impairment of learning and blockade of long-term potentiation by an N-methyl-D-aspartate receptor antagonist AP5. *Nature* 319:774-776.
- Murphy TH, Worley PF, Baraban JM (1991) L-type voltage-sensitive calcium channels mediate synaptic activation of immediate early genes. *Neuron* 7:625-635.
- Murrell J, Farlow M, Ghetti B, Benson M (1991) A mutation in the amyloid precursor protein associated with hereditary Alzheimer's disease. *Science* 254:97-99.
- Myhrer T (1998) Adverse psychological impact, glutamatergic dysfunction, and risk factors for Alzheimer's disease. *Neurosci Biobehav Rev* 23:131-139.
- Nawrath H, Wegener JW (1997) Kinetics and state-dependent effects of verapamil on cardiac L-type calcium channels. *Naunyn Schmiedebergs Arch Pharmacol* 355:79-86.
- Neary D, Snowden JS, Mann DM, Bowen DM, Sims NR, Northen B, Yates PO, Davison AN (1986) Alzheimer's disease: a correlative study. *J Neurol Neurosurg Psychiatry* 49:229-237.
- Neher E, Sakmann B (1976) Single-channel currents recorded from membrane of denervated frog muscle fibres. *Nature* 260:799-802.

- Nelson MT, Todorovic SM, Perez-Reyes E (2006) The role of T-type calcium channels in epilepsy and pain. *Curr Pharm Des* 12:2189-2197.
- Nimmrich V, Ebert U (2009) Is Alzheimer's disease a result of presynaptic failure? Synaptic dysfunctions induced by oligomeric β -amyloid. *Rev Neurosci* 20:1-12.
- Nimmrich V, Grimm C, Draguhn A, Barghorn S, Lehmann A, Schoemaker H, Hillen H, Gross G, Ebert U, Bruehl C (2008a) Amyloid β oligomers ($A\beta_{1-42}$ globulomer) suppress spontaneous synaptic activity by inhibition of P/Q-type calcium currents. *J Neurosci* 28:788-797.
- Nimmrich V, Gross G (2012) P/Q-type calcium channel modulators. *Br J Pharmacol* 167:741-759.
- Nimmrich V, Reymann KG, Strassburger M, Schoder UH, Gross G, Hahn A, Schoemaker H, Wicke K, Moller A (2010) Inhibition of calpain prevents NMDA-induced cell death and β -amyloid-induced synaptic dysfunction in hippocampal slice cultures. *Br J Pharmacol* 159:1523-1531.
- Nimmrich V, Szabo R, Nyakas C, Granic I, Reymann KG, Schroder UH, Gross G, Schoemaker H, Wicke K, Moller A, Luiten P (2008b) Inhibition of calpain prevents N-Methyl-D-aspartate-induced degeneration of the nucleus basalis and associated behavioral dysfunction. *J Pharmacol Exp Ther* 327:343-352.
- Noguchi A, Matsumura S, Dezawa M, Tada M, Yanazawa M, Ito A, Akioka M, Kikuchi S, Sato M, Ideno S, Noda M, Fukunari A, Muramatsu S, Itokazu Y, Sato K, Takahashi H, Teplow DB, Nabeshima Y, Kakita A, Imahori K, Hoshi M (2009) Isolation and characterization of patient-derived, toxic, high mass amyloid β -protein ($A\beta$) assembly from Alzheimer disease brains. *J Biol Chem* 284:32895-32905.
- Nordin M, Nystrom B, Wallin U, Hagbarth KE (1984) Ectopic sensory discharges and paresthesiae in patients with disorders of peripheral nerves, dorsal roots and dorsal columns. *Pain* 20:231-245.
- Nowycky MC, Fox AP, Tsien RW (1985) Three types of neuronal calcium channel with different calcium agonist sensitivity. *Nature* 316:440-443.
- Numberger M, Draguhn A (1996) *Patch-Clamp Technik: Spektrum Akademischer Verlag Heidelberg*.
- Nussbaum RL, Ellis CE (2003) Alzheimer's disease and Parkinson's disease. *N Engl J Med* 348:1356-1364.
- O'Keefe J, Dostrovsky J (1971) The hippocampus as a spatial map. Preliminary evidence from unit activity in the freely-moving rat. *Brain Res* 34:171-175.
- O'Keefe J, Recce ML (1993) Phase relationship between hippocampal place units and the EEG theta rhythm. *Hippocampus* 3:317-330.
- Oddo S, Billings L, Kesslak JP, Cribbs DH, LaFerla FM (2004) $A\beta$ immunotherapy leads to clearance of early, but not late, hyperphosphorylated tau aggregates via the proteasome. *Neuron* 43:321-332.
- Oddo S, Caccamo A, Tran L, Lambert MP, Glabe CG, Klein WL, LaFerla FM (2006) Temporal profile of amyloid- β ($A\beta$) oligomerization in an in vivo model of Alzheimer disease. A link between $A\beta$ and tau pathology. *J Biol Chem* 281:1599-1604.
- Olivera BM, Cruz LJ, Desantos V, Lecheminant GW, Griffin D, Zeikus R, McIntosh JM, Galyean R, Varga J, Gray WR, Rivier J (1987) Neuronal calcium-channel antagonists - discrimination between calcium-channel subtypes using ω -conotoxin from conus-magus venom. *Biochemistry* 26:2086-2090.

- Olivera BM, Miljanich GP, Ramachandran J, Adams ME (1994) Calcium channel diversity and neurotransmitter release: the ω -conotoxins and ω -agatoxins. *Annu Rev Biochem* 63:823-867.
- Olney J, Labruyere J, Wang G, Wozniak D, Price M, Sesma M (1991) NMDA antagonist neurotoxicity: mechanism and prevention. *Science* 254:1515-1518.
- Olson MI, Shaw C-M (1969) Presenile dementia and Alzheimer's disease in mongolism. *Brain* 92:147-156.
- Ono K, Condrón MM, Teplow DB (2009) Structure-neurotoxicity relationships of amyloid β -protein oligomers. *Proc Natl Acad Sci U S A* 106:14745-14750.
- Ophoff RA, Terwindt GM, Frants RR, Ferrari MD (1998) P/Q-type Ca^{2+} channel defects in migraine, ataxia and epilepsy. *Trends Pharmacol Sci* 19:121-127.
- Orgogozo JM, Rigaud AS, Stöffler A, Möbius HJ, Forette F (1991) Efficacy and safety of memantine in patients with mild to moderate vascular dementia. *Stroke* 33:1834-1839.
- Orrenius S, McConkey DJ, Bellomo G, Nicotera P (1989) Role of Ca^{2+} in toxic cell killing. *Trends Pharmacol Sci* 10:281-285.
- Overington JP, Al-Lazikani B, Hopkins AL (2006) How many drug targets are there? *Nat Rev Drug Discov* 5:993-996.
- Palmer AM, Gershon S (1990) Is the neuronal basis of Alzheimer disease cholinergic or glutamatergic. *FASEB J* 4:2745-2752.
- Palop JJ, Chin J, Roberson ED, Wang J, Thwin MT, Bien-Ly N, Yoo J, Ho KO, Yu GQ, Kreitzer A, Finkbeiner S, Noebels JL, Mucke L (2007) Aberrant excitatory neuronal activity and compensatory remodeling of inhibitory hippocampal circuits in mouse models of Alzheimer's disease. *Neuron* 55:697-711.
- Parsons CG, Gruner R, Rozental J, Millar J, Lodge D (1993) Patch clamp studies on the kinetics and selectivity of N-methyl-D-aspartate receptor antagonism by memantine (1-amino-3,5-dimethyladamantan). *Neuropharmacology* 32:1337-1350.
- Patil PG, Brody DL, Yue DT (1998) Preferential closed-state inactivation of neuronal calcium channels. *Neuron* 20:1027-1038.
- Pazzaglia PJ, Post RM, Ketter TA, Callahan AM, Marangell LB, Frye MA, George MS, Kimbrell TA, Leverich GS, Cora-Locatelli G, Luckenbaugh D (1998) Nimodipine monotherapy and carbamazepine augmentation in patients with refractory recurrent affective illness. *J Clin Psychopharmacol* 18:404-413.
- Perez-Reyes E (2003) Molecular physiology of low-voltage-activated T-type calcium channels. *Physiol Rev* 83:117-161.
- Perry EK, Gibson PH, Blessed G, Perry RH, Tomlinson BE (1977) Neurotransmitter enzyme abnormalities in senile dementia. *J Neurol Sci* 34:247-265.
- Perry EK, Tomlinson BE, Blessed G, Bergmann K, Gibson PH, Perry RH (1978) Correlation of cholinergic abnormalities with senile plaques and mental test scores in senile dementia. *Br Med J* 2:1457-1459.
- Petersen RC, Thomas RG, Grundman M, Bennett D, Doody R, Ferris S, Galasko D, Jin S, Kaye J, Levey A, Pfeiffer E, Sano M, van Dyck CH, Thal LJ (2005) Vitamin E and donepezil for the treatment of mild cognitive impairment. *N Engl J Med* 352:2379-2388.
- Peterson BZ, DeMaria CD, Yue DT (1999) Calmodulin is the Ca^{2+} sensor for Ca^{2+} -dependent inactivation of L-Type calcium channels. *Neuron* 22:549-558.

- Pietrobon D (2005) Function and dysfunction of synaptic calcium channels: insights from mouse models. *Curr Opin Neurobiol* 15:257-265.
- Pietrobon D (2010) Ca_v2.1 channelopathies. *Pflugers Arch* 460:375-393.
- Plummer MR, Logothetis DE, Hess P (1989) Elementary properties and pharmacological sensitivities of calcium channels in mammalian peripheral neurons. *Neuron* 2:1453-1463.
- Polo-Parada L, Korn SJ (1997) Block of N-type calcium channels in chick sensory neurons by external sodium. *J Gen Physiol* 109:693-702.
- Potier B, Dutar P, Lamour Y (1993) Different effects of ω -conotoxin GVIA at excitatory and inhibitory synapses in rat CA1 hippocampal neurons. *Brain Res* 616:236-241.
- Prickaerts J, van Goethem NP, Chesworth R, Shapiro G, Boess FG, Methfessel C, Reneerkens OA, Flood DG, Hilt D, Gawryl M, Bertrand S, Bertrand D, König G (2012) EVP-6124, a novel and selective $\alpha 7$ nicotinic acetylcholine receptor partial agonist, improves memory performance by potentiating the acetylcholine response of $\alpha 7$ nicotinic acetylcholine receptors. *Neuropharmacology* 62:1099-1110.
- Puzzo D, Privitera L, Leznik E, Fa M, Staniszewski A, Palmeri A, Arancio O (2008) Picomolar amyloid- β positively modulates synaptic plasticity and memory in hippocampus. *J Neurosci* 28:14537-14545.
- Qin N, Platano D, Olcese R, Costantin JL, Stefani E, Birnbaumer L (1998) Unique regulatory properties of the type 2a Ca²⁺ channel β subunit caused by palmitoylation. *Proc Natl Acad Sci U S A* 95:4690-4695.
- Rajakulendran S, Kaski D, Hanna MG (2012) Neuronal P/Q-type calcium channel dysfunction in inherited disorders of the CNS. *Nat Rev Neurol* 8:86-96.
- Ramsden M, Henderson Z, Pearson HA (2002) Modulation of Ca²⁺ channel currents in primary cultures of rat cortical neurones by amyloid β protein (1–40) is dependent on solubility status. *Brain Res* 956:254-261.
- Reisberg B, Doody R, Stoffler A, Schmitt F, Ferris S, Möbius HJ (2003) Memantine in moderate-to-severe Alzheimer's disease. *N Engl J Med* 348:1333-1341.
- Relkin N, Bettger L, Tsakanikas D, Ravdin L (2012) Three-year follow-up on the IVIg for Alzheimer's phase II study. *Alzheimers Dement* 8:580.
- Rezazadeh S, Hesketh JC, Fedida D (2004) Rb⁺ flux through hERG channels affects the potency of channel blocking drugs: correlation with data obtained using a high-throughput Rb⁺ efflux assay. *J Biomol Screen* 9:588-597.
- Riedel G, Platt B, Micheau J (2003) Glutamate receptor function in learning and memory. *Behav Brain Res* 140:1-47.
- Rogawski MA, Wenk GL (2003) The neuropharmacological basis for the use of memantine in the treatment of Alzheimer's disease. *CNS Drug Rev* 9:275-308.
- Rossé G, Schaffhauser H (2010) 5-HT₆ receptor antagonists as potential therapeutics for cognitive impairment. *Curr Top Med Chem* 10:207-221.
- Rovira C, Arbez N, Mariani J (2002) A β (25-35) and A β (1-40) act on different calcium channels in CA1 hippocampal neurons. *Biochem Biophys Res Commun* 296:1317-1321.
- Rowan MJ, Klyubin I, Cullen WK, Anwyl R (2003) Synaptic plasticity in animal models of early Alzheimer's disease. *Philos Trans R Soc Lond B Biol Sci* 358:821-828.
- Sah DW, Bean BP (1994) Inhibition of P-type and N-type calcium channels by dopamine receptor antagonists. *Mol Pharmacol* 45:84-92.

- Sanchez PE, Zhu L, Verret L, Vossel KA, Orr AG, Cirrito JR, Devidze N, Ho K, Yu GQ, Palop JJ, Mucke L (2012) Levetiracetam suppresses neuronal network dysfunction and reverses synaptic and cognitive deficits in an Alzheimer's disease model. *Proc Natl Acad Sci U S A* 109:E2895-2903.
- Sandoz G, Bichet D, Cornet V, Mori Y, Felix R, De Waard M (2001) Distinct properties and differential β subunit regulation of two C-terminal isoforms of the P/Q-type Ca^{2+} -channel α_{1A} subunit. *Eur J Neurosci* 14:987-997.
- Sanguinetti MC, Jiang C, Curran ME, Keating MT (1995) A mechanistic link between an inherited and an acquired cardiac arrhythmia: HERG encodes the I_{Kr} potassium channel. *Cell* 81:299-307.
- Sanguinetti MC, Krafte DS, Kass RS (1986) Voltage-dependent modulation of Ca channel current in heart cells by Bay K8644. *J Gen Physiol* 88:369-392.
- Sato H (2003) Sino-atrial nodal cells of mammalian hearts: ionic currents and gene expression of pacemaker ionic channels. *J Smooth Muscle Res* 39:175-193.
- Sberna G, Sáez-Valero J, Beyreuther K, Masters CL, Small DH (1997) The amyloid β -protein of Alzheimer's disease increases acetylcholinesterase expression by increasing intracellular calcium in embryonal carcinoma P19 cells. *J Neurochem* 69:1177-1184.
- Schenk D, Barbour R, Dunn W, Gordon G, Grajeda H, Guido T, Hu K, Huang J, Johnson-Wood K, Khan K, Kholodenko D, Lee M, Liao Z, Lieberburg I, Motter R, Mutter L, Soriano F, Shopp G, Vasquez N, Vandeventer C, Walker S, Wogulis M, Yednock T, Games D, Seubert P (1999) Immunization with amyloid-beta attenuates Alzheimer-disease-like pathology in the PDAPP mouse. *Nature* 400:173-177.
- Scheuner D, Eckman C, Jensen M, Song X, Citron M, Suzuki N, Bird TD, Hardy J, Hutton M, Kukull W, Larson E, Levy-Lahad L, Viitanen M, Peskind E, Poorkaj P, Schellenberg G, Tanzi R, Wasco W, Lannfelt L, Selkoe D, Younkin S (1996) Secreted amyloid β -protein similar to that in the senile plaques of Alzheimer's disease is increased in vivo by the presenilin 1 and 2 and APP mutations linked to familial Alzheimer's disease. *Nat Med* 2:864-870.
- Schmidtko A, Lotsch J, Freynhagen R, Geisslinger G (2010) Ziconotide for treatment of severe chronic pain. *Lancet* 375:1569-1577.
- Schmitz C, Rutten BPF, Pielen A, Schäfer S, Wirths O, Tremp G, Czech C, Blanchard V, Multhaup G, Rezaie P, Korr H, Steinbusch HWM, Pradier L, Bayer TA (2004) Hippocampal neuron loss exceeds amyloid plaque load in a transgenic mouse model of Alzheimer's disease. *Am J Pathol* 164:1495-1502.
- Schneider LS, Dagerman KS, Higgins JP, McShane R (2011) Lack of evidence for the efficacy of memantine in mild Alzheimer disease. *Arch Neurol* 68:991-998.
- Schreibmayer W, Tripathi O, Tritthart HA (1992) Kinetic modulation of guinea-pig cardiac L-type calcium channels by fendiline and reversal of the effects of Bay K 8644. *Br J Pharmacol* 106:151-156.
- Scott VE, Vortherms TA, Niforatos W, Swensen AM, Neelands T, Milicic I, Banfor PN, King A, Zhong C, Simler G, Zhan C, Bratcher N, Boyce-Rustay JM, Zhu CZ, Bhatia P, Doherty G, Mack H, Stewart AO, Jarvis MF (2012) A-1048400 is a novel, orally active, state-dependent neuronal calcium channel blocker that produces dose-dependent antinociception without altering hemodynamic function in rats. *Biochem Pharmacol* 83:406-418.
- Scoville WB, Milner BM (1957) Loss of recent memory after bilateral hippocampal lesions. *J Neurol Neurosurg Psychiatr* 20:11-21.
- Selkoe D (1996) Amyloid β -protein and the genetics of Alzheimer's disease. *J Biol Chem* 271:18295-18298.

- Selkoe DJ (2002) Alzheimer's disease is a synaptic failure. *Science* 298:789-791.
- Shankar GM, Bloodgood BL, Townsend M, Walsh DM, Selkoe DJ, Sabatini BL (2007) Natural oligomers of the Alzheimer amyloid- β protein induce reversible synapse loss by modulating an NMDA-type glutamate receptor-dependent signaling pathway. *J Neurosci* 27:2866-2875.
- Shankar GM, Li S, Mehta TH, Garcia-Munoz A, Shepardson NE, Smith I, Brett FM, Farrell MA, Rowan MJ, Lemere CA, Regan CM, Walsh DM, Sabatini BL, Selkoe DJ (2008a) Amyloid- β protein dimers isolated directly from Alzheimer's brains impair synaptic plasticity and memory. *Nat Med* 14:837-842.
- Shankar GM, Li S, Mehta TH, Garcia-Munoz A, Shepardson NE, Smith I, Brett FM, Farrell MA, Rowan MJ, Lemere CA, Regan CM, Walsh DM, Sabatini BL, Selkoe DJ (2008b) Amyloid-beta protein dimers isolated directly from Alzheimer's brains impair synaptic plasticity and memory. *Nat Med* 14:837-842.
- Shaw G, Morse S, Ararat M, Graham FL (2002) Preferential transformation of human neuronal cells by human adenoviruses and the origin of HEK 293 cells. *FASEB J* 16:869-871.
- Sheng Z-H, Rettig J, Takahashi M, Catterall WA (1994) Identification of a syntaxin-binding site on N-Type calcium channels. *Neuron* 13:1303-1313.
- Shi C, Soldatov NM (2002) Molecular determinants of voltage-dependent slow inactivation of the Ca^{2+} channel. *J Biol Chem* 277:6813-6821.
- Simic G, Kostovi I, Winblad B, Bogdanovi N (1997) Volume and number of neurons of the human hippocampal formation in normal aging and Alzheimer's disease. *J Comp Neurol* 379:482-494.
- Small DL, Monette R, Mealing G, Buchan AM, Morley P (1995) Neuroprotective effects of ω -Aga-IVA against in vitro ischaemia in the rat hippocampal slice. *Neuroreport* 6:1617-1620.
- Snutch TP (2005) Targeting chronic and neuropathic pain: the N-type calcium channel comes of age. *NeuroRx* 2:662-670.
- Snyder EM, Nong Y, Almeida CG, Paul S, Moran T, Choi EY, Nairn AC, Salter MW, Lombroso PJ, Gouras GK, Greengard P (2005) Regulation of NMDA receptor trafficking by amyloid-beta. *Nat Neurosci* 8:1051-1058.
- Sokolov S, Weiss RG, Timin EN, Hering S (2000) Modulation of slow inactivation in class A Ca^{2+} channels by β -subunits. *J Physiol* 527:445-454.
- Soldatov NM (1998) Molecular Determinants of L-type Ca^{2+} Channel Inactivation. *J Biol Chem* 273:957-963.
- Soong TW, DeMaria CD, Alvania RS, Zweifel LS, Liang MC, Mittman S, Agnew WS, Yue DT (2002) Systematic identification of splice variants in human P/Q-type channel $\alpha_12.1$ subunits: implications for current density and Ca^{2+} -dependent inactivation. *J Neurosci* 22:10142-10152.
- Spiers HJ, Maguire EA, Burgess N (2001) Hippocampal amnesia. *Neurocase* 7:357-382.
- Spillantini MG, Murrell JR, Goedert M, Farlow MR, Klug A, Ghetti B (1998) Mutation in the tau gene in familial multiple system tauopathy with presenile dementia. *Proc Natl Acad Sci U S A* 95:7737-7741.
- Staats PS, Yearwood T, Charapata SG, Presley RW, Wallace MS, Byas-Smith M, Fisher R, Bryce DA, Mangieri EA, Luther RR, Mayo M, McGuire D, Ellis D (2004) Intrathecal ziconotide in the treatment of refractory pain in patients with cancer or AIDS: a randomized controlled trial. *JAMA* 291:63-70.

- Stea A, Tomlinson WJ, Soong TW, Bourinet E, Dubel SJ, Vincent SR, Snutch TP (1994) Localization and functional properties of a rat brain α_{1A} calcium channel reflect similarities to neuronal Q- and P-type channels. *Proc Natl Acad Sci U S A* 91:10576-10580.
- Steele LS, Glazier RH (1999) Is donepezil effective for treating Alzheimer's disease? *Can Fam Physician* 45:917-919.
- Stephens GJ, Page KM, Bogdanov Y, Dolphin AC (2000) The α_{1B} Ca^{2+} channel amino terminus contributes determinants for β subunit-mediated voltage-dependent inactivation properties. *J Physiol* 525:377-390.
- Stine WB, Jr., Dahlgren KN, Krafft GA, LaDu MJ (2003) In vitro characterization of conditions for amyloid- β peptide oligomerization and fibrillogenesis. *J Biol Chem* 278:11612-11622.
- Stocker JW, Nadasdi L, Aldrich RW, Tsien RW (1997) Preferential interaction of ω -conotoxins with inactivated N-type Ca^{2+} channels. *J Neurosci* 17:3002-3013.
- Stoppini L, Buchs PA, Muller D (1991) A simple method for organotypic cultures of nervous tissue. *J Neurosci Methods* 37:173-182.
- Stotz SC, Hamid J, Spaetgens RL, Jarvis SE, Zamponi GW (2000) Fast inactivation of voltage-dependent calcium channels. A hinged-lid mechanism? *J Biol Chem* 275:24575-24582.
- Stotz SC, Zamponi GW (2001) Identification of inactivation determinants in the domain IIS6 region of high voltage-activated calcium channels. *J Biol Chem* 276:33001-33010.
- Strittmatter WJ, Weisgraber KH, Huang DY, Dong LM, Salvesen GS, Pericak-Vance M, Schmechel D, Saunders AM, Goldgaber D, Roses AD (1993) Binding of human apolipoprotein E to synthetic amyloid β peptide: isoform-specific effects and implications for late-onset Alzheimer disease. *Proc Natl Acad Sci U S A* 90:8098-8102.
- Study RE (1994) Isoflurane inhibits multiple voltage-gated calcium currents in hippocampal pyramidal neurons. *Anesthesiology* 81:104-116.
- Sutton KG, McRory JE, Guthrie H, Murphy TH, Snutch TP (1999) P/Q-type calcium channels mediate the activity-dependent feedback of syntaxin-1A. *Nature* 401:800-804.
- Suzuki N, Cheung T, Cai X, Odaka A, Otvos L, Eckman C, Golde T, Younkin S (1994) An increased percentage of long amyloid β protein secreted by familial amyloid β protein precursor (beta APP717) mutants. *Science* 264:1336-1340.
- Swensen AM, Niforatos W, Vortherms TA, Perner RJ, Li T, Schrimpf MR, Scott VE, Lee L, Jarvis MF, McGaraughty S (2012) An automated electrophysiological assay for differentiating $Ca_v2.2$ inhibitors based on state dependence and kinetics. *Assay Drug Dev Technol* 10:542-550.
- Tabet N, Feldman H (2003) Ibuprofen for Alzheimer's disease. *Cochrane Database Syst Rev* CD004031.
- Tajima Y, Ono K, Akaike A (1996) Perforated patch-clamp recording in cardiac myocytes using cation-selective ionophore gramicidin. *Am J Physiol Cell Physiol* 271:C524-C532.
- Tang W, Kang J, Wu X, Rampe D, Wang L, Shen H, Li Z, Dunnington D, Garyantes T (2001) Development and evaluation of high throughput functional assay methods for hERG potassium channel. *J Biomol Screen* 6:325-331.
- Tariot PN, Farlow MR, Grossberg GT, Graham SM, McDonald S, Gergel I (2004) Memantine treatment in patients with moderate to severe Alzheimer disease already receiving donepezil: a randomized controlled trial. *JAMA* 291:317-324.

- Taylor CP, Angelotti T, Fauman E (2007) Pharmacology and mechanism of action of pregabalin: the calcium channel $\alpha_2\delta$ (alpha₂-delta) subunit as a target for antiepileptic drug discovery. *Epilepsy Res* 73:137-150.
- Teller JK, Russo C, Debusk LM, Angelini G, Zaccheo D, Dagna-Bricarelli F, Scartezzini P, Bertolini S, Mann DMA, Tabaton M, Gambetti P (1996) Presence of soluble amyloid β -peptide precedes amyloid plaque formation in Down's syndrome. *Nat Med* 2:93-95.
- Teramoto T, Kuwada M, Niidome T, Sawada K, Nishizawa Y, Katayama K (1993) A novel peptide from funnel web spider venom, ω -Aga-TK, selectively blocks, P-type calcium channels. *Biochem Biophys Res Commun* 196:134-140.
- Terry RD, Masliah E, Salmon DP, Butters N, DeTeresa R, Hill R, Hansen LA, Katzman R (1991) Physical basis of cognitive alterations in Alzheimer's disease: synapse loss is the major correlate of cognitive impairment. *Ann Neurol* 30:572-580.
- Terstappen GC (1999) Functional analysis of native and recombinant ion channels using a high-capacity nonradioactive rubidium efflux assay. *Anal Biochem* 272:149-155.
- Terstappen GC (2005) Ion channel screening technologies today. *Drug Discov Today* 2:133-140.
- Terstappen GC, Roncarati R, Dunlop J, Peri R (2010) Screening technologies for ion channel drug discovery. *Future Med Chem* 2:715-730.
- Texido L, Martin-Satue M, Alberdi E, Solsona C, Matute C (2011) Amyloid β peptide oligomers directly activate NMDA receptors. *Cell Calcium* 49:184-190.
- Thibault O, Gant JC, Landfield PW (2007) Expansion of the calcium hypothesis of brain aging and Alzheimer's disease: minding the store. *Aging Cell* 6:307-317.
- Thies W, Bleiter L (2012) 2012 Alzheimer's disease facts and figures. *Alzheimers Dement* 8:131-168.
- Thomas P, Smart TG (2005) HEK293 cell line: a vehicle for the expression of recombinant proteins. *J Pharmacol Toxicol Methods* 51:187-200.
- Ting JT, Kelley BG, Lambert TJ, Cook DG, Sullivan JM (2007) Amyloid precursor protein overexpression depresses excitatory transmission through both presynaptic and postsynaptic mechanisms. *Proc Natl Acad Sci U S A* 104:353-358.
- Toru S, Murakoshi T, Ishikawa K, Saegusa H, Fujigasaki H, Uchihara T, Nagayama S, Osanai M, Mizusawa H, Tanabe T (2000) Spinocerebellar ataxia type 6 mutation alters P-type calcium channel function. *J Biol Chem* 275:10893-10898.
- Tottene A, Conti R, Fabbro A, Vecchia D, Shapovalova M, Santello M, van den Maagdenberg AM, Ferrari MD, Pietrobon D (2009) Enhanced excitatory transmission at cortical synapses as the basis for facilitated spreading depression in Ca(v)2.1 knockin migraine mice. *Neuron* 61:762-773.
- Tottene A, Fellin T, Pagnutti S, Luvisetto S, Striessnig J, Fletcher C, Pietrobon D (2002) Familial hemiplegic migraine mutations increase Ca²⁺ influx through single human Ca_v2.1 channels and decrease maximal Ca_v2.1 current density in neurons. *Proc Natl Acad Sci USA* 99:13284-13289.
- Tottene A, Urbani A, Pietrobon D (2011) Role of different voltage-gated Ca²⁺ channels in cortical spreading depression: Specific requirement of P/Q-type Ca²⁺ channels. *Channels* 5:110-114.
- Townsend M, Shankar GM, Mehta T, Walsh DM, Selkoe DJ (2006) Effects of secreted oligomers of amyloid β -protein on hippocampal synaptic plasticity: a potent role for trimers. *J Physiol* 572:477.
- Tsien RW, Ellinor PT, Horne WA (1991) Molecular diversity of voltage-dependent Ca²⁺ channels. *Trends Pharmacol Sci* 12:349-354.

- Tsunemi T, Saegusa H, Ishikawa K, Nagayama S, Murakoshi T, Mizusawa H, Tanabe T (2002) Novel Cav2.1 splice variants isolated from Purkinje cells do not generate P-type Ca²⁺ current. *J Biol Chem* 277:7214-7221.
- Uchitel OD, Di Guilmi MN, Urbano FJ, Gonzalez-Inchauspe C (2010) Acute modulation of calcium currents and synaptic transmission by gabapentinoids. *Channels (Austin)* 4:490-496.
- Ueda K, Shinohara S, Yagami T, Asakura K, Kawasaki K (1997) Amyloid β protein potentiates Ca²⁺ influx through L-type voltage-sensitive Ca²⁺ channels: A possible involvement of free radicals. *J Neurochem* 68:265-271.
- Ulas J, Brunner LC, Geddes JW, Choe W, Cotman CW (1992) N-methyl-d-aspartate receptor complex in the hippocampus of elderly, normal individuals and those with Alzheimer's disease. *Neuroscience* 49:45-61.
- Uneyama H, Uchida H, Konda T, Yoshimoto R (1999) Cilnidipine: preclinical profile and clinical evaluation. *Cardiovasc Drug Rev* 17:341-357.
- Upton N, Chuang TT, Hunter AJ, Virley DJ (2008) 5-HT₆ receptor antagonists as novel cognitive enhancing agents for Alzheimer's disease. *Neurotherapeutics* 5:458-469.
- Urban JD, Clarke WP, von Zastrow M, Nichols DE, Kobilka B, Weinstein H, Javitch JA, Roth BL, Christopoulos A, Sexton PM, Miller KJ, Spedding M, Mailman RB (2007) Functional selectivity and classical concepts of quantitative pharmacology. *J Pharmacol Exp Ther* 320:1-13.
- Valentino K, Newcomb R, Gadbois T, Singh T, Bowersox S, Bitner S, Justice A, Yamashiro D, Hoffman BB, Ciaranello R (1993) A selective N-type calcium channel antagonist protects against neuronal loss after global cerebral ischemia. *Proc Natl Acad Sci U S A* 90:7894-7897.
- van den Maagdenberg AM, Pietrobon D, Pizzorusso T, Kaja S, Broos LA, Cesetti T, van de Ven RC, Tottene A, van der Kaa J, Plomp JJ, Frants RR, Ferrari MD (2004) A Cacna1a knockin migraine mouse model with increased susceptibility to cortical spreading depression. *Neuron* 41:701-710.
- Varadi G, Lory P, Schultz D, Varadi M, Schwartz A (1991) Acceleration of activation and inactivation by the β subunit of the skeletal muscle calcium channel. *Nature* 352:159-162.
- Venter JC, Adams MD, Myers EW, Li PW, Mural RJ, Sutton GG, Smith HO, Yandell M, Evans CA, Holt RA, Gocayne JD, Amanatides P, Ballew RM, Huson DH, Wortman JR, Zhang Q, Kodira CD, Zheng XH, Chen L, Skupski M, Subramanian G, Thomas PD, Zhang J, Gabor Miklos GL, Nelson C, Broder S, Clark AG, Nadeau J, McKusick VA, Zinder N, et al. (2001) The sequence of the human genome. *Science* 291:1304-1351.
- Verweij BH, Muizelaar JP, Vinas FC, Peterson PL, Xiong Y, Lee CP (1997) Mitochondrial dysfunction after experimental and human brain injury and its possible reversal with a selective N-type calcium channel antagonist (SNX-111). *Neurol Res* 19:334-339.
- Vortherms TA, Swensen AM, Niforatos W, Limberis JT, Neelands TR, Janis RS, Thimmapaya R, Donnelly-Roberts DL, Namovic MT, Zhang D, Brent Putman C, Martin RL, Surowy CS, Jarvis MF, Scott VE (2011) Comparative analysis of inactivated-state block of N-type (Ca_v2.2) calcium channels. *Inflamm Res* 60:683-693.
- Wallace MS, Rauck R, Fisher R, Charapata SG, Ellis D, Dissanayake S (2008) Intrathecal ziconotide for severe chronic pain: safety and tolerability results of an open-label, long-term trial. *Anesth Analg* 106:628-637.

- Walsh DM, Klyubin I, Fadeeva JV, Cullen WK, Anwyl R, Wolfe MS, Rowan MJ, Selkoe DJ (2002) Naturally secreted oligomers of amyloid β protein potently inhibit hippocampal long-term potentiation in vivo. *Nature* 416:535-539.
- Walsh DM, Selkoe DJ (2007) A β beta oligomers - a decade of discovery. *J Neurochem* 101:1172-1184.
- Wang J, Dickson DW, Trojanowski JQ, Lee VM (1999) The levels of soluble versus insoluble brain A β distinguish Alzheimer's disease from normal and pathologic aging. *Exp Neurol* 158:328-337.
- Wang Z, Wang B, Yang L, Guo Q, Aithmitti N, Songyang Z, Zheng H (2009) Presynaptic and postsynaptic interaction of the amyloid precursor protein promotes peripheral and central synaptogenesis. *J Neurosci* 29:10788-10801.
- Wappl E, Koschak A, Poteser M, Sinnegger MJ, Walter D, Eberhart A, Groschner K, Glossmann H, Kraus RL, Grabner M, Striessnig J (2002) Functional consequences of P/Q-type Ca²⁺ channel Ca_v2.1 missense mutations associated with episodic ataxia type 2 and progressive ataxia. *J Biol Chem* 277:6960-6966.
- Westenbroek RE, Hell JW, Warner C, Dubel SJ, Snutch TP, Catterall WA (1992) Biochemical properties and subcellular distribution of an N-type calcium channel α 1 subunit. *Neuron* 9:1099-1115.
- Westenbroek RE, Sakurai T, Elliott EM, Hell JW, Starr TV, Snutch TP, Catterall WA (1995) Immunochemical identification and subcellular distribution of the α _{1A} subunits of brain calcium channels. *J Neurosci* 15:6403-6418.
- Westerman MA, Cooper-Blacketer D, Mariash A, Kotilinek L, Kawarabayashi T, Younkin L, Carlson GA, Younkin SG, Ashe KH (2002) The relationship between A β and memory in the Tg2576 mouse model of Alzheimer's disease. *J Neurosci* 22:1858-1867.
- Wheeler D, Randall A, Tsien R (1994) Roles of N-type and Q-type Ca²⁺ channels in supporting hippocampal synaptic transmission. *Science* 264:107-111.
- Whitehouse P, Price D, Struble R, Clark A, Coyle J, Delon M (1982) Alzheimer's disease and senile dementia: loss of neurons in the basal forebrain. *Science* 215:1237-1239.
- Wildburger NC, Lin-Ye A, Baird MA, Lei D, Bao J (2009) Neuroprotective effects of blockers for T-type calcium channels. *Mol Neurodegener* 4:44.
- Wilson SM, Toth PT, Oh SB, Gillard SE, Volsen S, Ren D, Philipson LH, Lee EC, Fletcher CF, Tessarollo L, Copeland NG, Jenkins NA, Miller RJ (2000) The status of voltage-dependent calcium channels in alpha 1E knock-out mice. *J Neurosci* 20:8566-8571.
- Wimo A, Prince M (2010) World Alzheimer Report 2010 - the global economic impact of dementia. <http://www.alz.co.uk/research/files/WorldAlzheimerReport2010.pdf>: Alzheimer's Disease International.
- Winblad B, Poritis N (1999) Memantine in severe dementia: results of the 9M-Best Study. *Int J Geriatr Psychiatry* 14:135-146.
- Winquist RJ, Pan JQ, Gribkoff VK (2005) Use-dependent blockade of Ca_v2.2 voltage-gated calcium channels for neuropathic pain. *Biochem Pharmacol* 70:489-499.
- Wisniewski KE, Wisniewski HM, Wen GY (1985) Occurrence of neuropathological changes and dementia of Alzheimer's disease in Down's syndrome. *Ann Neurol* 17:278-282.
- Wolfe MS, Xia W, Ostaszewski BL, Diehl TS, Kimberly WT, Selkoe DJ (1999) Two transmembrane aspartates in presenilin-1 required for presenilin endoproteolysis and γ -secretase activity. *Nature* 398:513-517.
- Wolff C, Fuks B, Chatelain P (2003) Comparative study of membrane potential-sensitive fluorescent probes and their use in ion channel screening assays. *J Biomol Screen* 8:533-543.

- Woodhall G, Evans ID, Cunningham MO, Jones RSG (2001) NR2B-containing NMDA autoreceptors at synapses on entorhinal cortical neurons. *J Neurophysiol* 86:1644-1651.
- Wu G, Kim HK, Zornow MH (1995) Transient brain ischemia in rabbits: the effect of ω -conopeptide MVIIC on hippocampal excitatory amino acids. *Brain Res* 692:118-122.
- Wyss JM, Swanson LW, Cowan WM (1979) A study of subcortical afferents to the hippocampal formation in the rat. *Neuroscience* 4:463-476.
- Xie X, Lancaster B, Peakman T, Garthwaite J (1995) Interaction of the antiepileptic drug lamotrigine with recombinant rat brain type IIA Na^+ channels and with native Na^+ channels in rat hippocampal neurones. *Pflugers Arch* 430:437-446.
- Xu W, Lipscombe D (2001) Neuronal $\text{Ca}_v1.3\alpha_1$ L-type channels activate at relatively hyperpolarized membrane potentials and are incompletely inhibited by dihydropyridines *J Neurosci* 21:5944-5951.
- Yamamoto T, Takahara A (2009) Recent updates of N-type calcium channel blockers with therapeutic potential for neuropathic pain and stroke. *Curr Top Med Chem* 9:377-395.
- Yang J, Ellinor PT, Sather WA, Zhang JF, Tsien RW (1993) Molecular determinants of Ca^{2+} selectivity and ion permeation in L-type Ca^{2+} channels. *Nature* 366:158-161.
- Yang L, Katchman A, Morrow JP, Doshi D, Marx SO (2011) Cardiac L-type calcium channel ($\text{Ca}_v1.2$) associates with γ subunits. *FASEB J* 25:928-936.
- Yankner BA, Duffy LK, Kirschner DA (1990) Neurotrophic and neurotoxic effects of amyloid β protein: reversal by tachykinin neuropeptides. *Science* 250:279-282.
- Yao PJ, Zhu M, Pyun EI, Brooks AI, Therianos S, Meyers VE, Coleman PD (2003) Defects in expression of genes related to synaptic vesicle trafficking in frontal cortex of Alzheimer's disease. *Neurobiol Dis* 12:97-109.
- Yu JT, Chang RC, Tan L (2009a) Calcium dysregulation in Alzheimer's disease: from mechanisms to therapeutic opportunities. *Prog Neurobiol* 89:240-255.
- Yu L, Edalji R, Harlan JE, Holzman TF, Lopez AP, Labkovsky B, Hillen H, Barghorn S, Ebert U, Richardson PL, Miesbauer L, Solomon L, Bartley D, Walter K, Johnson RW, Hajduk PJ, Olejniczak ET (2009b) Structural characterization of a soluble amyloid β -peptide oligomer. *Biochemistry* 48:1870-1877.
- Zamponi GW (2005) Voltage-gated calcium channels: Kluwer Academic / Plenum Publishers.
- Zhang JF, Randall A, Ellinor PT, Horne WA, Sather WA, Tanabe T, Schwarz TL, Tsien RW (1993) Distinctive pharmacology and kinetics of cloned neuronal Ca^{2+} channels and their possible counterparts in mammalian CNS neurons *Neuropharmacology* 32:1075-1088.
- Zhou Q, Homma KJ, Poo MM (2004) Shrinkage of dendritic spines associated with long-term depression of hippocampal synapses. *Neuron* 44:749-757.
- Zhuchenko O, Bailey J, Bonnen P, Ashizawa T, Stockton DW, Amos C, Dobyns WB, Subramony SH, Zoghbi HY, Lee CC (1997) Autosomal dominant cerebellar ataxia (SCA6) associated with small polyglutamine expansions in the α_{1A} -voltage-dependent calcium channel. *Nat Genet* 15:62-69.
- Zimmer T (2010) Effects of tetrodotoxin on the mammalian cardiovascular system. *Mar Drugs* 8:741-762.
- Zou K, Gong JS, Yanagisawa K, Michikawa M (2002) A novel function of monomeric amyloid β -protein serving as an antioxidant molecule against metal-induced oxidative damage. *J Neurosci* 22:4833.

Zuhlke RD, Pitt GS, Deisseroth K, Tsien RW, Reuter H (1999) Calmodulin supports both inactivation and facilitation of L-type calcium channels. *Nature* 399:159-162.

List of Tables and Figures

Table 1.1 Genetic factors predisposing to AD (adapted from Selkoe, 1996)	9
Figure 1.1 Scheme of different natural and synthetic Aβ assemblies (from Benilova et al., 2012).	17
Figure 1.2 Voltage-gated calcium channels (from Dolphin, 2012).	21
Figure 1.3 Nomenclature of channel state transitions	23
Figure 1.4 Hinged-lid model of fast voltage-dependent inactivation of HVA calcium channels (from Zamponi, 2005).	26
Figure 2.1 The Patchliner – an automated planar patch clamp system (from Nanion GmbH, Munich, Germany)	47
Figure 2.2 The rat hippocampal formation (from Amaral and Witter, 1989).	49
Figure 3.1 Characterization of the Aβ globulomer preparation	55
Figure 3.2 Effects of P/Q calcium channel modulation on Aβ globulomer-induced functional synaptic deficits	57
Figure 3.3 Effects of N-type and L-type calcium channel blockers on Aβ globulomer-induced functional deficits in synaptic transmission	58
Figure 3.4 Characterization of selected cell lines with inducible P/Q-type calcium channel expression	60
Figure 3.5 Basic biophysical characterization of P/Q-type calcium channels	61
Figure 3.6 Pharmacological validation of P/Q-type calcium channels	63
Figure 3.7 Biophysical and pharmacological validation of N-type calcium channel channels	65
Figure 3.8 Modulation of P/Q-type calcium channels by Aβ globulomer	67
Figure 3.9 Modulation of N-type calcium channels by Aβ globulomer	70
Figure 3.10 Effect of Aβ globulomer on different P/Q-type calcium channel states	72
Figure 3.11 Inactivation properties of P/Q-type calcium channels	75
Figure 3.12 Automated electrophysiological recordings from P/Q-type calcium channels	78
Figure 3.13 Validation of the automated patch clamp recordings for secondary screening on P/Q-type calcium channels	79
Figure 3.14 Membrane potential of P/Q-type calcium channels during FLIPR assay conditions	81
Figure 3.15 Implementation of patch clamp recordings to support the discovery of novel P/Q-type calcium channel blockers	84
Figure 3.16 Characterization of state-dependent properties of two novel P/Q-type calcium channel blockers	87
Figure 3.17 State-dependent P/Q-type calcium channel block prevents Aβ globulomer-induced functional synaptic deficits	89